New insights into sphingolipid metabolism and functions by using chemical tools

Francesca Cingolani



UNIVERSITAT DE BARCELONA

FACULTAT DE FARMÀCIA
PROGRAMA DE DOCTORAT EN BIOMEDICINA

New insights into sphingolipid metabolism and functions by using chemical tools

Memòria presentada per Francesca Cingolani per optar al títol de Doctor per la Universitat de Barcelona

Tesis realitzada en el Departament de Química Biomèdica, Institut de Química Avançada de Catalunya (IQAC-CSIC)

Directora
Josefina Casas Brugulat

Tutor
Timothy M. Thomson

Doctoranda
Francesca Cingolani

FRANCESCA CINGOLANI-2015

Ai miei genitori

This work was supported by grants from the Ministry of Science and Innovation (SAF2011-22444), the Agència de Gestió d'Ajuts Universitaris i de Recerca de la Generalitat de Catalunya (2009SGR1072; FI-DGR2011; BE-DGR2012) and Fundació La Marató de TV3 (20112130).

ACKNOWLEDGEMENTS

A la Dra. Josefina Casas, mi directora de Tesis, y a la Dra. Gemma Fabriàs por haberme acogido en el RUBAM, y por haber confiado en mis capacidades. Al Dr. Antonio Delgado y al Dr. José Luís Abad, por vuestros consejos y ayuda.

Al Dr. Timothy Thomson por la tutoría de esta Tesis.

A todos los compañeros que son o han sido parte del RUBAM por haber compartido conmigo éxitos, decepciones y tantas horas en el laboratorio. Y a todos los compañeros que han aliviado las horas interminables en la biblioteca del CSIC.

A todos los que han hecho que Barcelona sea un lugar acogedor y familiar. A los amigos que he encontrado durante estos años, por los buenos momentos compartidos.

To Prof. A. Futerman to give me the opportunity to work in his lab. To Futerman's lab people for giving me a great welcome in Israel.

To Mody for supporting me at any time, and for telling me what is English and what is not.

Ai miei amici, cosi lontani ma vicini, per esserci sempre anche se il dove e il quando è incerto.

Alla mia famiglia per il vostro affetto. Ai miei genitori, per tutto cio che significa per voi non avermi li, e per la fiducia che avete in me.

Grazie.

The following list includes the publications that were published during this PhD Thesis:

Cingolani, F., Casasampere, M., Sanllehí, P., Casas, J., Bujons J., Fabriàs, G. **Inhibition of dihydroceramide desaturase activity by the sphingosine kinase inhibitor SKI II.** *J. Lipid Res.*55, 1711–1720 (2014).

Camacho, L., Meca-Cortés, O., Luis Abad, J., García, S., Rubio, N., Díaz, A., Celià-Terrassa, T., Cingolani, F., Bermudo, R., Fernández, P. L., Blanco, J.,Delgado, A.,Casas, J., Fabriàs, G., Thomson, T.M. **Acid ceramidase as a therapeutic target in metastatic prostate cancer.** *J. Lipid Res.*54**,** 1207–20 (2013).

Fabriàs, G., Muñoz-Olaya, J., Cingolani, F., Signorelli P., Casas J., Gagliostro V., Ghidoni*, R.* **Dihydroceramide desaturase and dihydrosphingolipids: debutant players in the sphingolipid arena**. *Prog. Lipid Res.*51, 82–94 (2012).

ABSTRACT

Sphingolipids (SLs), a family of lipids characterized by a sphingoid backbone, are essential components of cell membranes. In the last two decades they emerged as bioactive molecules involved in the regulation of a variety of cellular processes. Ceramide (Cer) and sphingosine (So) generally mediate anti-proliferative stimuli, such as cell growth arrest and apoptosis, while sphingosine-1-phosphate (S1P) plays opposite roles by inducing cell proliferation and apoptosis resistance. The bioactive role of dihydroceramide (dhCer) has also been recently described, showing its involvement in processes like apoptosis and autophagy. Alteration of SLs levels are the base of human sphingolipidosis, and are also related to the onset and progression of other diseases, including cancer, inflammation and neurological disorders. SL metabolism is a complex network of anabolic and catabolic reactions catalyzed by specific enzymes. Consistent with the key role of SLs in cell biology, the modulation of key-enzyme of the SL metabolism such as dihydroceramide desaturase (Des1), ceramide synthase (CerS), ceramidases (CDases) and sphingosine kinase (SK) represent a strategy to better understand the role of SLs in physiophatological processes. During this PhD Thesis three different studies that show the use of SL analogues and SL metabolism inhibitors as pharmacological tools for biomedical investigation in cancer cells were performed.

The first study was focused on the alteration of SL metabolism and cytotoxic effect induced by Jaspine B (JB) in cancer cells. JB, a natural SL analogue from marine origin, is cytotoxic in a variety of cancer cell lines, including HGC-27 gastric cancer cells. JB induces changes in the sphingolipidome in this cell line, mainly the accumulation of dihydrosphingosine (dhSo) and So, and their phosphorylated forms. Moreover lipidomic analyses show the formation of acyl-JB. These effects appear to be due to inhibitory action of JB on CerS that uses the natural sphingolipid as substrate. The hallmark of JB cytotoxicity in HGC-27 cells is the formation of cytoplasmic vacuoles in a time and dose-dependent manner. Apoptosis is not involved in cytoplasmic vacuolization and JB induced cytotoxicity. In addition, despite the accumulation of the autophagic marker LC3-II, autophagy is probably not activated by JB treatment. The micropinocytic nature of vacuoles suggests the involvement of methuosis in JB-induced cell death.

The second study was focused on SKI II, a well-known SK inhibitor. In a study on HGC-27 cells we show that SKI II is also an uncompetitive inhibitor of Des1. Des1 inhibition in intact cells is not connected to protein degradation. SKI II, but not the SK1-specific inhibitor PF-543, provoked a remarkable accumulation of dhCers and their metabolites, while both SKI II and PF-543 reduced S1P to almost undetectable levels. SKI

II, but not PF-543, reduced cell proliferation, with accumulation of cells in the G0/G1 phase. Similarly SKI II, but not PF-543 increased LC3-II levels in HGC-27 cells, suggesting autophagy induction. These overall findings indicate that some of the effects attributed to decreased S1P may actually be caused by augmented dhCers and/or their metabolites.

The use of ceramide analogues as chemical tool for ceramidases investigation is the topic of the third study. RBM14 are coumarinic ceramide analogues that differ from the acyl chain length. Among them RBM14C12 was reported as the best substrate for acid ceramidase (AC). In this study it was shown that RBM14 molecules are also hydrolyzed by neutral (NC) and alkaline ceramidases (ACER). NC from *Pseudomonas aeuriginosa* prefers C12 and C14 analogues, while human recombinant NC better hydrolyzes RBM14C14 and RBM14C16 molecules. RBM14 substrates are hydrolyzed by MEF cells lacking NC, with higher activity at basic pH, suggesting ACER activity. SABRAC and RBM1-12 have been designed to inhibit the cysteine protease AC. In this study it was shown that papain, a protein belonging to the same protein family, is not inhibited by SABRAC and RBM1-12. Moreover preliminary studies suggest an irreversible inhibition of AC. These molecules can be used in combination with RBM14C12 substrate as a suitable tool for AC activity determination in intact cancer cells.

ABBREVIATIONS

4-HPR	N-(4-hydroxyphenyl)retinamide or fenretinide
AC	Acid ceramidase
ACER	Alkaline ceramidase
ACER1	Alkaline ceramidase 1
ACER2	Alkaline ceramidase 2
ACER3	Alkaline ceramidase 3
Acyl-CoA	Acyl-coenzyme A
ASAH1	Acid ceramidase gene
ASAH2	Neutral ceramidase gene
ASAH3	Alkaline ceramidase 1 gene
aSMase	Acid sphingomyelinase
Atg	Autophagy related protein
AV	Annexin-V
C1P	Ceramide-1-phosphate
CAPPs	Ceramide-activated protein phosphatases
CB5R	NADH-cytochrome b5 reductase
CDase	Ceramidase
CDH	Ceramide dihexoside (lactosylceramide)
Cer	Ceramide
CerC6NBD	*N*-[6-[(7-nitro-2-1,3-benzoxadiazol-4-yl)amino]hexanoyl]-D-*erythro* sphingosine
CERK	Ceramide kinase
CerS	Ceramide synthase
CK	Ceramide kinase
CMH	Ceramide monohexoside (glucosylceramide and galactosylceramide)
Des1	Dihydroceramide desaturase
dhCDH	Dihydroceramide dihexoside (lactosyldihydroceramide)
DhCerC6NBD	*N*-[6-[(7-nitro-2-1,3-benzoxadiazol-4-yl)amino]hexanoyl]-D-*erythro* dihydrosphingosine
dhCerS	Dihydroceramide synthase
dhSo	Dihydrosphingosine
dhSoP	Dihydrosphingosine-1-phosphate
DMS	*N,N*-dimethyl-D-*erythro*-sphingosine

EIPA	5-(N-Ethyl-N-isopropyl)amiloride
ER	Endoplasmic reticulum
ERK	Extracellular signal regulated kinase
FB1	Fumonisin B1
GalCer	Galactosylceramide
GalCerS	Galactosylceramide synthase
GCase	Glicosidase
GlcCer/GluCer	Glucosylceramide
GSLs	Glycosphingolipids
hNC	Human recombinant neutral ceramidase
IC_{50}	Half maximal inhibitory concentration
JB	Jaspine B
KDSR	3-keto-dihydrosphingosine reductase
K_m	Michaelis-Menten constant
LC3	Microtubule-associated protein 1 light chain 3
LD_{50}	Median lethal dose
MMP/MOMP	Mitochondrial outer membrane permeabilization
mTOR	Mammalian target or rapamycin
Myr	Myriocin
NC	Neutral ceramidase
NDB-Sa	NBD-sphinganine
nSMase	Neutral sphingomyelinase
PCD	Programmed cell death
pCDase	*Pseudomomas aeuruginosa* ceramidase
PHS	Phytosphingosine
PI	Propidium iodide
PI3K	Phosphatidylinositol-3-kinase
PKC	Protein kinase C
Rap	Rapamycin
S1PP	Sphingosine-1-phosphate phosphatase
Sa	Sphinganine
SK/Sphk	Sphingosine kinase
SK1/Sphk1	Sphingosine Kinase isoforms 1
SK2/Sphk2	Sphingosine kinase isoforms 2
SKI II	Sphingosine kinase inhibitor II
SLs	Sphingolipids

SM	Sphingomyelin
SMase	Sphingomyelinase
SMS	Sphingomyelin synthase
So/Sph	Sphingosine
SoP/S1P	Sphingosine-1-phosphate
SPL/S1PL	Sphingosine-1-phosphate lyase
SPT	Serine palmitoyltransferase
TNFα	Tumour necrosis factor-α
TRAIL	Tumour necrosis factor–related apoptosis-inducing ligand
V_{max}	Maximum reaction rate
Wt	Wortmannin

INTRODUCTION

1. Sphingolipids

Sphingolipids (SLs) consist of a family of lipids that are essential components of cell membranes. Their name was given by J.L.W. Thudichum in 1884 due to their enigmatic nature and unknown function. In the last two decades research progress in the SLs field shed light on their role as components of membrane microdomains called "lipid rafts", as well as on their function as signalling molecules[1].

1.1. Sphingolipids in cell biology

The concept of lipid rafts has pointed out the dynamic and functional role of SLs, that used to be considered for long time as structural elements of cell membranes[2]. Although the nature of lipid rafts has been extensively questioned in the last years[3,4], they are now described as ordered, fluctuating nanoscale assemblies of lipids and proteins enri-

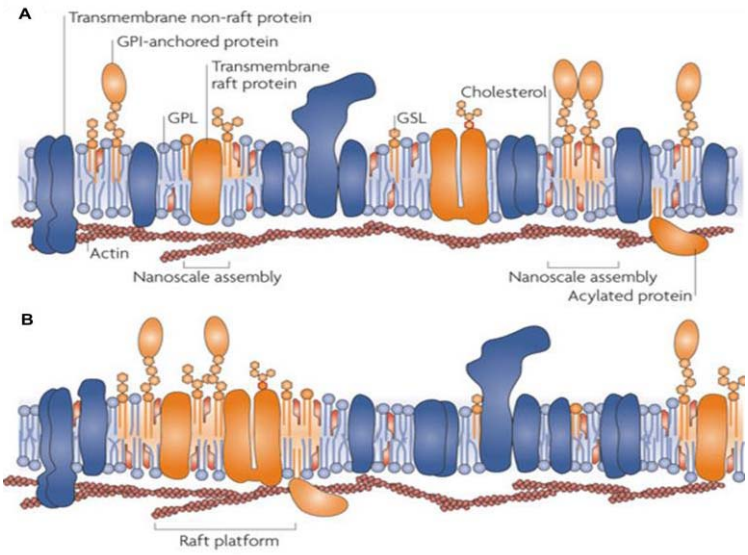

Figure 1.1: Lipid rafts in cell membranes. A. Nanoscale assemblies of sterols, sphingolipids and proteins originate lipid rafts that fluctuate in the plasma membrane. Glycosyl phosphatidylinositol (GPI) anchored proteins, transmembrane raft proteins and acylated cytosolic proteins also are assumed as rafts components. GPL, glycerophospholipid. **B.** Lipid-lipid, protein-lipid and protein-protein interactions organize nanoscale assemblies in raft platforms that are involved in biological membrane processes. Modified from *Simons K. and Gerl M.J., Nature (2010)*[5].

ched in SLs, such as sphingomyelin (SM) and glycosphingolipids (GSLs). This structures can coalesce into larger and more stable domains called raft platforms, that are involved in membrane signalling and trafficking[5] (**Figure 1.1**).

The role of sphingolipids as bioactive compounds in cell physiology and in pathological processes has emerged in the last two decades. SLs are activated by a variety of stimuli as second messengers to trigger biological effects (**Figure 1.2**).

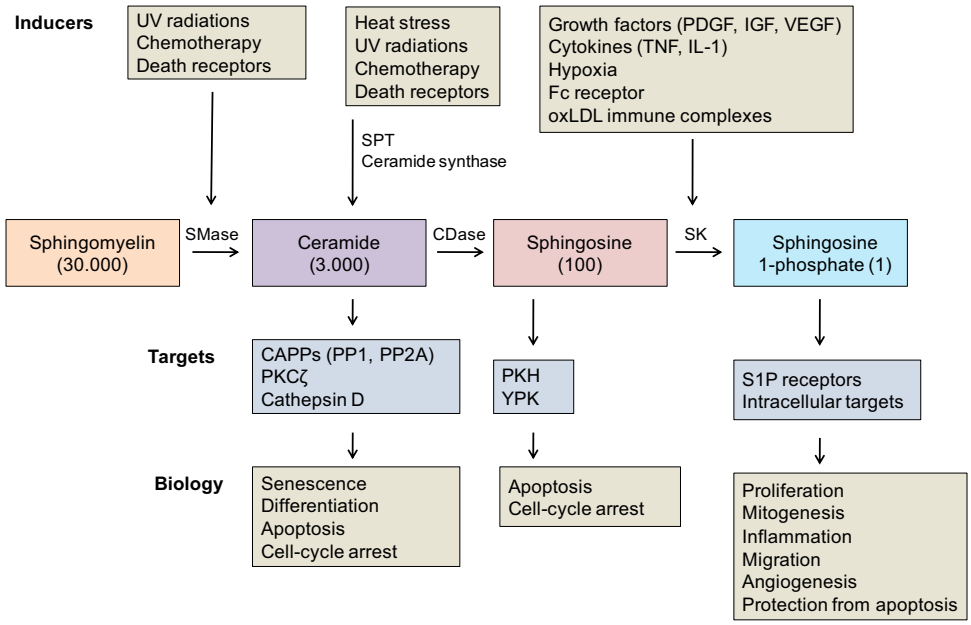

Figure 1.2: An overview of the roles of SLs in biology. The scheme shows potential participation of the bioactive lipids ceramide, sphingosine and sphingosine-1-phosphate in cell biological responses. The numbers in brackets indicate the relative levels of these SLs, pointing out that bioactive SLs levels exhibit great differences in cells. CAPP, ceramide-activated Ser–Thr phosphatase; IGF, insulin-like growth factor; IL-1, interleukin-1; oxLDL, oxidized low-density lipoprotein; PDGF; platelet-derived growth factor; PKC, protein kinase C; PKH, PKB homologue; TNFα, tumour necrosis factor-α; VEGF, vascular endothelial growth factor; YPK, yeast protein kinase. From: *Hannun Y. A. et al., Nat. Rev. Mol. Cell Biol*. (2008)[6].

Ceramide (Cer), sphingosine (So or Sph) and sphingosine-1-phosphate (S1P or SoP) are the most explored bioactive compounds. Cer signalling has been connected to a variety of biological effects, including apoptosis, cell growth arrest, cell differentiation and

senescence[7]. So is also involved in non-proliferating cellular processes like cell growth arrest and apoptosis[8–10]. On the contrary S1P can be described as a tumour-promoting lipid involved in the regulation of proliferation, cell growth, survival, migration, and resistance to apoptotic cell death, antagonizing the effects of Cer[11]. As these metabolites are interconvertible, it is not their absolute amount, but rather than their relative levels that determine the cell fate. In this contest ceramide synthase (CerS), ceramidase (CDase) and sphingosine kinase (SK or Sphk) come out as essential regulators of this machinery called "sphingolipid rheostat" (**Figure 1.3**). Moreover dysregulation of SLs metabolism is the origin of human diseases called sphingolipidosis and is also related to other different diseases[12], among them cancer[13,14], inflammation[15] and neurological disorders[16,17].

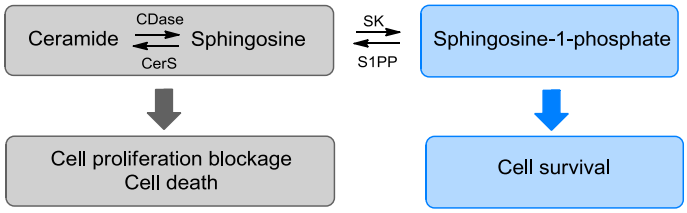

Figure 1.3: Sphingolipid rheostat. Cell fate depends on the equilibrium between bioactive sphingolipids with opposite roles in cell signalling.

1.2. Structure

SLs are characterized by eighteen carbon amino-alcohol backbones: sphingosine has an insaturation at C4, while its two natural analogues, dihydrosphingosine (dhSo; also named sphinganine Sa) and phytosphingosine (PHS), are saturated compounds. Moreover PHS has an additional hydroxyl group in position 4 of the hydrocarbon chain (**Figure 1.4**). So is mainly found in higher eukaryotes (such as humans and animals), PHS is especially detected in lower eukaryotes (such as yeast, fungi, and plants), whereas dhSo exists in both higher and lower eukaryotes [18,19].

Modifications of the backbones give rise to more complex molecules. Phosphorylation of C1 hydroxyl group originates the respective phosphorylated forms of the sphingoid bases, dihydropshingosine-1-phosphate (dhSoP) and S1P. On the other hand, acylation of the sphingoid backbone via an amide bond with fatty acids of variable

length and desaturation generate a diversity of ceramide species. More complex SLs are represented by glycosphingolipids that differ by both the order and type of sugar residues attached to their headgroups. Since these molecules are produced from ceramide precursors, they too may have differences in their acyl chain composition. Sphingomyelin species are also produced from ceramide, however they are defined by a phosphocholine headgroup rather than the addition of sugar residues[20] (**Figure 1.4**).

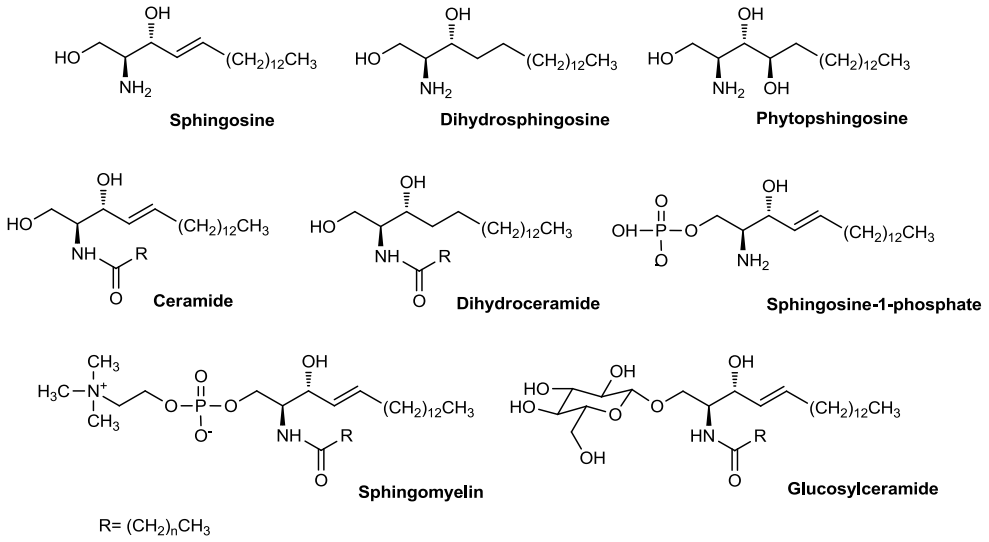

Figure 1.4: SLs structures.

1.3. Sphingolipid metabolism

The central molecule of SL metabolism is Cer, that is mainly synthesized trough the *de novo* pathway from non-sphingolipidic precursors. Two alternative pathways that contribute to Cer production are the sphingomyelin pathway and the salvage pathway (**Figure 1.5**).

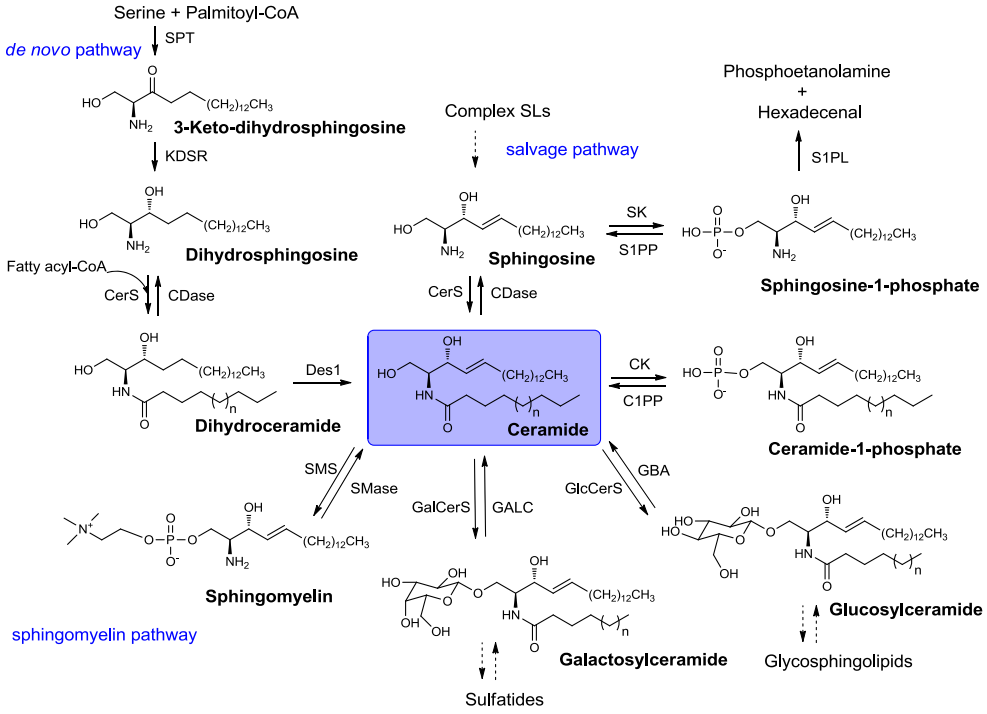

Figure 1.5: Pathways of SLs metabolism. GALC, galactosylceramidase; GlcCerS, glucosylceramide synthase; GBA; glucocerebrosidase; C1PP, ceramide-1-phosphate phosphatase. Other abbreviations are found in the text.

The *de novo* synthesis begins with the condensation of serine and palmitoyl-CoA, catalyzed by serine palmitoyl transferase (SPT) to give 3-keto-dihydrosphingosine. This is reduced to dihydrosphingosine by 3-keto-dihydrosphingosine reductase[21] (KDSR), followed by the acylation of the sphingoid backbone by Cer to produce dihydroceramide (dhCer)[22].

The final reaction is the Δ4-desaturation of dhCer to Cer by dihydroceramide desaturase (Des1)[23]. In the following biosynthetic reactions, Cer is transported to the Golgi apparatus by a non vesicular mechanism[24], and there further metabolized to sphingomyelin with the addition of a phosphocoline headgroup by sphingomyelin synthase (SMS)[25], or converted to ceramide-1-phosphate (C1P) by ceramide kinase (CK or CERK)[26]. Cer can also be converted into glucosylceramide (GlcCer or GluCer), in turn metabolized to GSLs[24]. Galactosylceramide (GalCer) is produced starting from Cer by galactosylceramide synthase (GalCerS), and in turn is used for the synthesis of sulfatidies[27]. Cer can also be metabolized by ceramidases that remove the amide-linked fatty acid to form sphingosine, which is available for recycling into SLs pathway trough the acylation by CerS, or for phosphorilation to S1P by sphingosine kinase[28]. The last and irreversible step of the sphingolipids metabolism is represented by the reaction of sphingosine-1-phosphate lyase (S1PL or SPL) that breakdown S1P to ethanolamine phosphate and hexadecenal[29]. Alternatively S1P can be degraded by sphingosine-1-phosphate phosphatase (S1PP) to sphingosine.

In the sphingomyelin pathway, Cer is produced from the hydrolysis of SM through the action of either acid or neutral sphingomyelinases (aSMases; nSMases) that break down sphingomyelin to produce ceramide and phosphocoline[30]. The last source of Cer is represented by the catabolism of S1P or C1P by phosphatases or the breakdown of complex sphingolipids as GlcCer and GalCer by specific hydrolases in a process referred as salvage pathway[31].

1.4. Compartmentalization and regulation

Enzymatic reactions in SL metabolism take place in different cellular compartments (**Figure 1.6**). *De novo* synthesis of Cer occurs on the cytosolic surface of the endoplasmic reticulum (ER) and potentially in ER-associated membranes, such as the perinuclear membrane and mitochondria-associated membranes[32]. Two specific pathways are known for the transport of Cer from the ER to the Golgi, were SM and GluCer are synthesized. First, SM is formed of Cer provided by the Cer transfer protein, CERT. Second, the synthesis of GluCer is based on Cer deriving from vesicular transport. FAPP2 transport protein mediates a non-vesicular transport of GluCer from *cis*-Golgi, its site of synthesis, to the *trans*-Golgi compartments, where the enzymes for more complex GSLs synthesis are localized[24,33]. The synthesis of complex GSLs (e.g., gangliosides) occurs in

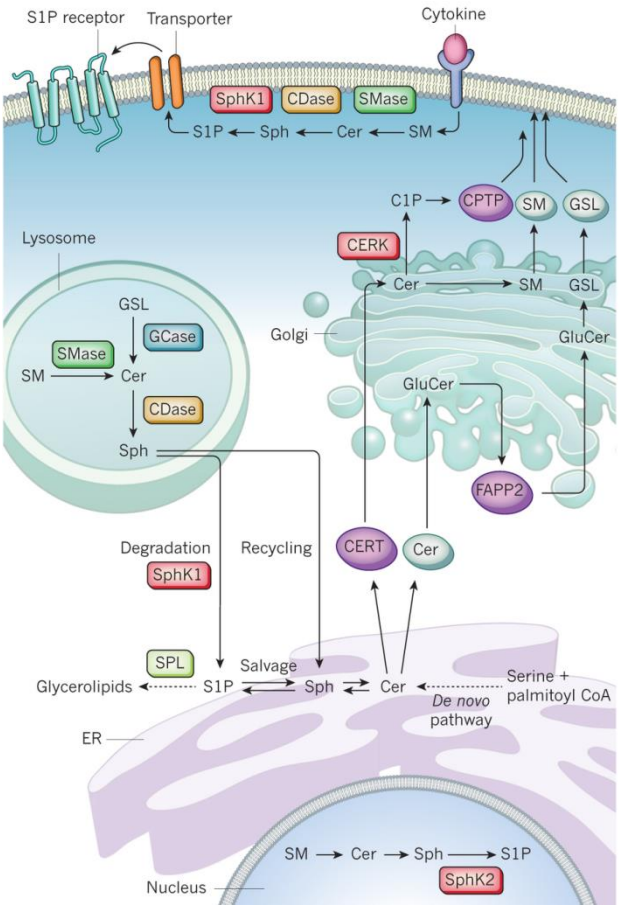

Figure 1.6: Compartmentalization and regulation of SL metabolism. *From Maceyk M. et al., Nature (2014)* [15]

the luminal side of the Golgi. Therefore, GluCer needs to flip from the cytosolic surface to the inside of the Golgi[34]. This mechanism is supported by the ABC transporter, P-glycoprotein[34]. Subsequently, SM and complex GSLs are transported to the plasma membrane via vesicular trafficking; C1P-specific transfer protein (CPTP) is responsible for the transport of C1P. There SMase, CDase and SK produce the bioactive metabolites Cer, So and S1P, respectively. S1P can be transported across the membrane. Membrane sphingolipids are internalized by the endocytic pathway and in the lysosome they are degraded by acidic forms of SMase, glycosidase (GCase) and CDase. Due to its ionizable

positive charge, the salvaged So is able to leave the lysosome and shows adequate solubility in the cytosol to move between membranes, including the ER, where it would be available for recycling[35]. Alternatively So can be metabolized to glycerolipids after phosphorilation by SK and cleavage by S1PL. In the nucleus SK2, a SK isoforms, is responsible for S1P synthesis[36]. Cer synthesis has been reported in mitochondria, that contain CerS[37] and a reverse neutral ceramidase, that been has recently identified as a new source for Cer synthesis[38].

2. Sphingolipid metabolism in cellular responses and diseases

The recent advances in SLs research allowed to better understand their involvement in biological functions and cell homeostasis, as well as their connection with different diseases, particularly with cancer. Some of the most important features of key bioactive sphingolipids and their related metabolic enzymes that were direct object, or related to the present work, will be discussed, pointing out their involvement in physiopathological processes.

2.1. Bioactive sphingolipids

2.1.1. Ceramide

The role of Cer as an essential second messenger in cells has been deeply investigated. Elevation of Cer levels has been associated to apoptotic cell death after a variety of stimuli, including serum deprivation[39], ionizing radiations[40], vitamins[41] and after cell treatment with chemotherapeutic agents such as taxol[42], daunorubicin[43] or cannabinoids[44]. Apoptosis is also stimulated when cells are treated exogenously with short-chain ceramides (D-e-C2-ceramide or D-e-C6-ceramide)[45]. One of the mechanisms by which ceramide regulates apoptosis is via the induction of Fas capping[46]. More recently it was shown that the pro-apoptotic protein Bax is regulated by Cer, leading to mitochondrial outer membrane permeabilization (MOMP or MMP), one of the characterizing events of apoptosis[47]. The anti-proliferative effects of Cer also inhabits in the inhibition of cell growth[48], and stimulation of cell differentiation[49]. Moreover it is involved in cell senescence by inhibiting the mitogenic stimulation[50] or by regulating telomere length[51,52]. Several direct targets of Cer have been identified, including cathepsin D, CAPPs and kinase suppressor of RAS (KSR) that in turn regulates downstream pathways[13]. Protein modulated by these signaling cascade include caspases[53], cyclin-dependen kinases[54] and telomerase[52], that respectively control apoptosis, cell cycle and senescence. Cer has also been shown to induce autophagy by activating different mechanisms such as the up-regulation of the autophagic gene Beclin[55], and the activation of death-inducing mitochondrial protein BNIP3[56]. Low Cer levels have been reported in cancer disease[57,58], in line with the anti-survival effects of the molecule. Moreover different studies show that cancer cells are able to reduce ceramide levels as a survival strategy by overexpressing enzyme from the SLs pathway such as ceramidase[59,60] or sphingosine kinase[61,62].

In the last years improvements in the sphingolipidomic analysis by mass spectrometry[63,64] allowed to identify different ceramide species, thus correlating chain length composition with specific effects and cellular alterations. At cellular level, many studies reported the effect of different ceramides in the balance between cell death and survival. For instance connection between the pro-apoptotic protein Bak and long-chain ceramide induced apoptotic cell death has been reported[65]. In CerS2 knock-out mouse the lack of very-long chain Cer inhibits TNFR1 (tumour necrosis factor-α receptor-1) internalization, impairing downstream signalling for apoptosis [66]. Many studies showed the effect of different ceramides in the balance between cell death and survival. C18-ceramide produced by CerS1 and C16-ceramides produced by CerS5 were shown to have pro-survival and anti-apoptotic role respectively in head and neck squamous cell carcinoma (HNSCC)[67]. In HeLa cells CerS2 overexpression offered partial protection for irradiation-induced apoptosis, while CerS5 overexpression increased apoptosis[68]. Moreover upregulation of CerS2 increases cell proliferation, whereas upregulation of CerS4 and CerS6 causes cell death in both breast and colon cancer[69]. Specific ceramide species have also been connected to cancer progression and treatment. In breast cancer elevation of total ceramides, in particular C16-, C24- and C24:1-ceramides was reported[70]. In HNSCC low levels of C18-ceramide have been reported and their elevation by CerS1 transfection led to cell growth inhibition[71]; in colon cancer cells different sensitivity to TRAIL (tumour necrosis factor–related apoptosis-inducing ligand) induced apoptosis was related to C16-, C18- and C-24 levels[72]. The involvement of specific ceramide species have also been related to other pathologies as multiple sclerosis[73,74] and obesity[75–77].

2.1.2. Dihydroceramide

The role of dihydroceramide in cell biology was recently reviewed[78], pointing out the bioactive function of this sphingolipid that was considered for a long time as an ineffective molecule. Many studies have reported that dhCer inhibits cells cycle. Inhibition of Des1 by genetic ablation or pharmacological tools reduced cell growth provoking cell arrest in G0/G1 by decreasing phosphorylated retinoblastoma protein[79], or by modulating the expression of cyclin D1, delaying G1/S transition[80]. The role of dhCer in apoptosis induction is not so clear as the one of ceramide. Treatment with in vitro exogenous short chain dhCer, conversely to Cer, was unable to induce apoptosis in different cancer cells line[81,82]. Other studies have shown that dhCer induces apoptosis in leukemia cells[83], but to a lesser extent than Cer. Moreover it was recently reported that increased dhCer was

associated with cytotoxic effects of combined temozolomide and SK inhibitory treatment in glioblastoma cells, including apoptosis[84]. Increased levels of dhCer have also been associated to autophagy induction in cancer cells[85]. Interestingly the built up in dhCer generated by Des1 inhibition was able to reduce etoposide cytoxicity in gastric and colon cancer cells[80]. However increase in dhCer levels originating after treatment with the anticancer agent fenretinide (N-(4-hydroxyphenyl)retinamide or 4-HPR)[86] or the antioxidant γ-tocotrienol[87] triggered to cancer cell death, pointing out both the protective and lethal effects of dhCer induced autophagy. Similarly to Cer, also dhCer with different acyl chain length seems to have specific effects. For instance very-long chain dhCers were responsible for cytotoxicity in leukemic cell line[88]. In a different study high levels of C16-, C24- and C24:1-dhCer after celecoxib treatment were related to an anti-proliferative effect in different in cancer cell lines[89]. Elevated dhCer levels were reported in endometrial cancer[90] and might also be induced by hypoxia in tumour cells and *in vivo*[91,92].

2.1.3. Sphingoid bases

Sphingosine was the first species to be identified between sphingolipids and has been described as mediator of cell-growth arrest[10] and apoptosis in many cell types after treatment with dexamethasone[8], doxorubicine[9] or serum deprivation[93]. So has been described as a protein kinase C (PKC) inhibitor both in vitro[94] and in intact cells[95]. Because activation of some PKC isoforms has been implicated in cell proliferation and survival, inhibition of PKC by So may be associated with its inhibitory effects on these processes. In addition So has been shown to inhibit other kinases such the MAPK ERK1/2[96] and protein kinase B (PKB/AKT)[97]. Apart from protein targets, So has been shown to alter the integrity of intracellular membrane systems: it increases the permeability of lysosomes leading to activation of the lysosomal pathway of apoptosis[98] as well as of mitochondria, resulting in the release of cytochrome c, and activation of the intrinsic pathway of apoptosis[9]. Similarly So was shown to mediates tumour necrosis factor-α (TNFα)-induced lysosomal membrane permeabilization in hepatoma cells, leading to apoptotic-like cell death[99]. So has also been described as responsible of Golgi fragmentation, leading to cell-growth arrest, defects in cell adhesion and anoikis, a subtype of programmed cell death[100].

Similarly to So, dihydrosphingosine also mediate cell growth arrest and apoptosis[101,102] when either applied exogenously[103] or endogenously accumulated after CerS inhibition[104]. Moreover the cytotoxic effect of the anticancer agent fenretinide was shown to be connected to dhSo accumulation in different cell lines[86,105]. More recently

increased levels of both dhSo and dhCer have been connected to induction of apoptosis and autophagy by γ-tocotrienol in prostate cancer cell[87].

The role of PHS in mediating various cellular responses such as growth inhibition[106] and activation of protein kinases[107] has been reported in yeast. However different studies show cellular effect of the natural sphingoind base in mammals. For instance addition of exogenous PHS induces the differentiation and growth arrest of epidermal keratinocytes by activating PPAR-γ[108]. PHS also causes apoptosis of Jurkat cells through the mitochondrial pathway[109] and sensitizes the same cell line to TRAIL-induced apoptosis[110], although its role as a second messenger has yet to be clearly defined.

2.1.4. Sphingosine-1-phosphate

An opposite role to the pro-apoptotic function of Cer and So is empowered by the proliferating molecule S1P. It has shown mitogenic properties in various cell types[111–113]. Moreover it has been known for a long time that it is a potent suppressor of apoptosis as demonstrated in different studies in T-cells[114],endothelial cells[115] and mouse fibroblasts[116]. The pro-survival role of S1P is also related to the induction of protective autophagy that allow cells to survive under nutrient starvation[117,118]. Other effects related to S1P signalling are cell adhesion, migration[119,120] and angiogenesis[121,122]. Most of the biological functions exploited by S1P are regulated through the binding to G-protein-coupled receptors family. Five S1P receptors ($S1P_{1-5}$) have been reported until now and they activate downstream signalling pathways, including phosphatidylinositol-3-kinase (PI3K), phospholipase C (PLC), PKC, and extracellular signal regulated kinase (ERK)[123]. Alternatively S1P can act on intracellular targets, including TRAF2 (tumor necrosis factor-α receptor-associated factor 2), which can lead to pro-survival signalling via activation of the transcription factor NF-KB[124]. Considering the effects above described, it is not surprising that S1P is involved in cancer. Indeed, increased levels of the SK1 mRNA transcript and/or protein in different kinds of cancer including stomach, lung, brain, colon and kidney cancer as well as in non-Hodgkins lymphoma and breast cancer have been reported[125]. S1P is also involved in inflammatory conditions[126], such as the autoimmune disease multiple sclerosis.

2.2. Metabolic enzymes

2.2.1. Ceramide synthase

Ceramide synthases are a group of six enzymes that catalyse the formation of dhCer or Cer through the acylation of sphingoid bases, respectively dihydrosphingosine and sphingosine in mammals, with a variety of fatty acyl-coenzyme A (acyl-CoA)[127].

2.2.1.1. Identification and characterization of mammalian CerS

Each of the CerS enzymes is the product of unique genes located on different chromosomes[22]. The first gene responsible for ceramide synthesis was identified as *LAG1* in *Saccharomyces Cerevisiae*[128], that was later described as a longevity assurance gene (LASS), because its deletion promoted longer chronological lifespan in yeast[129]. Several years later, *LAG1* and its homologue *LAC1* were found to be necessary for the synthesis of very long chain ceramides (C26-Cer) in yeast[130]. In 1991, a mammalian gene, upstream of growth and differentiation factor-1 (UOG-1), was discovered[131] and it was able to functionally complement the LAG1 and LAC1 double deletion in yeast[132]. However only in 2002 it was demonstrated that UOG-1 overexpression in mammalian cells resulted in increased ceramide synthesis, leading to the confirmation that this gene codifies for CerS[133]. Moreover the ceramide produced by UOG-1 only contained C18-fatty acid, showing the specificity of the enzyme, now known as CerS1, for stearic acid in ceramide synthesis. Additional mammalian Lag homologues were identified trough bioinformatic analysis[132,134,135]. Moreover the overexpression of two of the sequences, originally characterized as translocating chain-associating membrane protein homologues (TRH) was associated to enrichment in stearic and arachidic acid for THR1 (now called CerS4) in ceramide composition, whereas SLs synthesized by TRH4-overexpressing cells (known as CerS5) were preferentially enriched in palmitic acid[136]. CerS2 sequence was cloned in 2001 as LASS2[137] and subsequently also CerS6[138] and CerS3[139] were identified and cloned as LASS6 and LASS3 respectively.

2.2.1.2. Subcellular localization and tissue distribution

The subcellular localization of the CerS protein is the endoplasmic reticulum (ER)[140], although CerS has been partially purified from a mitochondria-enriched fraction[141].

CerS are integral membrane proteins[142], with their active site probably facing the cytosol[140]. Although the transmembrane topology of the mammalian CerS has not been resolved experimentally, the comparison of several prediction programs to assess the topology was performed by Tidhar *el at*. Most of the programs suggested that CerS have six membrane-spanning domains. However, significant disagreement between the various prediction programs was noted for the fourth putative transmembrane domain, in which the Lag1p motif is located, with some programs suggesting one membrane-spanning domain in this region and others, two[143]. However an odd-number of trans-membrane domains is supported by recent experimental data[144].

Many studies on the tissue distribution of mammalian CerS have shown that each tissue has different profiles of CerS expression and that it can change during development. CerS1 is mainly expressed in brain and at low levels in skeletal muscle and testis[145]. It was also shown that it is upregulated postanatally, which may reflect the synthesis of neuronal plasma membrane[146]. CerS2 is much more widely expressed than CerS1 and two different studies showed that they are abundant in many tissues, mainly kidney and liver[145,147]. CerS3 is found mainly in skin and testis[139], it is highly expressed in keratinocytes and its expression increases during their differentiation[148]. Less information are available about CerS4 that has been found at high levels in skin, leukocytes, heart and liver, however its absolute mRNA expression levels in this tissues are significantly lower than those of other CerS, such as CerS2[145]. CerS5 is the main CerS detected in lung epithelia[149]. In brain CerS5 mRNA is detected in most cells within the gray and white matter[146]. CerS6 shows high homology to CerS5, however much less is known about this isoform. CerS6 is found in different tissues as intestine and kidney[145]. Decreased expression of CerS6, together with CerS2, has been described during mouse brain development, especially in myelin-producing cells[146]. However it has been observed that CerS mRNA expression not always correlate with the sphingolipid acyl chain composition in a particular tissue, suggesting a variety of post-translation and activity regulatory mechanism that regulate CerS, determining the presence of ceramides containing specific acyl chains[145].

2.2.1.3. Structural and functional features

The Tram-Lag-CLN8 (TLC) domain, a region of ~200 residues found in different proteins, is a shared domain between all mammalian CerS[134]. Within this region, the Lag1p motif is a conserved sequence of 52 amino acids[132] considered to be involved in CerS activity, with some conserved residues probably implicated in the catalysis or substrate

binding[134]. Moreover all mammalian CerS, except for CerS1, they have a homobox (Hox)-like domain[135], of which the last 12 residues functionally important for CerS activity since their modification or removal leads to a loss of CerS activity[150]. One of the most notable characteristic of CerS is the ability of the single isoforms to produce ceramides with characteristic acyl-chain distribution. For this each CerS utilizes a restricted subset of fatty acyl-CoA to synthesize Cer with defined acyl chain length (**Figure 2.1**). Recently Tidhar *et al*. showed in a structure activity experiment based on chimeric CerS that a region of 150

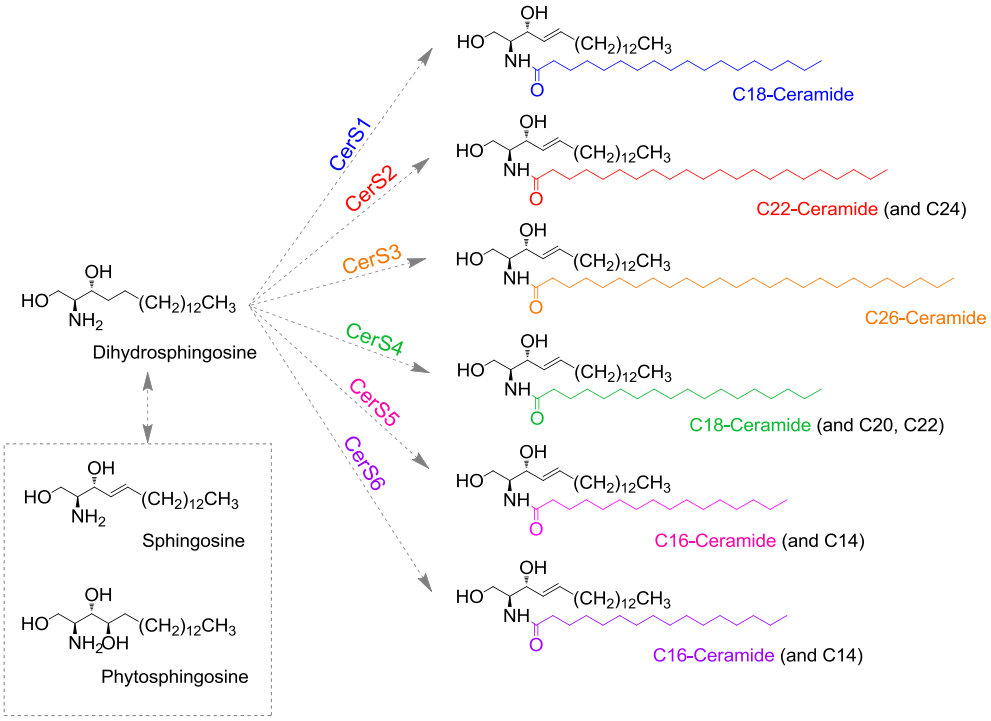

Figure 2.1: CerS specificity. Different CerS isoforms can use a restricted subset of acyl-CoA, producing ceramides with specific fatty acid chain length. Less specificity is shown toward the sphingoid base: ceramide synthesis originates from dihydrosphingosine produced in the *de novo* synthetic pathway of SLs; sphingosine and phytosphingosine represent alternative natural substrates of CerS.

residues within the TLC domain is sufficient for maintaining CerS specificity[143]. Conversely CerS show less specificity towards the sphingoid chain base, since they are able to *N*-acylate a variety of natural long chain bases (dihydrosphingosine, sphinsosine, phytosphingosine)[20] (**Figure 2.1**) as well as their analogues such as Fumonisin B1[151], NBD-sphinganine (NBD-Sa)[152] and FTY720[153].

2.2.1.4. Biological functions and involvement in disease

CerS is involved in the physiological regulation of the *de novo* synthesis of sphingolipids, with the acylation of dihydrosphingosine, as well as in the recycling of sphingosine originating from the breakdown of complex sphingolipids[127]. Thus CerS role in physiological and pathological processes is strictly related to the biological effects of the molecules that are regulated by this enzyme. Since (dihydro)ceramides and their precursors dhSo and So has been shown to have an important role as signal molecules in different processes, including cell growth, apoptosis and to be involved in different diseases as described above, the modulation of CerS activity might have cellular effects triggered by those molecules.

Although the direct involvement of CerS in pathological processes is not completely understood, some examples of CerS genetic alteration suggest their implication in human diseases. A genetic association study of rhegmatogenous retinal detachment, an important cause of vision loss, recently showed an association with a missense coding single-nucleotide polymorphism located within CerS2 gene[154]. Since the blockade of ceramides synthesis already showed to have a protective effect in a retinitis pigmentosa mouse model[155] and light-induced degeneration of retina[156], it is reasonable to consider the involvement of very-long chain ceramides, or their corresponding metabolites, in retina disorders. Moreover genetic mutations in CerS3 gene have been recently related to a disturb in keratinisation, named ichthyoses, showing the importance of very long ceramides in the formation and function of human epidermis[157,158].

Other information on CerS biology come from the generation of CerS null mice. The characteristics of this animal models, the alteration in SLs composition and the associated phenotype have been reviewed by Park *et al.*[159]. The measurement of ceramides levels shows generally that the decrease in ceramide with a specific acyl chain length, due to the depletion of the corresponding CerS isoforms, is related to elevated levels of a different ceramide specie. Nevertheless in most of the cases this replacements does not avoid mice phenotype to display several alterations, pointing out the relevance of

different ceramide species in cell functions. More recently a CerS4 deficient mouse has been generated[160], with decrease in C18- and C20-ceramides, higher levels of very long-chain ceramides and age dependent hair loss. In agreement the same phenotype was reported in a different work that showed the crucial role of CerS4 in epidermal stem/progenitor cell homeostasis and hair follicle cycling regulation[161].

2.2.1.5. CerS inhibitors

Although in the last years the knowledge about CerS specificity and the distinct role of ceramides with different acyl chain has highly increased, the CerS inhibitors that are now available show no specificity towards the different isoforms of the enzymes.

Fumonisin B1 (FB1) (**Figure 2.2**) is the most used and characterized CerS inhibitor and belongs to a family of toxins of fungal origin (*Fusarium verticilloides*) that are found as food contaminants in cereals, causing a variety of diseases in humans and animals[162–164]. FB1 is responsible for the dysregulation of the sphingolipid metabolism, representing a possible explanation to fumonisins toxic effect[165,166]. It has been shown to inhibit CerS via competitive-like inhibition towards both dihydrosphingosine and acyl-CoA[167], with an IC_{50} value of ~100 nM[168], causing a bulk accumulation of dihydrosphingosine and, to a lesser extent, sphingosine. Cell cycle arrest[169] and apoptosis[104,170,171] have been shown in different cells lines after FB1 treatment and correlated to the elevation in sphingoid bases. Other effects of FB1 on the sphingolipid metabolism include the increase of sphingosine-1-phosphate[172] and dyhydrosphingosine-1-phosphate[166] and in turn, of fatty aldehyde and ethanolamine phosphate[165], as well as the depletion of complex sphingolipids[167].

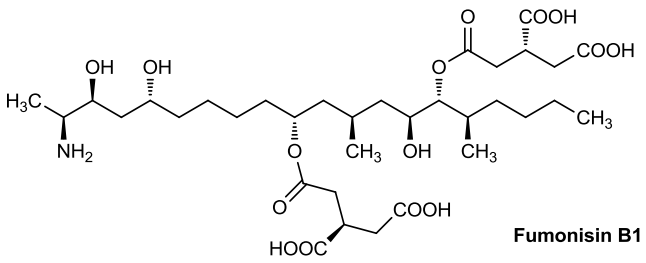

Figure 2.2: Structure of Fumonisin B1

Other CerS inhibitors are represented by alternaria aleternate toxin (AAT) and australifungin, both originating from fungi. AAT is structural related to fumonisins and causes the accumulation of sphingoid bases[173], while australiafungin[174] is an antifungal compound with different structural features from sphingolipids**.** Another molecules that show inhibitory activity towards CerS is FTY720, a sphingoid base-like compound that also acts as an agonist of S1P receptors[175].

2.2.2. Ceramidases

Ceramidases (CDases) are amidohydrolases that break down ceramides to form sphingosine and fatty acids. Five human ceramidases encoded by five distinct genes have been reported. They differ for the subcellular localization and they have been grouped as acid ceramidase (AC), neutral ceramidase (NC) or alkaline ceramidase (ACER), depending on the optimum pH of their ceramidase activity (**Table 2.1**)[176]. AC catabolizes ceramide in lysosomes and is found only in vertebrates. In contrast NC and ACER have a broader distribution, and can be found in different species ranging from lower eukaryotes to mammals. However, only NC[177] is found in prokaryotes, including some pathogenic bacteria. A reverse activity has also been described for most of CDases[178,179], with that for AC showing a pH optimum slightly less acidic (pH 5.5) than that of the forward reaction[180]. The reverse activity of ceramidases uses a free fatty acid as a substrate, while CerS uses acyl-CoAs as substrates.

Table 2.1 Ceramidases

Enzyme	Gene	pH optimal	Subcelular localization
Acid ceramidase (AC)	*ASAH1*	4.5	Lysosome
Neutral ceramidase (NC)	*ASAH2*	7.6	Plasma Membrane, mitochondria, secreted
Alkaline ceramidase 1 (ACER1)	*ASAH3*	8.5	Endoplasmic reticulum
Alkaline ceramidase 2 (ACER2)	*ASAH3L*	7-9	Golgi apparatus
Alkaline ceramidase 3 (ACER3)	*PHCA*	9.5	Endoplasmic reticulum, Golgi apparatus

2.2.2.1. Acid ceramidase

Acid ceramidase activity was first described by Gatt in 1963[181]. The protein was purified from human urine in early 1990s[182], and its cDNA was cloned few years later[183]. Although AC has been localized mainly in lysosomes, a portion of the enzyme is secreted to the medium as a 47 kDa monomer[182]. Substrate specificity studies suggest that ceramides with medium acyl chain are better hydrolyzed by AC than short chain (≤ C6) or long chain (≥ C16). Optimun pH is 4.5 and no cations are required for its activity[176]. Structurally AC is a heterodimeric glycoprotein derived from a single enzymatically inactive precursor. Biosynthesis starts with the production of a ~53–55 kDa precursor, which is processed into a mature heterodimeric enzyme composed of an α (13 kDa) and a β subunit (40 kDa)[184]. Proteolytic processing of the precursor occurs in either late endosomal and/or lysosomal compartment[185] and it is most likely an autoproteolytic event with Cys143, Arg159 and Asp162 as a functional triad to form the two subunits[186]. The acid ceramidase amino acid sequence reveals high homology with the *N*-terminal nucleophile (Ntm) hydrolase family[187], a superfamily of enzymes that hydrolyze a varietry of substrates with the common feature of having a *N*-terminal nucleophile. In acid ceramidase it is represented by the nucleophilic thiol in the cysteine residue (Cys 143) that is exposed at the *N*-terminus of the β subunit after cleavage of the precursor protein[186]. Complete deglycosylation of AC reduces the apparent molecular weight of the β subunit to 28 kDa, but does not alter the α subunit[182] suggesting that the β subunit is highly glycosylated. Of six individual potential *N*-glycosylation sites, five of them are used[188], and some of them are required for correct lysosomal processing or enzymatic activity, and for the formation of the heterodimeric enzyme[185].

Increasing evidence points to important role of AC in cancer outcome, progression and resistance to therapy. The enzyme is overexpressed in several cancer cell lines like prostate cancer[59,189], head and neck cancer[190], and melanoma[191]. In addition overexpression of AC has been shown to suppress apoptotic cell death induced by TNFα[192] and radiation[193]. This made AC an interesting target for anticancer drugs development because the inhibition of its activity leads to the accumulation of pro-apoptotic ceramide and cell death. Consistent with the notion that AC has a protective role in survival, it was found that AC knockout in mouse lead to embryos death at a very early stage, that was delayed buy the addition of exogenous S1P[194].

The significance of AC in mammalian system is reinforced by its role in human lipid storage disease (LSD) Farber lipogranulomatosis, first described in 1957 by Sidney Farber[195]. It is an autosomal-recessively lysosomal storage disease due to a dysfunctional

AC gene product. That results in the accumulation of ceramide in lysosomes, leading to different phenotypes including deformed joints and subcutaneous nodules, with neurological involvement and a shortened lifespan[196].

AC has been implicated in other metabolic complications; for example was shown to have a role in preventing type 2 diabetes and modulating insulin signalling[197]. In 2004 it was also reported that AC might play a role in controlling neuronal apoptosis and that AC-mediated signalling pathways might be involved in the molecular mechanism of Alzheimer's disease[198].

2.2.2.2. Neutral ceramidase

Neutral ceramidase (NC) is encoded by *ASAH2* gene. Its activity was described first in 1969 in human intestine with an optimal pH of 7.6[199]. This data was confirmed by using NC purified from mouse liver, however the pH range was shown to be quite broad[178]. NC has been cloned first from the bacteria *Pseudomona aeruginosa*[200] then in humans[201] and in many other different specie[202]. No cations are required to activate NC, even if enzymatic activity was enhanced by Na^+ and Ca^{2+}. Mg^{2+} and Mn^{2+} were somewhat stimulatory, but Zn^{2+}, Cu^{2+} and Fe^{2+} inhibited the enzyme[203]. The substrate specificity of human NC has not been established, however it was reported that in mouse the enzyme prefers long-chain ceramides[176].

NC localization varies in different organisms: it can be secreted or localized at the plasma membrane[177,204] as a type II integral membrane protein[205]. The presence of a serine/threonine/proline-rich domain named mucin box (that is present just in vertebrates) in the *N*-terminal region is the responsible for NC presence in the plasma membrane[177]. In addition, NC has also been localized in endosome-like structures[206], and in mitochondria in MCF-7 and HEK293 cells[201]. NC was also found to be secreted into the intestine lumen for SL digestion, being resistant to pancreatic proteases[207]. Northern blotting analysis revealed that NC is expressed ubiquitously[201], but highly expressed in kidney, liver, heart [208] and intestine[209].

The comparison of enzymatic sequences from different species to investigate NC catalytic mechanism, find out a motif comprised of six amino acids core (GDVSPN) with the serine residue (Ser 354) as possible responsible for the nucleophile attack to the amide bond of ceramide[203]. More recently the crystal structures of neutral ceramidase from *Pseudomonas aeruginosa* (pCDase) was determined, suggesting that cleavage of the *N*-acyl linkage of Cer by NC proceeds by a mechanism similar to that described for zinc-

dependent carboxylpeptidase. Moreover authors indicated that the hexapeptide may be integral for the Zn^{+2} dependent catalytic mechanism of the enzyme[210].

ASAH2 null mice showed a significantly increased C16:0 ceramide content but a reduced sphingosine content in the intestine and the inability to metabolize dietary ceramides. Due to an absence of visible pathology in the *ASAH2* null mice, it is unclear what role NC plays in non-intestinal tissues, if any[211]. As a key regulator of the S1P-Cer balance with the other ceramidase, NC has been described as an essential component of an innate detoxifying mechanism to prevent ceramide-induced apoptosis[209]. Moreover it has been reported that cytokines such as TNFα and interferon-γ increased activity, mRNA and NC protein synthesis, where this elevation was shown to protect cells from cytokine-induced cell death[212]. Moreover a protective role of NC was reported in inflammation in a mouse model of bowel inflammatory disease[213].

2.2.2.3. Alkaline ceramidases

Three human alkaine ceramidases (ACER) have been described: ACER1; ACER2 and ACER3, which contain 264[214], 275[215] and 267[216] amino acids, respectively, with a similar molecular weight around 31 kDa. All of them present multiple transmembrane domains and their activities are enhanced by Ca^{2+}[176]. Alkaline ceramidase belong to a superfamily of putative transmembrane hydrolases called CREST (alkaline ceramidase, PAQR receptor, Per1, SID-1 and TMEM8), that shares three conserved sequence motifs with semi-invariant residues[217]. Alkalyne ceramidase activity is the only ceramidase activity found in erythrocytes. Recently, plasma S1P has been reported to derive from So generated from ACER activity in that cells. Furthermore, ACER has also been shown to be important for erythroid differentiation in an erythroblastic leukemia cell line[218].

ACER1 is localized in the ER, has a pH optimum of 8.5 and preferentially hydrolyze ceramides with very long-chain unsaturated fatty acid. It fails to hydrolyse any dihydroceramides or phytoceramides. This enzyme is mainly expressed in the epidermal keratinocyte. It has been reported that ACER1, together with AC, is upregulated in this cells in response to increasing concentration of Ca^{2+} in the tissue culture medium and in turn induced differentiation of human keratinocytes, probably with the involvement of changes in So and S1P levels[214].

ACER2 is localized in the Golgi apparatus and is highly expressed in the placenta and modestly expressed in many other tissues[215]. It has a high degree of similarity in protein sequence to ACER1. This enzyme catalyze the reaction in a rage of pH between 7-9

and prefers long chain or very long chain ceramides like D-e-C_{16}-ceramide and D-e-C_{20}-ceramide over dihydroceramides or phytoceramides as substrate, while has no activity toward dihydroceramide and phytoceramide with saturated fatty acids[176]. ACER2 has been show to have a double role in cell destiny depending on a balance between So and S1P: high ectopic expression of ACER2 causes growth arrest of HeLa cells by generating high levels of So, whereas low ectopic expression of ACER2 promotes the proliferation of HeLa cells in serum-free medium by elevating S1P and activating S1P/S1PR1 pathway, without accumulating cytotoxic levels of So. Moreover ACER2 expression is upregulated in HeLa cells in response to serum deprivation, and knockdown of ACER2 inhibits the serum-independent proliferation of HeLa cells and causes apoptosis of cells in serum-free medium, suggesting that ACER2 upregulation has a protective role in cell survival against serum-deprivation[215]. ACER2 activity and mRNA has been shown to increase after treatment with the dihydroceramide desaturase inhibitor N-(4-hydroxyphenyl)retinamide (4-HPR). Moreover over-expression of ACER2 enhanced 4-HPR-induced DhSo formation and cell death, suggesting that ACER2 also regulates the levels of dihdyrosphingosine by controling the hydrolysis of certain dihydroceramides with unsaturated acyl chains[105]. Moreover ACER2 has been shown to be upregulated in tumours, and its upregulation promotes tumour cell proliferation and survival likely through increasing the generation of S1P and activating the S1P receptor S1P1[202].

ACER3 was the first human alkaline ceramidase to be cloned and was originally called alkaline phytoceramidase because it was able to hydrolyzes phytoceramide selectively. It has a pH optimum of 9.5, is activated by Ca^{2+}, but is inhibited by Zn^{2+} and sphingosine. ACER3 is localized in both ER and Golgi apparatus, and is highly expressed in most tissues, especially in the placenta. It shows a specifity for unsaturated long–chain ceramides, dihydroceramides and phytoceramides as substrate. ACER3 prefers unsaturated long–chain ceramides, minor ceramide species in mammalian cells and tissues, so ACER3 knockdown results in an increase in the levels of unsaturated long-chain ceramides (D-e-C18:1- ceramide and D-e-C20:1-ceramide) in tumour cells. Interestingly, ACER3 down-regulation decreases the levels of other ceramide species while increasing the levels of both So and S1P by increasing the expression of ACER2, which hydrolyses most mammalian ceramide species[216]. ACER3 knockdown inhibited cell proliferation by up-regulation of the cyclin-dependent kinase inhibitor, but also inhibited serum-deprivation induced apoptosis[219].

2.2.2.4. Chemical tools for ceramidases investigation

The interest on ceramidases in cell biology prompt the development of different substrates that allow the measurement of CDase enzymatic activity. Radioactively labelled ceramides[220,221] with ^{14}C or ^{3}H and fluorescent NBD-labelled ceramides[222] represent some of the most used substrates. Alternatively fluorescent BODIPY-ceramides have been employed[221]. A quenched fluorescent ceramide analogue that becomes fluorescent upon hydrolysis of its *N*-acyl bond was reported for bacterial ceramidase activity determination[223]. Bedia *et al.*[224,225] developed in our group coumarinic *N*-acylaminiodiols named RBM14 that are suitable for high throughput screening of ceramidases. Particularly RBM14C12 was shown to be highly hydrolyzed by AC, thus representing a eligible system in Farber disease diagnosis[225]. More recently alternative ceramide derivatives labelled with the lipophilic-dye Nile Red (NR) instead of NBD have been synthesized as substrates for acid and neutral ceramidases[226]. Moreover the same group developed two novel NR-NBD doubly labelled fluorescent ceramide analogues that exhibit significant FRET and are suitable for determination of enzyme activity in real-time[227].

Progresses in understanding ceramidases role in different systems are related to the use of enzymatic inhibitors. Among the most used molecules, B-13 and *N*-oleoylethanolamine (NOE) specifically inhibit AC, while D-erythro-N-myristoyl-2-amino-1-phenyl-1-propanol (D-*e*-MAPP) inhibits both NC and ACER. Camacho *et at.*[228] recently reported the development of ceramide analogues as AC inhibitors, showing the potential therapeutic of two α-bromoamides in metastatic prostate cancer cells.

2.2.3. Dihydroceramide desaturase

Dihydroceramide desaturase is responsible for inserting the 4,5-*trans*-double bond into the sphingoid backbone after the *de novo* synthesis of dhCer and it is crucial in the regulation of the balance between sphingolipids and dihydroshingolipids.

2.2.3.1. Identification and characterization of Des1

The *DES1* gene was first cloned in 1996 in *Drosophila melanogaster* as *DESG1* (Drosophila degenerative spermatocyte 1) while investigating the role of the gene in the

initiation of meiosis during spermatogenesis[229]. Soon after a second a orthologue of this gene was found in mice[230]. Finally, Cadena *et al.* demonstrated that Degs1 was a membrane desaturase, localized to the ER membrane, where it has access to newly synthesized dihydroceramide species[231]. The involvement of a desaturase in the last step of the *de novo* pathway of ceramide was reported for the first time in *in vitro* studies by using dihydroceramide analogues[232–234], by observing the desaturation reaction needed NADPH[232] or NADH[233] as electron donor and oxygen as electron acceptor. Since other well-know desaturases are characterized by intermediaries that are involved in a series of coupled reactions that transport electrons from NAD(P)H to a terminal desaturase that reduces oxygen, the same complex was hypothesized for Des1. This assumption was subsequently confirmed by using specific inhibitors[232] or antibodies[233] for the postulated intermediaries, suggesting the involvement of a flavoprotein, the cytochomre b5 and the presence of a non-haem iron in the catalytic complex. According to these results, a model was postulated in which dihydroceramide desaturase was regarded as a part of a larger enzymatic complex[232] (**Figure 2.3**). More recently, Enomoto *et al.*[235] further developed this idea and proposed a similar mechanism of action with the involvement of a NADH-cytochrome b5 reductase in regards of the homologue, Des2.

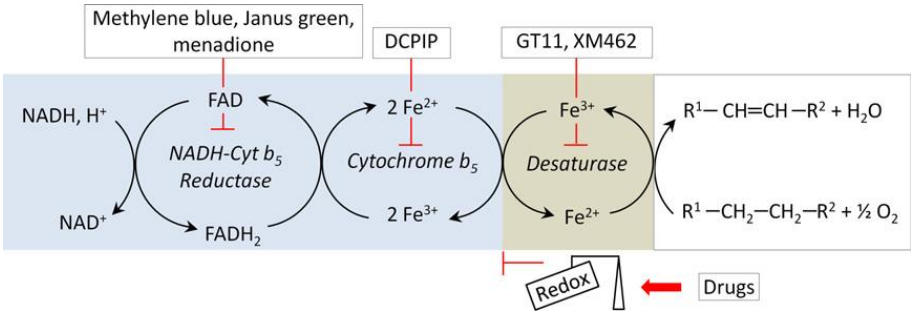

Figure 2.3 Des1 enzyme complex and inhibition. Methylene blue, Janus green and menadione were used as inhibitors to consider the involvement of a flavoprotein, while 2,6-dichlorophenolindophenol (DCPIP) suggested the presence of cytochrome b_5 in the complex. Desaturase inhibitors include different drugs that alter the redox potential in the cell; GT11 and XM462 are active site directed inhibitors. From *Fabrias et al., Progress in lipid research, (2012)*[236].

2.2.3.2. Structural and functional features

In a study based on bioinformatic approaches, Ternes *et al.*[237] found that several putative Des1 sequences share highly-conserved histidine motifs essential for catalytic activity: $HX_{(3-4)}H$, $HX_{(2-3)}HH$, and $H/QX_{(2-3)}HH$. These histidine boxes are also present in membrane fatty acid desaturases and membrane hydrocarbon hydroxylases[238]. Mizutani *et al.*[239] reported that both murine and human Des2 have an additional histidine motif (HX2–3HH) near the C-terminus. The alignment of Des1 protein from different species confirmed the presence of conserved His boxes that were represented as predicted transmembrane domains, together with iron bind histidine boxes and glycine myristoilation site[236](**Figure 2.4**). Myristoylation has shown to be necessary for the enzymatic activity[240]; moreover it has also reported that this modification alters Des1 subcellular localization, targeting the enzyme to the mitochondria, wherein causes an increase in Cer levels that in turn leads to apoptosis.

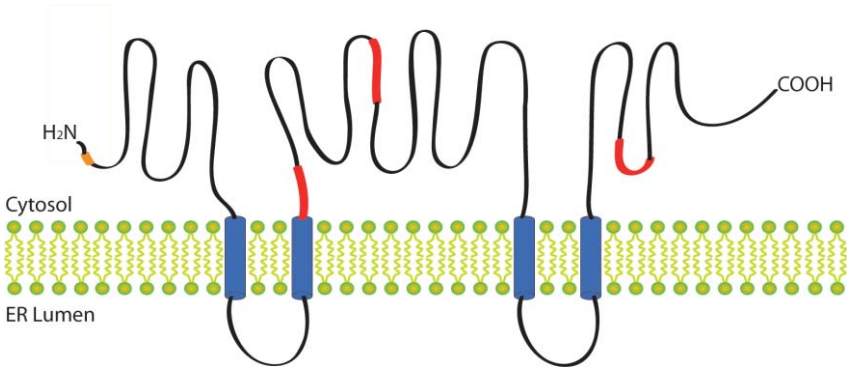

Figure 2.4: Schematic representation of human Des1. The four transmembrane domains (blue), the iron binding histidine boxes (red) and the glycine myristoylation site (orange) are illustrated. From Fabrias *et al*. *Progress in lipid research, (2012)*[236].

In terms of function, Des1 exhibits high dihydroceramide Δ4-desaturase and very low C-4 hydroxylase activities, whereas Des2, exhibits bifunctional sphingolipid C-4 hydroxylase and Δ4-desaturase activities[237]. Moreover human Des2 is capable of creating either phytoceramide or ceramide from dihydroceramide precursors[239]. Therefore, it is not surprising that Des2 is highly expressed in the intestines, kidneys, and skin where phytoceramides are present in high abundance[239,241].

Des1 activity is largely affected by the stereochemistry of the sphinganine moiety of the substrate: desaturation of the D-*erythro*-isomer is much higher than that of the L or D-*threo*-isomers. Other factors that influence the enzymatic activity are the length of the alkyl chains of the amide-linked fatty acid; for instance *in vitro* activity in rat liver microsomes decreases when the length of the chain is increased[233]. However in fetal rat skin and liver homogenates, C18/C14-Cer is a better substrate for desaturation than the dhCer analogues containing fatty acids with 18, 10, 6, or 2 carbon atoms[234]. The enzyme shows activity against dihydrosphingomyelin, whereas dhSo and glucosyldihydroceramide are not desaturated at all[236]. The enzyme is active over a broad pH range (6.5-9), being optimal around 8.5[232]. Dithiothreitol (DDT) strongly inhibits its activity, probably because it interferes with disulfide bonds that form impairing protein stability and catalytic activity[233].

2.2.3.3. Biological relevance of Des1

The production of Des1 homozygous (*Des1*$^{-/-}$) and heterozygous (*Des1*$^{+/-}$) describe both phenotype for *Des1* mutants. *Des1*$^{-/-}$ mice revealed an incompletely penetrant lethality. Surviving animals were small in size, showed abnormalities in skin and hair, tremors, and numerous blood chemistry and hematological alterations. The homozygous null mice were also characterized by signs of growth retardation and exhibited abnormal liver function. Moreover the study demonstrated that *Des1*$^{+/-}$ mice were refractory to dexamethasone-induced insulin resistance, revealing an important role of Cer in this process[242]. In a different study on metabolic diseases the ablation of *Des1* in mouse embryonic fibroblasts showed a marked increase in Akt/PKB signaling, anabolism, and protection from starvation-induced apoptosis[243], confirming that Des1 might represent a target in this kind of pathologies.

The increasing relevance of dhCer and its related metabolites in cellular response as apoptosis and autophagy, as well as in cancer onset and progression (see paragraph 2.1) point out the key function of Des1 as a regulatory enzyme in cancer diseases, encouraging the identification of molecular tools to better understand its role in the mentioned processes.

2.2.3.4. Des1 inhibitors

Several drugs have been reported to inhibit Des1 activity. A first group of compounds that repress Des1 activity includes the natural compound resveratrol (**Figure 2.5**)[85,244], a polyphenol with antioxidant properties. Other compounds are represented by curcumin, Δ^9-tetrahydrocannabinol, and celecoxib[236]. These aromatic compounds, structurally unrelated to (dh)Cer may act indirectly on Des1 activity by disturbing the redox status of the cell (**Figure 2.3**). Indeed, a specific study demonstrated that Des1 activity can be modulated by oxidative stress[245]. Also fenretinide has been extensively reported as Des1 inhibitor as reported by Rodriguez-Cuenca *et al*.[78]. Curiously it has been described as a competitive inhibitor at short incubation times and an irreversible inhibitor at longer incubation times[246]. Nevertheless, since the experiments were conducted with the entire desaturase complex, the possibility that fenretinide is not acting directly on the terminal desaturase cannot be completely ruled out.

The first rationally designed inhibitors of Des1 is compound GT11[247]. It is a cyclopropenylceramide that carries out a competitive inhibition[248] against the substrate and it is active both in vitro and in intact cells[249]. This opened up the possibility of selective disturbance of Des1, as shown by a second dhCer-related molecule named XM462 (**Figure 2.5**), that also inhibited Des1 both in vitro in rat liver microsomes and in Jurkat cells[250].

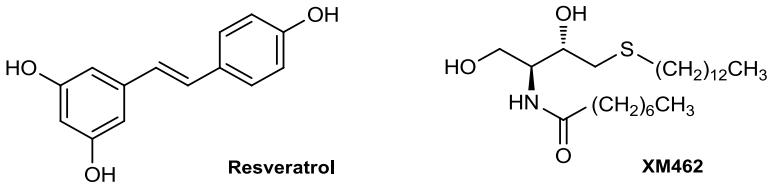

Figure 2.5: Des1 inhibitors. An example of aromatic inhibitor (Resveratrol) and a specific inhibitor (XM462).

2.2.4. Sphingosine kinase

Sphingosine kinase is a central enzyme of the sphingolipid metabolism, being the responsible for the conversion of proapoptotic sphingosine and ceramide to the mitogenic S1P.

2.2.4.1. Identification and characterization of SK

Humans express two SK genes, resulting in the formation of SK1 (or Sphk1) and SK2 (or Sphk2) proteins, each with a number of splice isoforms (a, b and c for SK1; a and b for SK2). The first cloning of mammalian SK1 was reported by Kohama *et al.*[251] and few years later SK2 isoform was also cloned in human and mouse[252]. Although SK1 and SK2 differ in size, they share high degree of polypeptide sequence similarity, with almost all of the SK1 polypeptide sequence aligning with regions of the larger SK2. Moreover five highly conserved regions called C1-C5 are shared by the two isoforms[124]. Both SK1 and SK2 can utilize D-*erythro*-sphingosine and D-*erythro*-dihydrosphingosine as substrates; however SK2 can phosphorylate a larger pool of substrates, between them phytosphingosine and the SK1 inhibitor D,L-*threo*- dihydrosphingosine, suggesting that the two isoforms differ in the conformation of the substrate binding pocket[253] .

Recently the crystal structures of human SK1 in the apo form was resolved, revealing a two-domain architecture in which the catalytic site is located between the two domains and a hydrophobic lipid-binding pocket is buried in the C-terminal domain[254]. Although crystal structure for SK2 is not currently available, it appears that a proline-rich region, not found in SK1, can be part of the sphingosine binding region of the enzyme[124].

While the activity of both SK isoforms can be enhanced by various cytokines and growth factors, both enzymes also possess intrinsic catalytic activity that has been proposed to equilibrate sphingosine and ceramide levels in absence of agonist stimulation. Moreover enzymatic SK1 and SK2 activation can occur via phosphorylation by ERK1/2[253]. SK1 activity is also regulated by proteolysis; for instance cathepsin B has been implicated in regulating lysosomal degradation of SK1 in podocytes[255]. The ubiquitin-proteosomal pathway has also been reported as a degradation system of SK1 in LNCaP prostate cancer and MCF-7 breast cancer cells[256].

SK1 and SK2 have different developmental expression, tissue distribution and subcellular localization patterns[257], suggesting that the two enzymes might have distinct physiological functions. SK1 appears to reside predominantly in the cytosol and undergoes

translocation to the plasma membrane after ERK phosphorylation[258]. To the contrary SK2 is more likely localized in the endoplasmic reticulum, nucleus and mitochondria[259]. The different localization appears to be connected with the different role of SK1 and SK2 in cell functions. It is well established that SK1 relocation to the plasma membrane is necessary to mediate pro-survival and oncogenic signalling[260]. By comparison SK2 subcellular localization reflects its complex and wide functions. For instance nuclear SK2 has been connected with DNA synthesis inhibition[261], while mitochondrial localization has been shown to promote apoptosis[262].

2.2.4.2. SK1 and SK2 functions and involvement in disease

SK1 has been described as a pro-survival and pro-proliferative enzyme[263]. Moreover there is evidence of a major role for SK1 in cancer development[264]. For instance, there is elevated *SK1* mRNA transcript and/or SK1 protein expression in stomach, lung, brain, colon, kidney and breast cancer and non-Hodgkin lymphoma[125]. High tumour expression of SK1 is also correlated with poor patient survival rates, angiogenesis and radiation or chemotherapy resistance[265–267]. Moreover SK1 appears to play a role in enhanced proliferation and metastasis, two major hallmarks of cancer progression[125,268]. A growing body of evidence show that SK1 suppress apoptosis, by altering the cellular ceramide:S1P ratio, leading to uncontrolled cell growth and chemotherapy resistance[267].

SK2 has not been as well characterized as SK1. Different studies carried out to understand its role in cellular processes have given contradictory results, making difficult to draw up a defined profile of SK2 in physiological and pathological processes. Early studies on SK2 function found that its overexpression induced cell cycle arrest and apoptosis[124], suggesting an opposite role to the pro-proliferative signalling of SK1. The interaction of the SK2 putative BH3 domain with Bcl-x_L[269], as well as BID-mediated activation of BAK[262] appear to be responsible for apoptosis activation. A part from the overexpression studies, also the endogenous SK2 has been confirmed as a pro-apoptotic stimuli as showed in SK2 knock-out mice[270]. Despite the described role of SK2 in mediating apoptotic stimuli and growth arrest, there are now many studies supporting an opposite role in promoting survival and proliferation, much like SK1. For instance inhibition of SK2 has been shown to sensitize cells to apoptotic stimuli[271]; similarly SK2 ablation by siRNA prevents tumour cell proliferation and migration[272]. Moreover a number of studies *in vivo* have reported that tumour growth can be attenuated by the genetic ablation of SK2 in

MCF-7 breast tumour xenografts[273] or the pharmacological inhibition of SK2 in a range of mouse tumour models[274,275].

Both SK1 and SK2 are shown to be involved in inflammation. Many studies agree on the SK1 role in promoting/enhancing inflammation, regulating monocyte, macrophages and neutrophil function during the inflammatory response[276]. Conversely the role of SK2 in the inflammatory response is controversial, with many of the studies suggesting that SK2 can be anti-inflammatory as indicated by increased levels of pro-inflammatory cytokines and decreased levels of anti-inflammatory IL-10 in a breast cancer xenograft model lacking SK2[273]. In contrast pharmacological inhibition of SK2 demonstrated anti-inflammatory effects in Crohn's disease[277] and in rodent models of inflammatory arthritis[278], suggesting that SK2 can promote inflammation.

Knockout studies showed that mice lacking either SK1 or SK2 are viable and fertile while deletion of both isoforms is lethal to the embryo, which exhibits severe defects in angiogenesis and neurogenesis[279]. These findings suggest that, despite their different role in cell biology, SK1 and SK2 appear to have at least some functional redundancy.

2.2.4.3. SK inhibitors

Due to SKs multiples roles in controlling cell fate, they became attractive targets in the development of cancer therapeutics. The first known SK inhibitors were long chain base analogues such as *N,N*-dimethyl-D-*erythro*-sphingosine (DMS)[280] that inhibits both SK isoforms, and L-*threo*-dihydrosphingosine (safingol)[281]. This is a competitive inhibitor of SK1 but, unlike DMS, it is a substrate of SK2; another SK inhibitor that exhibit the same behaviour is FTY720[282].

Since the mentioned compounds can also inhibit other kinases, more specific compounds for SK inhibition were developed. Between them one of the most widely used is the 2-(*p*-hydroxyanilino)-4-(*p*-chlorophenyl) thiazole known as SKI II (**Figure 2.6**), a polyaromatic molecule isolated from a library of synthetic compounds by French *et a.* in 2003[283]. It is a dual SK1 and SK2 inhibitor but does not show any activity against other human kinases as ERK2, PKC-α and PI3K. It is a not competitive inhibitor of the ATP-binding site of SK; inhibition experiments in recombinant human SK showed a IC_{50} of 0.5 μM. Moreover SKI II exhibits anti-proliferative activity on several human cancer cell lines with IC_{50} values in the low μM range (0.9-4.6 μM).

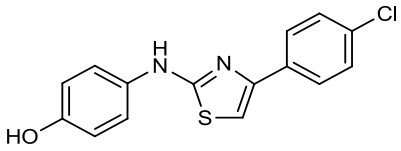

SKI II

Figure 2.6: Structure of SKI II inhibitor

Selective SK1 inhibitors include SK1-I[284] and SKI 178[285] and the most recently introduced PF-543[286]. In the last years also SK2 specific inhibitors, such ABC294640[287] have been described, making easier the study of this isoform in physiological processes and disease.

In light of the crucial role of sphingolipids in physiological processes and in different kind of diseases, it comes out how the introduction of new chemical tolls might be helpful for further investigation in this field. In particular the study and the modulation of the enzymes that regulate the biological balance between bioactive molecules is a promising strategy to deeply understand the involvement of SLs in different physiophatological processes and to find new therapies.

3. Natural sphingolipids

SLs are present not only in mammals but also in other organisms, both from the prokaryote and the eukaryote kingdoms[288]. The multiplicity of biosynthetic pathways implicated in the different organisms is responsible for the structural diversity found among the natural sphingoid bases, as reported by Pruett *et al*.[289] The variety of this natural occurring molecules represents a remarkable source of lead compounds for the design of synthetic analogues with therapeutic applications. Alternatively, they represent pharmacological tools suitable for basic biomedical research.

3.1. Sphingolipid metabolism inhibitors

Among eukaryotes, fungi represent a wide source or mycotoxines and other metabolites that exhibit a variety of biological activities[290]. Particularly fungal sphingolipid analogues might alter sphingolipid metabolism by inhibiting key enzymes of the metabolic pathway.

This is the case of SPT inhibitors such as sphingofungins, lipoxamycin, and the most used compound myriocin. These metabolites are assumed to be substrates of the target enzyme, giving rise to aberrant forms of a transient intermediate of SPT reaction. Moreover they were shown to inhibit fungal and mammalian enzyme in cell-free preparations with IC_{50} values in the nanomolar range[291]. In addition, viridiofungins are potent inhibitors of mammalian SPT, however they also inhibit squalene synthase[292]. Structural modification of myriocin, that has also immunosuppressant properties[293], gave rise to FTY720. This compound has been recently approved for the treatment of multiple sclerosis[294] and it is also being studied as anticancer agent for its properties as SK inhibitor[295]. Moreover it has been recently reported as a S1PL inhibitor[296].

Fumonisins are a family of fungal toxins that share structural similarity with the sphingoid base and were shown to inhibit CerS[162,165]. Among them FB1 is the compound of election used for the investigation of CerS inhibition. The characterization of FB1 and the biological effects related to CerS inhibition have been already treated in paragraph 2.2.1.5, together with other fungal metabolites that also inhibit CerS.

Other examples of SL metabolism inhibition by fungal metabolites are given by scyphostatin and manumycin A. Scyphostatin exhibited a potent, reversible[297], and selective inhibitory activity against nSMase in a rat brain microsome assay[298]. Synthetic analogues of scyphostatin have been developed looking for more potent nSMase inhibitors.

Among them, a series of *N*-acyl scyphostatin analogues, were shown to be irreversible inhibitors of nSMase[297]. Manumycin A is structurally related to scyphostatin, it is an irreversible inhibitor of nSMase with an affinity to the enzyme comparable to the natural substrate sphingomyelin. Some synthetic manumycin A analogues were shown to be irreversible inhibitors. Manumycin A has been shown to have antitumor activity. However, manumycin A has been shown to have Ras farnesyltransferase- and interleukin-1-converting enzyme inhibitory activities[299]. Manumycin A is currently used in cancer research, but its activity is mainly attributed to Ras farnesyltransferase inhibition.

The reported examples point out the importance of natural molecules that because of their similarity with natural SLs, they might alter the enzymatic activities and consequently the balance between bioactive molecules. Moreover they represent scaffolds for the synthesis of new molecules, aimed to improve pharmacological properties and effects of the original compounds.

3.2. Sphingolipids analogues from marine organisms: Jaspine B

Jaspine B (pachastrissamine) is a natural anhydrous derivative of phytosphingosine resulting from the cyclodehydration between C1 and C4 hydroxyl groups of the sphingoid backbone (**Figure 3.1**). It was first isolated by Kuroda *et al.* from marine sponge *Pachastrissa sp.* in 2002[300] and subsequently isolated from the sponge *Jaspis sp.*, together with an analogue called Jaspine A (**Figure 3.1**) by Ledroit *et al.* in 2003[301]. Early study on cell viability reported that JB was cytotoxic in different cancer cell lines, such as P388, MEL28, A549, HT29 and HeLa[300–302].

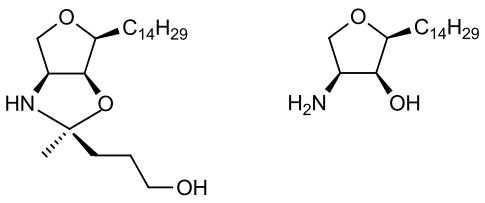

Jaspine A **Jaspine B**

Figure 3.1: Natural Jaspines

Because of its intriguing biological activity, JB has been an interesting target for chemical synthesis through different synthetic routes as reported by Kwon *et al*.[303]. Moreover JB analogues were produced by the modification of the heterocycle[304,305] or by changing the aliphatic chain[306]; however these changes did not strongly improved JB cytotoxicity.

The first study that more deeply investigated JB biological effects revealed that cytotoxicity in murine B16 and human SK-Mel28 melanoma cells was related to interference with SL metabolism via typical apoptosis, release of cytochrome c and caspase processing associated with increased Cer levels. In particular SMS was proposed as the putative target for JB to account for the observed effects in B16 melanoma cells[307]. Other biological effects were reported for structural analogues and isomers of the natural sphingolipid. For instance a series of five strereoisomers of "aza analogues" of Jaspine B ("aza-Jaspine B") (**Figure 3.2,** upper panel) also displayed cytotoxicity against various melanoma cells with potencies comparable to that of Jaspine B. Some of them impaired the conversion of Cer into SM in B16 cells, in agreement with the effects observed for the natural JB[308]. The investigation of the molecular mechanism that trigger apoptosis in melanoma cancer cells suggested that inhibition of ERK is involved[309].

In a research on diastereomeric JB at C2 and C3 position carried out in our group, JB with the natural configuration and three stereoisomers named 2,3-*epi*, 2-*epi* and 3-*epi* JB were synthesized (**Figure 3.2,** lower panel). Jaspine B was the most cytotoxic molecule, whereas the other compounds were about 10–20 times less toxic. Moreover JB showed increased levels of dhCer and cytotoxicity decreased in presence of the autophagy inhibitor 3-methyladenine, suggesting the involvement of the dhCer-mediated autophagy in JB induced cytotoxicity[310]. The above four molecules together with their enantiomeric analogues (**Figure 3.2,** *ent*-isomers) exhibited moderate to potent inhibitory activity against SK1 and SK2. Moreover atypical PKCs were inhibited by several pachastrissamine stereoisomers[311].

Two series of 1,2,3-triazole-Jaspine B hybrids with different side chain length (**Figure 3.2,** upper panel) were synthesized and tested for cytotoxicity in MGC-803, MCF-7 and EC-9706 cells: compounds with alkyl chain between C14 and C18 generally showed elevated cytototoxiciy. Moreover investigation of apoptosis and cell cycle analysis demonstrated that one of the most cytotoxic compounds caused early and late apoptosis and arrested the cell cycle at G2/M phase in a concentration- and time-independent manner[312].

Recently the cytotoxicity and SK inhibition properties of a series of carbocyclic JB-analogues with different alkyl-chain length have been reported (**Figure 3.2,** upper panel),

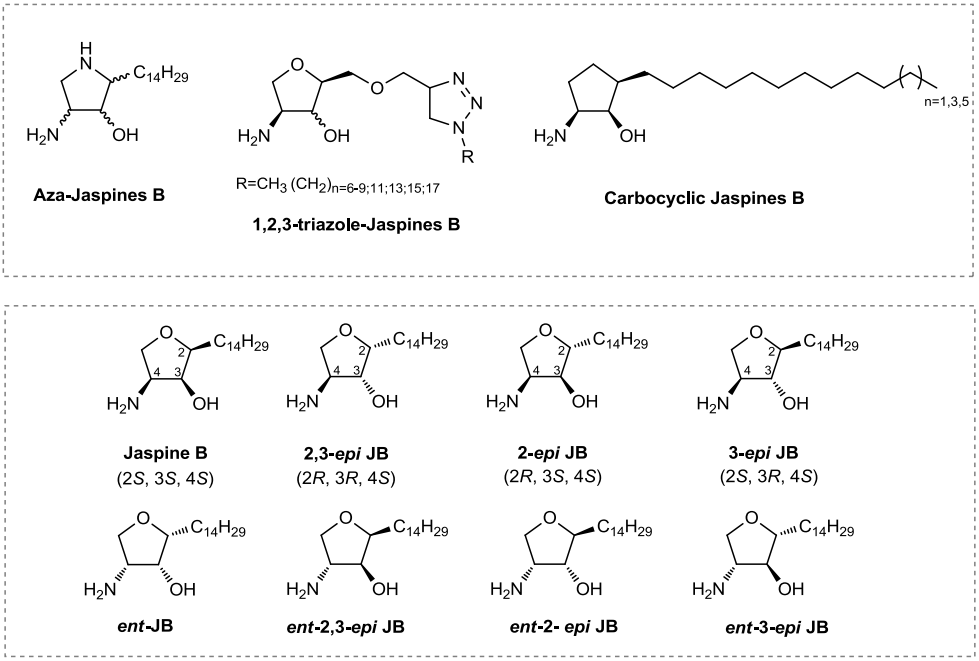

Figure 3.2: Jaspine B structural analogues and isomers

showing that both shorter and longer analogues were less effective than the analogue with the same chain length of natural JB. These results pointed out that the ring oxygen atom of pachastrissamine is dispensable, but the appropriate chain length is apparently required to retain its biological properties[303].

Due to its bioactivity and cytotoxicity in different cell lines JB represents a promising molecule in drug discovery and a valuable pharmacological tools to better understand the molecular basis of cellular alterations connected to cancer disease.

4. Cell death mechanisms

Cell death represents an homeostatic mechanism in cell physiology; however dysregulated cell death is a common feature of many human diseases, including cancer, stroke and neurodegeneration, and modulation of this cellular response has proved to be an effective therapeutic strategy[313]. Apoptosis and necrosis represents the two classical forms of cell death; autophagy, although more recently described, is also well characterized at molecular level. Moreover new findings pointed out the intricate interplay between these processes focusing on the relevance and impact of this crosstalk in normal development and in pathology[314]. A variety of new cell death mechanisms have been reported in the last years, by observing phenotypic features as well as by applying biochemical methods to find pathways that are activated in different cell death conditions. In this section a general overview of different cell death mechanisms is reported, with special attention for apoptosis, autophagy and methuosis.

4.1. Apoptosis and caspase-independent cell death

Apoptosis is a well known mechanism of programmed cell death (PCD) that is usually activated during development and aging as a homeostatic mechanism to maintain cell populations in tissues. Apoptosis also occurs as a defence mechanism such as in immune reactions or in case of cell damage by disease or toxic agents[315]. Alterations or defiance against these natural death mechanisms can lead to diseases such as diabetes mellitus, neurodegenerative diseases and cancer. In this regard, cancer cells often present defective apoptotic machinery that confer survival advantage. For instance upregulation of anti-apoptotic family of proteins, such as Bcl-2, Bcl-X_L and Mcl-1 has been often observed in cancer cells. In addition activation of pro-survival paths, like PI3K-Akt pathway, further help to resist death triggers. Suppression of pro-apoptotic proteins, such as Bax also contributes to resistance against apoptosis-inducing therapeutic regimens. Thus, improving therapeutic efficacy and selectivity and overcoming drug resistance are the major goals in developing anti cancer agents today[316].

Characterizing features of this mechanism are cell shrinkage (pyknosis), chromatin condensation, degradation of DNA by endogenous DNases, nuclear fragmentation and formation of apoptotic bodies. They consist of cytoplasm with tightly packed organelles with or without a nuclear fragments[317]. These bodies are subsequently

phagocytized by macrophages and degraded within phagolysosomes[318], thus avoiding inflammation process.

Apoptosis may be triggered either by extrinsic stimuli through cell surface death receptors, such as TNFα, Fas (CD95/APO1) and TRAIL receptors or by intrinsic stimuli, such as Ca^{2+} overload and overgeneration of reactive oxygen species (ROS), via the mitochondrial signalling pathway, characterized by mitochondrial membrane permeabilization (**Figure 4.1**). In either case, activation of cysteine aspartyl proteases, called caspases is a key event of this process.

In the extrinsic pathway the death-inducing sopramolecular complex (DISC) regulates the activation of caspase 8, while in the mitochondrial pathway the apoptosome activate caspase 9. Both pathways converge with the activation of caspase 3[319], which mediate (at least part of) the catabolic processes that characterize end-stage apoptosis. Apoptotic events are highly regulated by Bcl-2 proteins family, including Bcl-X_L, Bad and Bim. The inhibitors of apoptosis (IAPs) is family of protein that regulate the caspase cascade, and then, may influence both the intrinsic and extrinsic pathway. Another fundamental regulator of apoptosis is p53, that has been shown to regulate apoptosis either by activating expression of pro-apoptotic proteins, or in an trascription-independent manner by interaction with anti apoptotic proteins[316].

Alternatively pro-apoptotic triggers that cause mitochondrial MMP, also engage cell death even in the absence of caspase activity, producing the so called caspase-independent cell death[320] (also known as caspase-independent apoptosis[319]). Following MMP, various intermembrane-space proteins are released into the cytoplasm causing cellular alteration including DNA damage, progressive loss of respiratory chain function and reduced mitochondrial membrane potential, ultimately leading to bioenergetic crisis and cell death[320].

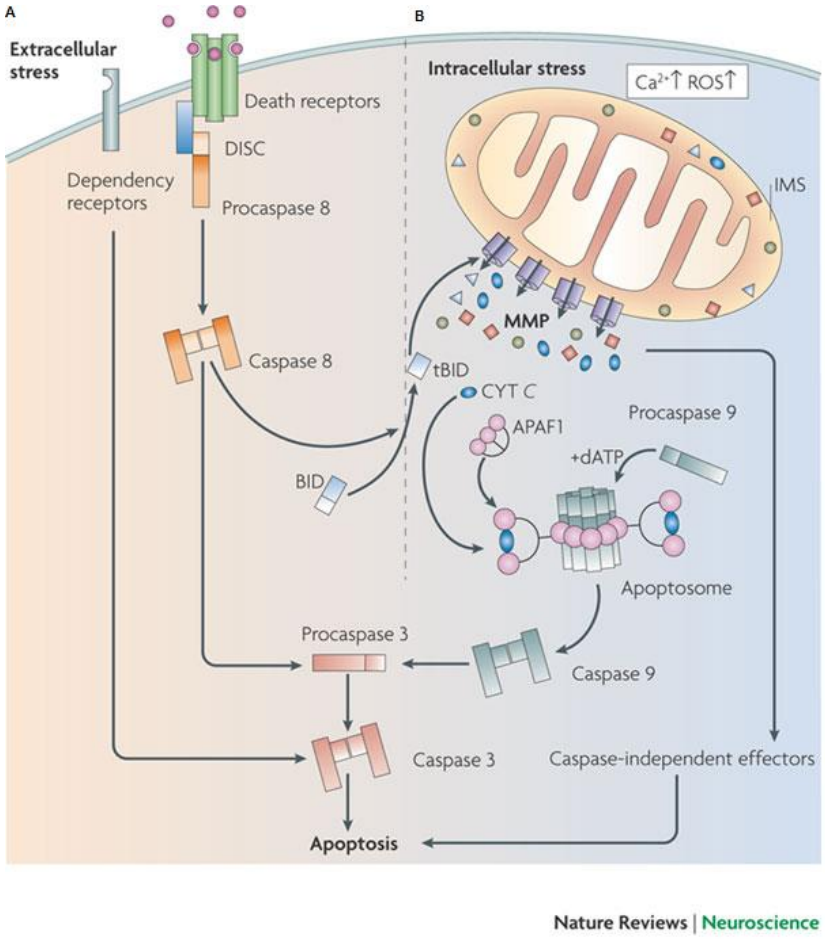

Figure 4.1: The extrinsic and intrinsic pathways of apoptosis. Apoptosis can result from the activation of two biochemical cascades: the extrinsic (**A**) and intrinsic (**B**) pathways that result in caspases activation. Mitochondrial membrane permeabilization (MMP) marks a point of no return in the mitochondrial pathway by activating both caspase-dependent and caspase-independent mechanisms that eventually execute cell death**.** Following MMP the mitochondrial intermembrane space (IMS) protein cytochrome *c* (CYT *C*) is released into the cytosol and interacts with the adaptor protein apoptotic peptidase activating factor 1 (APAF1) as well as with procaspase 9 to form the apoptosome, with activation of caspase 3. Alteratively IMS proteins activate caspase-independent effectors. One of the major links between extrinsic and mitochondrial apoptosis is provided by the BCL-2 homology domain 3 (BH3)-only protein BID, which can promote MMP following caspase 8-mediated cleavage. dATP, deoxyadenosine triphosphate; tBID, truncated BID. Figure modified from *Galluzzi et al., Nature Reviews Neuroscience, (2009)*[321].

4.2. Necrosis

In contrast to apoptosis, necrosis has been traditionally thought to be a unregulated form of cell death. It is characterized by cytoplasmatic swelling (oncosis), and cell membrane rupture, leading to release of the cellular components and inflammatory tissue response[322]. Cells that die by necrosis frequently exhibit changes in nuclear morphology but not the organized chromatin condensation and fragmentation of DNA that is characteristic of apoptotic cell death[323].

Recent genetic evidence, as well as the discovery of chemical inhibitors of necrosis, have greatly changed the idea of "accidental" cell death, and revealed the existence of multiple pathways of regulated necrosis. Between them necroptosis, that depends on protein RIPK1 and/or RIPK3 activity, is the most well characterized mechanism[324].

4.3. Autophagy

The word autophagy, derived from the Greek word for "self-eating", refers to the catabolic processes through which the cell turns over its own constituents[325].

In physiological conditions, autophagy has a homeostatic function. It proceeds at basal levels, ensuring the continuous removal of dysfunctional or damaged entities, including protein, organelles and/or their portions. Moreover, the autophagic flux can be upregulated in response to a wide panel of stimuli, including nutritional, metabolic, oxidative or pathogenic, representing an adaptive response to stress with cytoprotective functions[326]. However, the activation of the autophagic machinery can also let to cell death, as reported in different cellular models[327].

Autophagy also has a double-edged role in cancer. Defects of this pathway are associated with susceptibility to metabolic stress, genomic damage, and tumorigenesis, indicating a role for autophagy in tumour suppression[328]. On the other hand cancer cells take advantage from autophagy to overcome stress conditions, such as poor blood supply (specially in primary tumours) or limited nutrients conditions[329]. Moreover autophagy has shown to be activated as response to different cancer treatment, representing a possible risk for drug resistance[328].

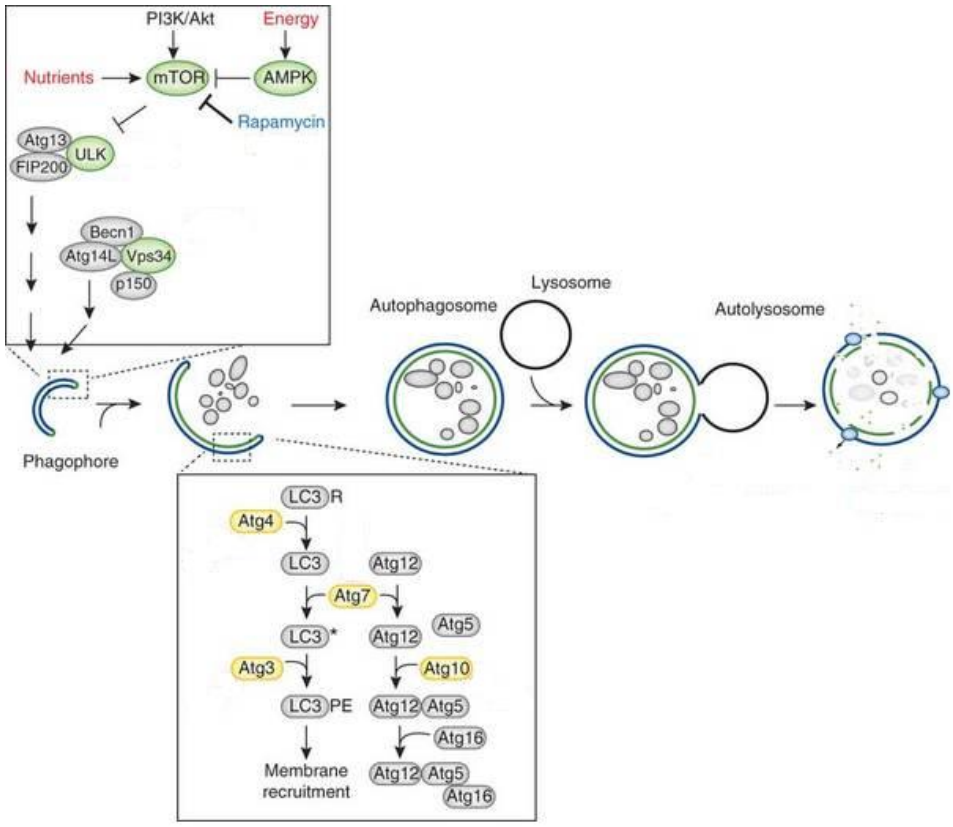

Figure 4.2: Autophagy. PI3K/Akt pathway or high levels of nutrients activate mTOR with consequent inhibition of the autophagic machinery, while other stimuli (including Rapamycin) can inhibit the protein, thus activating autophagy. The different steps of the autophagic pathway are regulated by different proteins, including Atg proteins , Becn1 (Beclin1) and PI3K (Vps34), some of them with enzymatic activity (shown in green and yellow). After completing the autophagosome formation, fusion with the lysosome originate the autolysosome where the autophagic cargo is degraded and recycled back to the cytoplasm. Figure modified from *Cheong et al., Nature biotechnology (2012)*[330]

Autophagy is characterized by the formation of double-membrane vesicles called autophagosomes, which sequester the cytoplasmic structures targeted for destruction (**Figure 4.2**). Following autophagy induction, the Atg (autophagy-related) proteins assemble at a specialized site that has been named the phagophore assembly site (PAS) and orchestrate fusion of Golgi-, endosome- and plasma-membrane-derived membranes to form the phagophore[331]. A characterizing event of the elongation of the phagophore is the conjugation of phosphatidylethanolamine (PE) to the microtubule-associated protein 1

light chain 3 (LC3; LC3-I indicate the soluble form of the protein), originating the lipidated form LC3-II, which is incorporated into the autophagosome membrane[332], thus representing an important marker of autophagy. Complete autophagosomes with autophagic cargo, which recruitment involve proteins such as p62, subsequently fuse with the lysosomes, originating autolysosomes, where the inner membrane and autolysosome content are degraded by lysosomal enzymes[331].

Autophagy is tightly regulated. The mammalian target of rapamycin (mTOR) is an autophagy repressor and represent one of the most important check point for this process (**Figure 4.2**). Upon different stimuli mTOR is inhibited with the activation of the ULK/Atg13/FIP200 complex, triggering the initiation of the autophagic process. The class III-PI3 kinase (Vps34)-Atg14L-Becn1 complex also regulates the autophagosome formation[330].

4.4. Emerging mechanisms of non-apoptotic cell death: methuosis

In the last report of the Nomenclature Committee on Cell Death, emerging mechanism of regulated cell death have been classified according to their biochemical features, caspase dependence and use of pharmacological or genetic inhibition. Among them several non-apoptotic mechanisms have been included, such as entosis, characterized by the "cell-in cell" phenotype, netosis, that is restricted to granulocytic cells, and parthanatos, that involve the DNA damage-responsive enzymes poly(ADP-ribose) polymerases (PARPs)[319]. More recently Kornienko *et al.* added to this list other forms of non-apoptotic cell death that have been reported after pharmacological treatment, named methuosis, paraptosis, oncosis, and lysosomal membrane permeabilization, pointing out the importance of alternative pathways in apoptosis-resistant cancer treatment[333].

Methuosis is one of the most recently reported mechanism, described by Overmeyer *et al.* in 2008[334]. The name, which is derived from the Greek methuo (to drink to intoxication), was selected because the most prominent attribute in cells undergoing this form of cell death is the accumulation of large fluid-filled cytoplasmic vacuoles that originate from macropinosomes (**Figure 4.3**). Features of methuosis, compared to other forms of non-apoptotic cell death mechanism have been reported by the same group as shown in **Table 4.1**.

Table 4.1: Features of methuosis compared with other forms of non-apoptotic cell death[a]

	Methuosis	**Oncosis**	**Paraptosis**	**Necroptosis**	**Ferroptosis**	**Pyroptosis**	**Parthanatos**	**Autophagic cell death**
Visible vacuoles; origin	Yes; macropinosomes and endosomes	Yes ER and mitoch.	Yes ER and mitoch.	Yes ER and mitoch.	No	No	No	Yes autophagosome
Rupture of plasma membrane	Yes	Yes	Yes	Yes	No	Yes	No	Varies
Cell swelling	Yes	Yes	Yes	Yes	No	Yes	No	No
Membrane blebbing	No	Yes	No	No	No	No	No	No
Chromatin condensation	No	Yes	No	Yes	Yes	Yes	Yes	Yes (late)
DNA fragmentation	Varies	No	No	No	No	Yes	Yes	Yes (late)
Activation of executer caspases (occurs but not required)	Yes	No	No	No	No	No	Yes	Varies
Accumulation of autophagosomes	Yes		Yes	Yes	No		No	Yes
Mitochondrial membrane permeability		Yes	Yes	Yes	No	No	Yes	Varies
Lysosomal membrane permeability		Yes	No	Yes	No	No		Varies
ATP depletion	Yes	Yes	Yes	Yes	Yes	No	Yes	Varies
Inhibitors		Glycine, PARP inh.		Necrostatin	Ferrostatin, iron chelators	Caspase-1-inh.	PARP inh.	3-MA, si-RNA vs Atg-5, Beclin-1

[a] *From Matlese et a., Am. J. Pathol. (2014)*[335]

Macropinocytosis is a clathrin-independent endocytic process by which mammalian cells internalize extracellular fluid, nutrients and proteins in vesicles (macropinosomes) generated from protrusion of the plasma membrane termed lamellipodia or ruffles[336]. After acquiring phosphatidylinositol-3-phosphate and the small GTAase, Rab 5, macropinosomes enter the endocytic pathway, where they either recycle back to the cell surface or mature to acquire characteristics of late endosomes (LAMP1 and Rab7) and ultimately fuse with lysosome. However macropinocytic process is dysfunctional in methuosis and micropinosomes do not recycle or fuse with lysosomes. Instead they choalesce to form progressively larger vacuoles. As vesicles of increasing size fill the cytoplasmic space, the cells detach from the support and lose membrane integrity in a

manner reminiscent of necrosis. However no protection is afforded by necrostation, distinguishing this form of cell death from necroptosis[335].

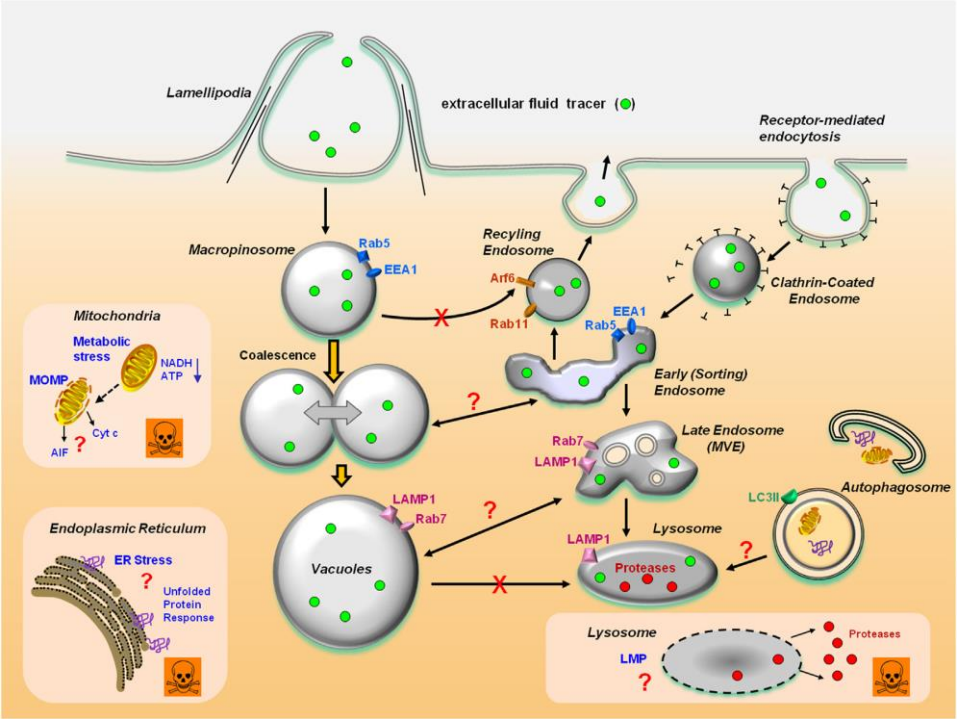

Figure 4.3: A working model of methuosis: Nascent macropinosomes generated from lamellipodial membrane projections enter the cell and coalesce to form large fluid-filled vacuoles. The latter are unable to recycle like normal macropinosomes, but rapidly mature to form a stable vacuole population with some characteristics of late endosomes (Rab7 and LAMP1). It remains to be determined if the vacuoles have the capacity to disrupt protein trafficking in the clathrin-dependent pathway or merge with early endosomes or late multivesicular endosomes. Although there is good evidence that the macropinosome-derived vacuoles are distinct from autophagosomes, it will be important to determine whether the accumulation of vacuoles or associated changes in the metabolic state of the cell may have an impact on autophagy. A central question for future study is how vacuolization of macropinosomes or late endosomes leads to loss of membrane integrity and necrotic cell death. Contributing factors, which are not mutually exclusive, could include compromised mitochondrial energy metabolism, mitochondrial outer membrane permeability (MOMP), lysosomal membrane permeability (LMP), or ER stress. AIF, apoptosis-inducing factor; Cyt c, cytochrome *c*. From *Maltese et al, Am. J. Pathol. (2014)*[335]

Vacuoles, that can be marked with an extracellular fluid tracer, neither originate from swollen ER membranes or mitochondria, as is typically the case in paraptosis and oncosis, nor share similar features with autophagosomes. Moreover, although LC3-II elevation was detected during methuosis, immunofluorescence staining and genetic inhibition of autophagy demonstrated that the two processes are independent[334].

Features that are common to the execution program of apoptosis can be detected in methuosis. These include activation of caspase-3 and cleavage of caspase substrates. Nevertheless in methuosis loss of cell viability is not prevented by the broad spectrum caspase inhibitor z-VAD and typical features of apoptosis such as cell shrinkage, chromation condensation and plasma membrane blebbing are generally absent[335].

After the initial identification of methuosis in glioblastoma cells after ectopic expression of constitutively active Ras protein[334], further studies have identified the small GTPases, Rac1 and Arf6, as key downstream components of the signaling pathway underlying Ras-induced methuosis[337]; however this mechanism has not been confirmed in a model of methuosis induced by a small molecule[338]. Moreover recent reports have described pharmacological tools than can induce the features of methuosis in a broad spectrum of cancer cells, including those that are resistant to conventional apoptosis-inducing drugs, such as temozolomide-resistant glioma[339] and doxorubicin-resistant breast cancer[340].

Although some morphological and molecular criteria that describe methuosis have been delineated suggesting a working model of methuosis (**Figure 4.3**), further studies are necessary to better understand the execution program and to answer open questions related to this newly-introduced form of cell death. The identification of alternative mechanisms of cell death, although not defined for their physiological importance, enclose significant interest in the fields of toxicology and cancer therapy. Indeed, they represent alternative mechanisms that cells use to die and provide new opportunities to manipulate cell death in a therapeutic context, for instance to enable the killing of apoptosis-resistant cancer cells.

OBJECTIVES

The main objectives pursued for this work are:

I. To investigate the effects of the natural sphingolipid Jaspine B on the sphingolipid metabolism and to shed light on its cytotoxic effect in HGC-27 gastric cancer cells.

II. To study the inhibition of dihydroceramide desaturase activity by the sphingosine kinase inhibitor SKI II and to evaluate the biological effects related to its inhibitory activity.

III. To investigate the use of ceramide analogues as chemical tools for ceramidases investigation:

   i. RBM14 coumarinic ceramide analogues as neutral and alkaline ceramidases substrates.
   ii. SABRAC and RBM1-12 as acid ceramidase inhibitors.

RESULTS AND DISCUSSION

5. Alterations of sphingolipid metabolism and cytotoxic effect of Jaspine B in gastric cancer cells

The natural sphingolipid Jaspine B (JB) (**Figure 5.1**) is a cyclic anhydro phytosphingosine that has cytotoxic properties in human and mouse cancer cell lines[300]. JB was shown to induce apoptotic and autophagy-mediated cell death in melanoma cell line[307] and A549 human alveolar epithelial carcinoma cells[310] that were associated with alterations in sphingolipid metabolism.

Further studies were planned to investigate the effect of JB on the sphingolipid content and metabolism as well as on the molecular mechanism that trigger cell death. For this end JB and its stereoisomers 2-*epi*, 3-*epi* and 2,3-*epi* JB were synthesized by Dr. José Luis Abad as previously described[310], together with two acylated forms of JB with C8- and C16-fatty acid chains, and an azide (N_3)-JB (**Figure 5.1**). Preliminary studies performed in our group reported that the 2,3-*epi*-isomer showed a cytotoxicity similar to JB, while 2-*epi* and 3-*epi*-isomers were slightly less cytotoxic. Acylated JB and N_3-JB did not show any cytotoxicity. Since the reported modification did not improve the cytotoxic properties of the molecule, most of the following studies were performed using the natural isomer of JB.

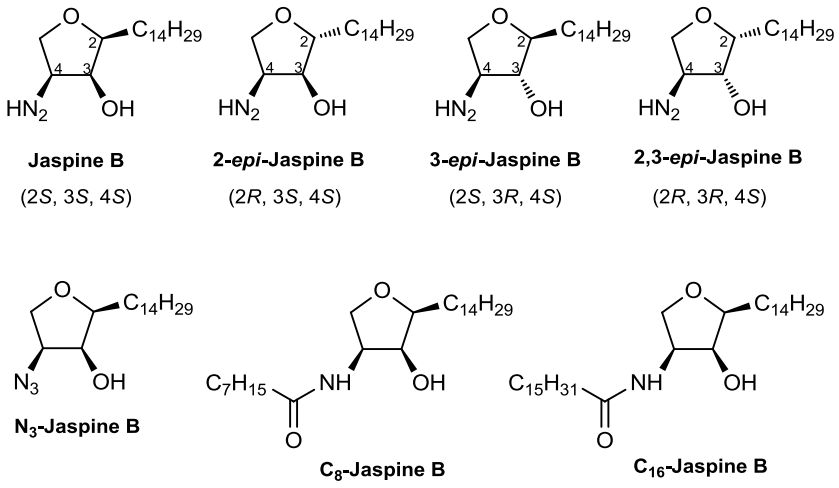

Figure 5.1: Structures of JB and its analogues.

This section discusses the effects of JB on the sphingolipid metabolism and its cytotoxic effects on the gastric cancer cells HGC-27. This cell line was chosen as a model to investigate the molecular basis of JB cytotoxicity in-depth, in light of its potential in autophagic response when SL metabolism is altered[80,85]. Moreover these cells present genetic alterations that confer resistance to anticancer pharmacological treatments[341], making the finding of new anticancer treatments necessary.

5.1. Evaluation of JB cytotoxicity in a panel of cancer cells

First the effect of JB on cell viability was evaluated in different cancer cell lines (**Figure 5.2**), showing cytotoxicity in a low micromolar range as reported in **Table 5.1**.

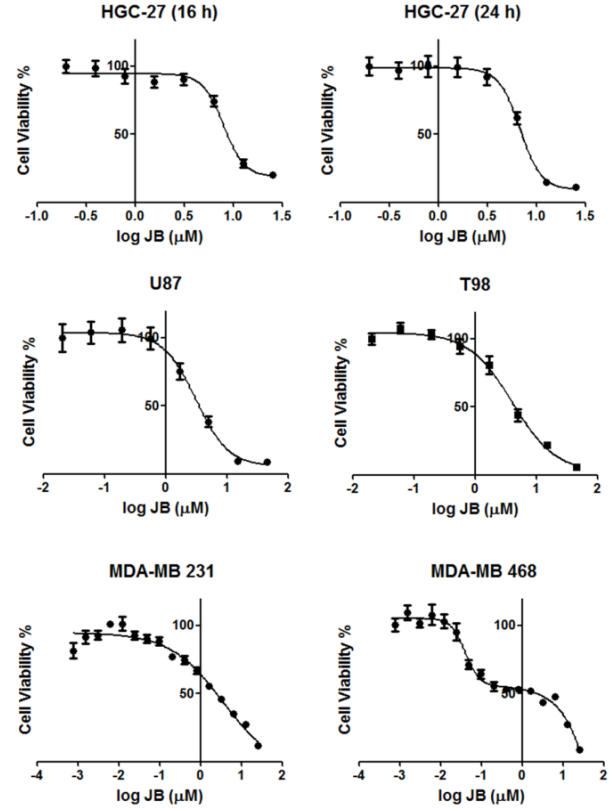

Figure 5.2: Effect of JB on cancer cell viability. Cells were incubated with different concentrations of JB or ethanol (≤0.25%) as a control for 16 (HGC-27) or 24 hours (HGC-27, U87, T98, MDA-MB 231, MDA-MB 468). MTT test was carried out to assess cell viability. Results are expressed as percentage of cell viability over control. Data are represented as mean ±SD of two to three independent experiments in triplicates.

Similar cytotoxicity was reported after 16 and 24 hours of treatment in HGC-27 cells. The highest cytotoxicity was observed in MDA-MB 231 cells, while MDA-MB 468 cells treatment gave a response that does not fit with the classical sigmoid model, thus LD_{50} was not calculated.

Table 5.1 Jaspine B cytotoxicity in cancer cells[a]

Cell line	Cancer Type	LD_{50} (μM)
HGC-27 (16 h)	Human gastric carcinoma	8.0±0.5
HGC-27 (24 h)	Human gastric carcinoma	7.3±0.7
T98	Human glioblastoma	4.5±2.0
U87	Human glioblastoma	3.2±0.9
MDA-MB 231	Human breast adenocarcinoma	2.1±0.2
MDA-MB 468	Human breast adenocarcinoma	N.D.

[a] LD_{50} was calculated as mean of two to three experiments in triplicates ± SD. N.D.: not determined

5.2. Effect of JB on the sphingolipid metabolism

5.2.1. JB increases sphingoid bases levels and their phosphorylated forms

The effect of JB on the sphingolipid metabolism was evaluated in HGC-27 cells. Previous experiments performed in our group showed the accumulation of dhCer after 10 hours of treatment in the same cell line. This was in agreement with data previously reported in A549 cells[310] which suggested a reduced Des1 activity. This hypothesis was rejected after demonstrating by Des1 activity assays that JB does not inhibit this enzyme neither in lysates nor in intact cells (Fabio Simbari, PhD Thesis).

In order to get a more detailed overview and to further investigate the effect of JB in bioactive sphingolipid levels, the sphingolipidome was analyzed in a time course study. For this end, cells were treated with JB at the concentration of 1 μM for 4, 8, 24 and 48 hours. Results from mass spectrometry analysis confirmed the increase in dhCer that almost doubled its level for all the time points of the treatment. Increase in dhSM was also detected after 24 and 48 hours of treatment. Triple-Quadrupole Mass Spectrometer analysis showed that dhSo exhibited the highest increase 4 hours (about 130 fold over the control) and 8 hours (about 220 fold over the control) after JB treatment. As a consequence also its phosphorylated derivate dhSoP, that was undetectable in ethanol

treated control samples, accumulated after 4, 8 and 24 hours of treatment. Sphingosine and SoP also highly increased, mainly after 8 hours of treatment, but not as dramatically as the corresponding unsaturated compounds. Conversely narrow changes were observed in Cer levels, as well as in its metabolite SM (**Figure 5.3**).

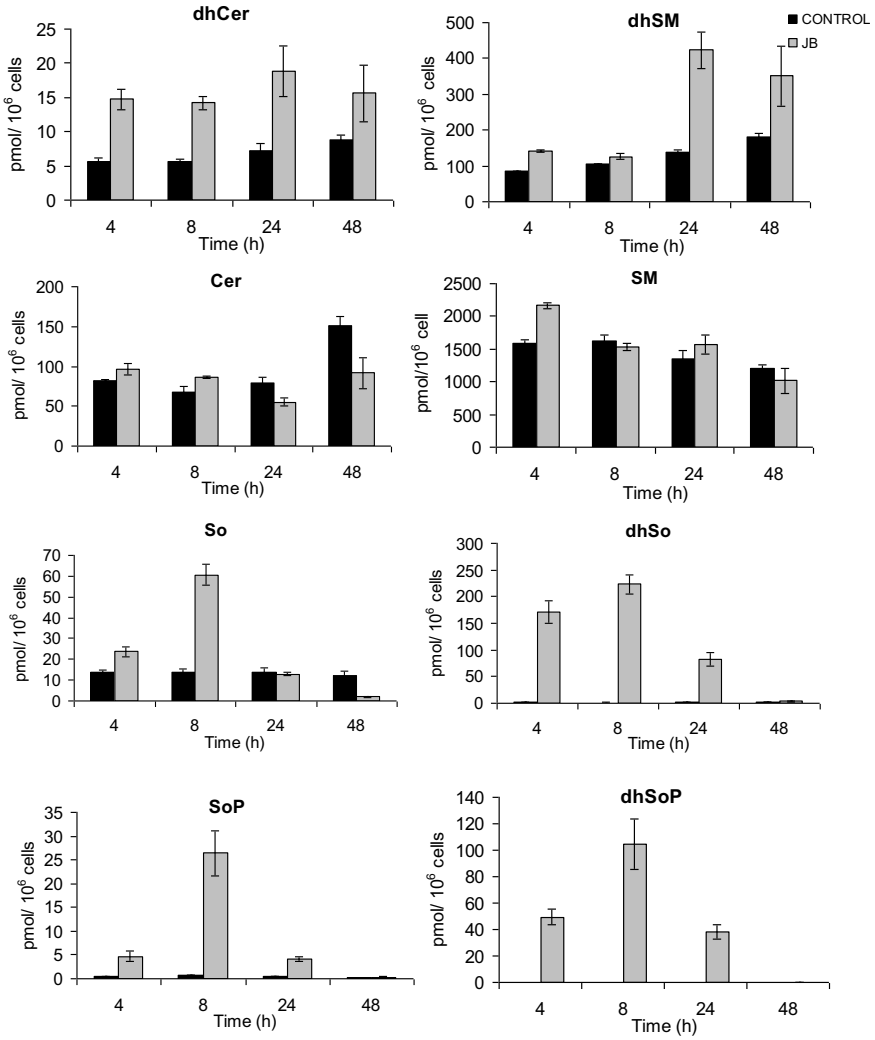

Figure 5.3: Effect of JB on HGC-27 sphingolipidome. HGC-27 cells were treated with 1 μM of JB for 4, 8, 24 and 48 h or ethanol (0.1%) as a control. Lipids were extracted and analyzed by UPLC/TOF and Triple Quadrupole Mass Spectrometer. Results are means ± SD of a typical experiment repeated three times in triplicates.

5.2.2. JB is acylated

The metabolism of JB in gastric cell line was evaluated. Mass spectrometry analysis of ceramides in JB treated samples revealed the presence of new peaks in the chromatogram belonging to species that have the same molecular weight of ceramides with different acyl-chain length, but different retention time. Since the natural sphingolipid has the same molecular weight of sphingosine, it was hypothesized that these signals were associated to acylated forms of JB. The most abundant acyl-JBs detected were C16-, C22-, C24- and C24:1-species (**Figure 5.4**).

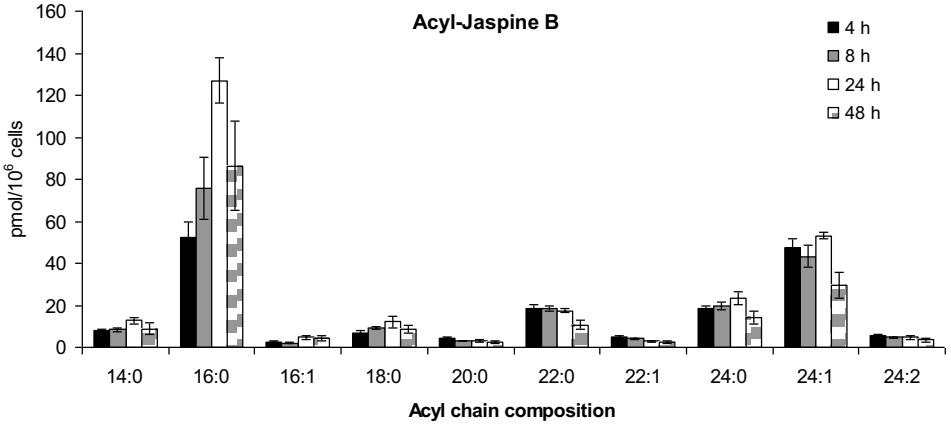

Figure 5.4: Production of acylated JB: HGC-27 cells were treated with 1 µM of JB for 4, 8, 24 and 48 h. Lipids were extracted and analyzed by UPLC/TOF as detailed in Materials and Methods section. Results are means ± SD of a typical experiment repeated three times in triplicates.

Altogether the lipidomic studies demonstrate that JB produces changes in the sphingolipidome, mainly increased levels of the sphingoid bases So and, to a larger extent, dhSo. Importantly, increased levels of SoP and dhSoP are reported as a consequence of the sphingoid bases phosphorylation by SK. Moreover JB induces the formation of acyl-JBs, mainly with long and very long acyl-chain length, probably due to the acylation of the natural sphingolipid analogue by CerS. This result resembles the effect of FB1 that was shown to be acylated by CerS[151], resulting in inhibition of CerS activity and accumulation of long chain bases[342]. These experiments also confirm the slight accumulation of dhCer

that was previously reported[310]. However the increase is in a very low range if compared to the accumulation of dhSo and So.

5.2.3. The study of JB as CerS substrate and inhibitor

5.2.3.1. Preliminary studies with RBM2-40 substrate

To assess the ability of JB to inhibit CerS, a preliminary study using RBM2-40, was performed. RBM2-40 is a ωN_3-sphinganine (ωN_3Sa) described in our group[343], which can be metabolized to the *N*-acyl amides ωN_3-ceramide (ωN_3Cer) and ωN_3-dihydroceramide (ωN_3dhCer) and their phosphocholine derivatives ωN_3-sphingomyelin (ωN_3SM) and ωN_3-dihydrosphingomyelin (ωN_3dhSM) (**Figure 5.5**).

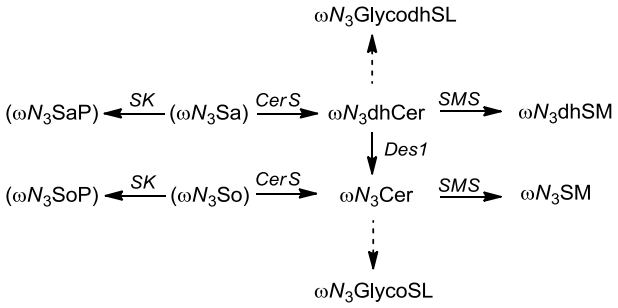

Figure 5.5: RBM2-40 metabolism in the sphingolipid pathway. *Modified from Garrido et. al., Chembiochem (2015)*[343]*.*

HCG-27 cells were incubated with RBM2-40 and its metabolism by the sphingolipid pathway, in presence or absence of JB, was evaluated. Results from the mass spectrometry analysis showed that RBM2-40 was metabolized by CerS, producing ωN_3dhCer, acylated mainly with 14, 16, or 18 carbon atoms fatty acid chains. ωN_3dhSM with C14- and C16- but also C22-, C24- and C24:1- fatty acid chains were found, suggesting that long chain ωN_3dhCers were produced from RBM2-40 acylation, and in turn metabolized to ωN_3dhSMs. No appreciable levels of ωN_3Cers were detected, however the presence ωN_3SMs suggests that ωN_3Cers were produced and quickly converted to ωN_3SMs by SMS, preventing its accumulation. Moreover the results clearly showed that C14- and

C16-ωN_3dhCer decreased in presence of Jaspine B. Similarly the production of ωN_3dhSM with C24- and C24:1- acyl chain and ωN_3SMs with C16-, C20-, C24- and C24:1- was reduced by Jaspine B in comparison to the respective controls (**Figure 5.6**). This results suggest that the natural sphingolipid alters RBM2-40 acylation, supporting the hypothesis of CerS inhibition.

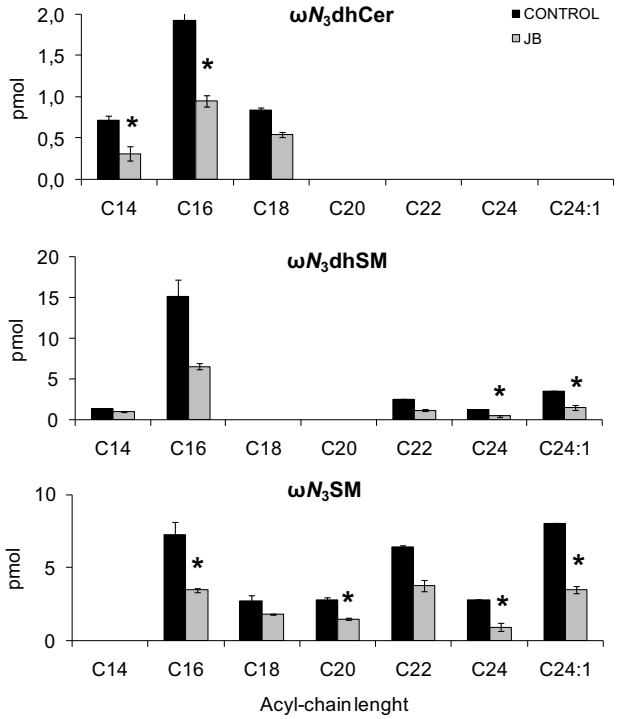

Figure 5.6: JB decreases RBM2-40 acylation. HGC-27 cells were incubated with 5 μM of RBM2-40, as CerS substrate, and 0.5 μM of Jaspine B (or ethanol as a control) for 10 hours. Lipids were extracted and analyzed by UPLC/TOF. Results are the mean ± SD, n =3. (*, $p<0.05$, *t* test).

5.2.3.2. Inhibition studies using a CerS fluorogenic activity assay

In order to confirm that JB inhibits CerS, a specific fluorogenic assay for the determination of CerS activity[152] was performed in Prof. Anthony H. Futerman's laboratory,

(Department of Biological Chemistry, Weizmann Institute of Science) during a short stay of 4 months. The assay takes advantage of the use of NBD-sphinganine (NBD-Sa) as CerS substrate instead of tritiated sphinganine or sphingosine used in other methods. Moreover the lack of detergents in the assay preserves the activity of CerS, that as a membrane-bound enzyme can be altered by detergents, as previously reported by Lahiri [344].

JB inhibition was checked in HEK293T cell lysates ectopicaly-expressing the different isoforms of human CerS. The enzymes acylate the fluorogenic NBD-Sa with different acyl chain lenght acyl-CoAs depending on the CerS specificity, producing fluorescent labelled dihydroceramides that were quantified after TLC separation of lipid extracts. In **Table 5.2** the specific activity assay conditions for CerS isoforms, that were established in previous experiments, are reported. Unfortunately CerS3 activity measurements were not included, due to technical difficulties in ectopic expression of CerS3.

In the first experiment the enzymatic assay was carried out with cell lysates expressing CerS2. Lysates from cells transfected with the empty plasmid (pcDNA3) were used as a negative control, while the well known inhibitor FB1 was used as a positive control of CerS inhibition. Results showed that JB treatment resulted in up to 56% reduction in CerS2 activity in comparison to the control. The inhibition achieved in presence of FB1 confirmed that the reduction in CerS2 activity was due to a specific inhibitory effect of JB and gave reliability for the following measurements (**Figure 5.7**).

Table 5.2: CerS fluorogenic assay conditions used for the different enzyme isoforms

Ceramide synthase	µgr of protein	Incubation time (min.)	Acyl-CoA
CerS1	25	20	C18
CerS2	40	10	C22
CerS4 (C18 CoA)	30	20	C18
CerS4 (C20 CoA)	30	20	C20
CerS5	1	5	C16
CerS6	5	10	C16

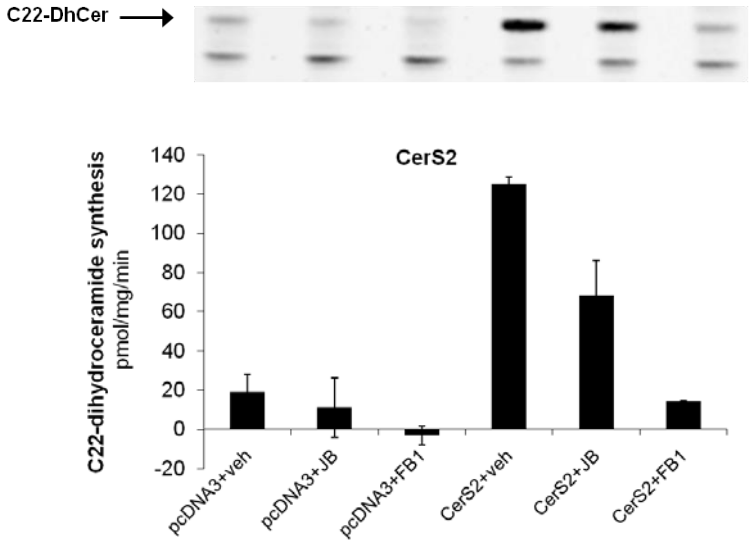

Figure 5.7: Effect of JB CerS2 overexpressing cells. Lysates coming from cells transfected with the empty plasmid (pcDNA3) or CerS2 plasmid were previously incubated with ethanol as a vehicle, JB 5 μM or FB1 1 μM for 5 minutes and then incubated for further 10 minutes after the addition of NBD-Sa. Lipids were extracted and NBD-labelled dihydroceramides were separated by TLC. In the upper panel the picture of the TLC showing the C22-dihydroceramide formed by CerS2 is reported. Results are represented as mean ±SD of one experiment with duplicates.

In the next experiment carried out on CerS6-expressing cell lysates, the inhibitory effects of JB, and its stereoisomers, and C8-acylated and C16-acylated JBs, and N_3-JB were tested. Results showed that JB is CerS6 inhibitor, causing 58% of inhibition compared to the control. Among the stereoisomers, only 2-*epi*-JB exhibited a 25% of inhibition over CerS6 compared to the control, while the other isomers and acylated JBs gave no significant inhibition. As expected also N_3-JB was not able to inhibit CerS (**Figure 5.8**).

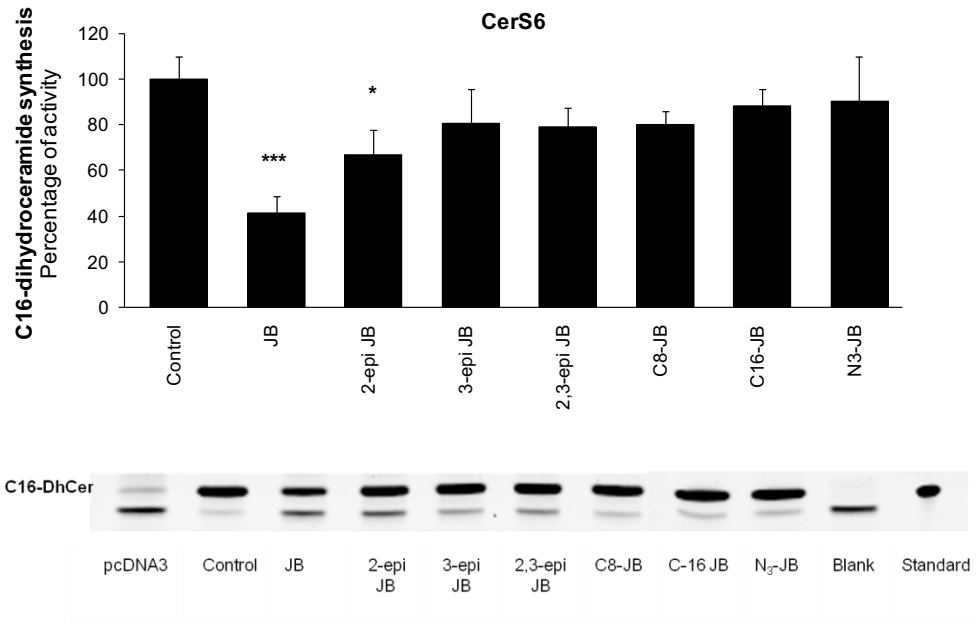

Figure 5.8: Effect of Jaspines on CerS6 over-expressing cells. Cell lysates were previously incubated with the indicated compounds (5 μM) or ethanol as a control vehicle for 5 minutes and the incubated for further 10 minutes after the addition of NBD-Sa. Lipids were extracted and NBD-labelled dihydroceramides were separated by TLC. A typical example of TLC showing the signals corresponding to the dhCer produced by CerS6 activity is reported in the bottom of the figure. C12-NBD-dhCer was used as a standard. Results are represented as the mean ± SD of two experiments in duplicates. (*, $p<0.05$; ***, $p<0.001$, *t* test).

These results prompt us to follow the investigation on CerS inhibition by using JB as it gave the highest inhibitory effect on CerS6 activity. The inhibitory effect of JB was then assessed in cell lysates ectopically-expressing CerS1, CerS2, CerS4 and CerS5. As shown in **Figure 5.9**, JB inhibited NBD-Sa acylation catalyzed by the different CerS isoforms tested. The percentage of inhibition was between 66% and 44% for all the enzymes as resumed in **Table 5.3.**

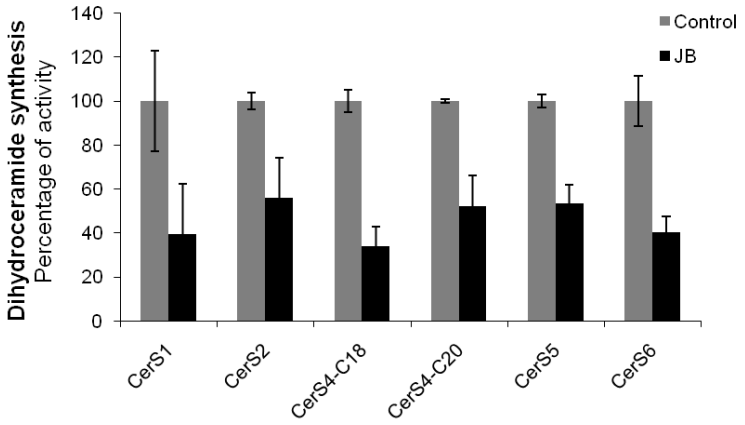

Figure 5.9: JB inhibits CerS. Different amount of protein were incubated for the indicated times (**Table 5.2**) after 5 minutes of preincubation with 5 µM of Jaspine B (or ethanol as a control). The assay starts when NBD-Sa is added and last for different incubation times. Lipids were extracted and NBD-labelled dihydroceramides were separated by TLC. Results are represented as mean ± SD of three experiments in duplicates*, $p<0.05$; **, $p<0.01$;***, $p<0.001$, *t* test

Table 5.3: Ceramide synthase inhibition by JB[a]	
CerS1	61 %
CerS2	44%
CerS4 (C18 Acyl-CoA)	66%
CerS4 (C20 Acyl-CoA)	48%
CerS5	47%
CerS6	60%

[a]CerS inhibition is expressed as percentage compared to the respective controls.

These results demonstrate that JB inhibits CerS activity. Although the lipidomic results showed that JB acylated forms were mainly represented by C16, C22, C24 and C24:1 species, suggesting a possible specific inhibition of the isoforms that produce long and very long chain Cer, this hypothesis was not confirmed in this assay. In fact for all the tested CerS isoforms, JB showed around 50% inhibition to all CerS isoforms, without any specificity for one or more specific enzyme. The accumulation of C16, C22, C24 and C24:1

acyl-JBs as the most abundant species is probably related to the abundance of the CerS isoforms that characterize HGC-27 gastric cancer cell line. This is also in agreement with the Cer content in untreated cells, that show the same composition in the acyl chain length of Cer (not shown).

Despite CerS3 was not included in the activity experiments because of problems in the protein ectopic-expression we expect to get a similar result as in CerS2. As both CerS2 and CerS3 synthesize very-long chain Cer with C22 and C24 acyl-chain length, it is reliable to assume that CerS3 would be inhibited similarly to CerS2.

Studies carried out by using JB stereoisomers, and C8-acylated and C16-acylated JB, and N_3-JB on CerS6 showed that 2-*epi* JB, characterized by *S* configuration in C3 as the natural JB, is the only isoform that can inhibit CerS activity but with a lower inhibition rate compared to the natural isomer (JB), while no effects were detected with the other molecules. These results suggest that the configuration of the carbon atoms of JB heterocycle might be relevant for CerS inhibition. Moreover the acylation of the natural sphingolipid represented an obstacle for its inhibitory activity, indicating the importance of a free amino group in carbon 4. The lack of inhibition of N_3-JB confirmed this evidence.

5.2.3.3. Jaspine B is a substrate of CerS

Based on the results obtained in the inhibition experiments, we next examined whether the inhibition of CerS was due to the direct acylation of JB by CerS. To verify this hypothesis, radioactive-based assays of CerS activity were performed as a part of the studies carried out in collaboration with Prof. Futerman in the Weizmann Institute of Science.

For this end cell lysates from HEK293T cells ectopically-expressing CerS5 were incubated with equimolar amounts of dihydrosphingosine or JB as substrates in presence of radioactive labelled acyl-CoA. Results showed that CerS5 acylated up to 50% of JB compared to the acylation of the natural substrate dihydrosphingosine (**Figure 5.10, A**). Moreover the addition of 1 μM of FB1 reduced the formation of acyl-JB confirming that CerS is responsible for the direct acylation of the natural sphingolipid (**Figure 5.10, B**).

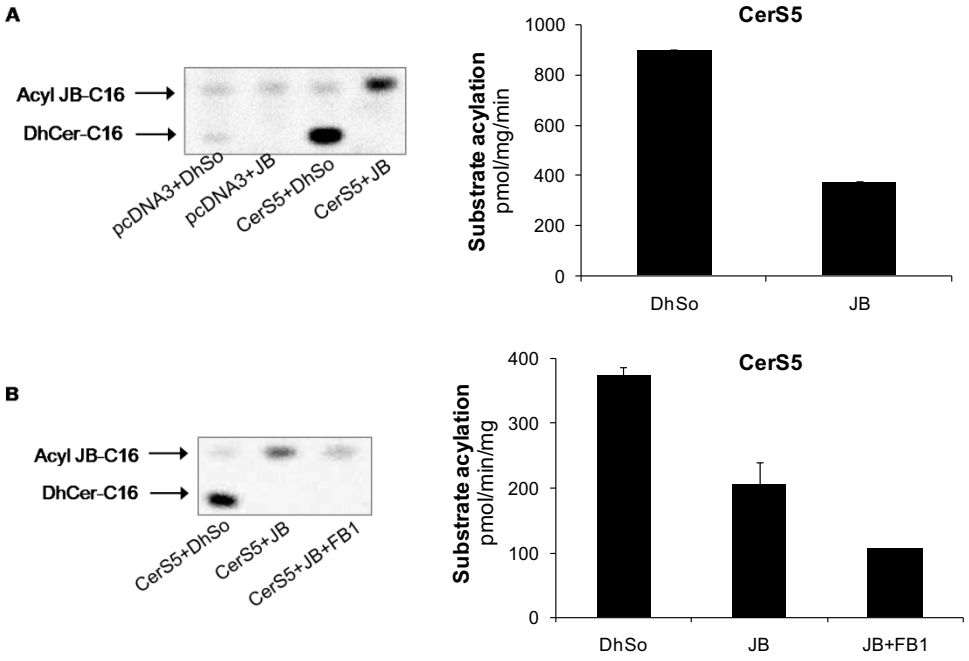

Figure 5.10: JB is acylated by CerS5. A. Lysates (50 µgr) from HGC-27 cells transfected with the empty plasmid (pcDNA3) or CerS5 were incubated with dhSo (15 µM) or JB (15 µM) and radioactive labelled C16-acyl CoA for 20 minutes. Lipids were extracted, separated by TLC and susbtrates acylation was determined as detailed in Material and Methods. Results are means ± SD of a typical experiment repeated two times in duplicates. **B.** Lysates (50 µgr) from HGC-27 cells overexpressing CerS5 were incubated with dhSo (15 µM), JB (15 µM) or JB (15 µM) together with FB1 (1µM) for two hours. Lipids were extracted, separated by TLC and substrates acylation was determined as detailed in Material and Methods. Results are means ± SD of one experiment in duplicates.

These results demonstrate that JB is directly acylated by CerS, and this results in the inhibition of CerS enzymatic activity. The reported acylation rate (around 50% compared to dhSo) is in agreement with the results obtained in the activity determination, where JB gave an inhibition between 44% and 66% for all the CerS isoforms. This result also confirms the presence of acyl-JB in the sphingolipidome of intact cells treated with the natural sphingolipid analogue (**Figure 5.4**). Nevertheless the accumulation in the same cells of dhCer remains a discrepant evidence, as it was already demonstrated that JB does not inhibit dihydroceramide desaturase activity neither in lysates nor in intact cells (Fabio Simbari, PhD Thesis).

In light of these results it is clear that CerS is inhibited by JB with the formation of acyl-JB coming from the direct acylation of the natural sphingolipid. On the other hand JB isomers have little (2-*epi*) or no effect (3 *epi* and 2,3-*epi*) on CerS activity. Nevertheless, it is known from previous studies in our laboratory (not published) that all the Jaspine isomers have similar cytotoxicity in intact cells. These findings suggest that there is no direct connection between JB acylation and its cytotoxic effect. The lack of effect on cell viability of C8-acyl and C16-acyl JB also confirms this hypothesis.

The acylation experiment in presence of FB1 confirmed that JB is used by CerS5 as substrate. The acylation was checked also in CerS6 and CerS4, but the radioactive quantification was not carried out. Nevertheless the image of the radioactive TLC plates of CerS4 and CerS6 gave a positive signal when JB was used a s a substrate, showing that also these CerS isoforms use JB as substrate. In light of these results it is likely that the JB inhibition of CerS activity for all the CerS isoforms is derived through the same mechanism.

5.2.4. JB does not inhibit ceramidases activity

Sphingolipidomic analysis has shown a bulk accumulation of dhSo in intact cells after JB treatment, that is in agreement with the inhibition of CerS. However the detection of doubled levels of dhCer for both short and long times of treatment suggested an additional effect of JB on the sphingolipid enzymatic activity. Since it was already proved that JB does not inhibit Des1, the increase in dhCer levels indicated a possible inhibition of ceramidases.

To assess this hypothesis, ceramidase enzymatic activity in presence of JB was determined by using a fluorimetric assay that was described by our group that employs a synthetic ceramide analogue[224]. Estimation of inhibition of ceramidase activity in intact cells was carried out using analogues of the indicated substrate that differ by the fatty acid chain length, namely RBM14C10, C12, C14 and C16[225] (see Chapter 7, **Figure 7.1, B**). Results showed that JB produced around 40% of inhibition in CDase activity compared to the control when RBM14C10 and C14 were used as a substrate; the inhibition rate increased to 80% in presence of the C12 substrate (**Figure 5.11, A**).

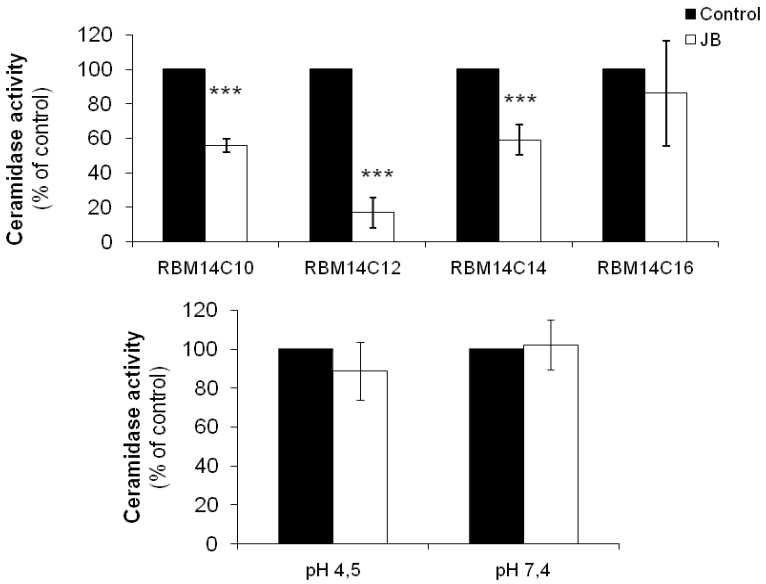

Figure 5.11: Ceramidase inhibition by JB. **A.** HGC-27 intact cells were incubated with Jaspine B 1 μM (or 0.1% of ethanol as a vehicle) for 3 hours and then with RBM14 substrates (40 μM) for additional 3 hours. **B.** Cell lysates (20 mg/ml) were incubated with Jaspine B (1 μM) or ethanol as a control for 3 hours in presence of RBM14C12 (40 μM) as a substrate in acetate buffer 100 mM, pH 4.5 or of phosphate buffer 100 nM, pH 7.4. Ceramidase activity was assessed as described in Material and Methods section. Results are mean ± SD of three different experiments in triplicates (* $p < 0.05$; *** $p < 0.001$, *t*-test)

The correlation between acyl-chain length and ceramidase specificity for the substrates is still an opened issue of investigation in our group. It was reported that RBM14C12 is a better substrate for acid ceramidase[225]. Nevertheless the investigation of RBM14s as neutral and alkaline ceramidases substrates has shown that RBM14C12 is highly hydrolysed by neutral ceramidase, while lower hydrolysis has been observed for alkaline ceramidases (see Chapter 7, paragraphs 7.1.1 and 7.1.2). This considerations prompt us to speculate that the reduction in ceramidase activity in presence of RBM14C12 was mainly due to the inhibition of acid ceramidase or neutral ceramidase by JB. To investigate this hypothesis ceramidase enzymatic assay was carried out in cell lysates by using appropriate pH conditions for both neutral and acid ceramidases. Results showed that JB was not able to decrease neither the acid ceramidase activity nor the neutral ceramidase activity compared to the control (**Figure 5.11, B**).

All together these results show that JB does not inhibit ceramidase activity. Although the enzymatic activity in presence of the natural sphingolipid in intact cells was altered suggesting a possible involvement of acid on neutral ceramidase, the activity assay in cell lysates revealed that this was a non-specific effect. A possible explanation is related to the structure of JB that as an ammine can easily go to lysosomes, penetrating the membrane as non-ionized weak base and get trapped inside when it becomes protonated[345]. The resulting high intra-organelle molecule concentration causes an influx of water to maintain osmotic balance, decreasing the internal pH. Since acid ceramidase activity is localized in lysosomes and its function depends on the pH, it might be that the decrease in ceramidase activity is connected to an altered function of the lysosomes. Similarly, the high amounts of dihydrosphingosine produced after JB treatment might also accumulate in this organelle causing the same effect.

As a conclusion of the studies on the effect of JB on sphingolipid content and enzymatic activity, we observe that JB is a CerS inhibitor and substrate, while it does not change ceramidases activity. The alterations in the sphingolipid content consist in the increase of dhSo and So and their phosphorylated forms, and in the formation of acyl-JB as a consequence of the effect on CerS activity (**Figure 5.12**). The slight accumulation of dhCer, although not expected, is not a completely unknown phenomena when CerS is inhibited. It was already reported that the sphingosine analogue FTY720 while showing CerS inhibition in cell lysates also determined accumulation of ceramide in intact cells[153], probably because of the mode of inhibition of CerS activity. Even though the kinetics of JB inhibition have not been described, we hypothesise that the bulk accumulation of dhSo is the driving force for dhCer synthesis. Since CerS inhibition is not completely blocked by JB and dhSo is one of the substrates of CerS and it competes with the natural substrate, it is likely that after a critical point dhSo is so elevated that it is in part acylated to dhCer, overcoming CerS inhibition partially. However further studies are needed to confirm this hypothesis.

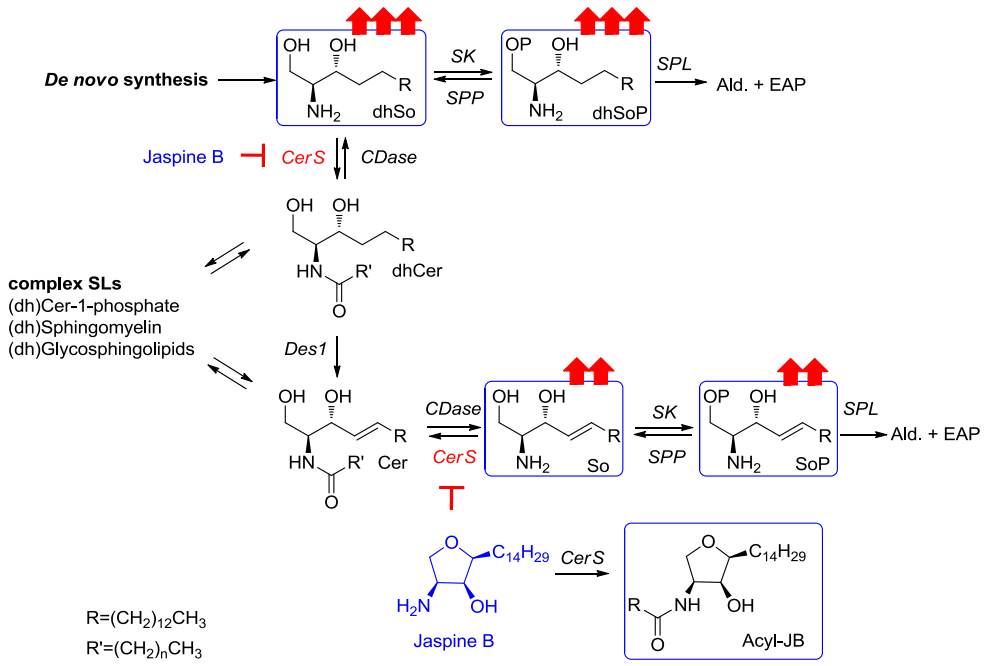

Figure 5.12: Effect of JB on the enzymes of the SLs metabolic pathway. In red the inhibition of CerS by JB is indicated. In the blue the principal molecules that are involved SL metabolism alteration is reported. Red arrows indicate increase of SLs level.

5.3. Investigation of JB induced cell death

5.3.1. JB induces cytoplasmic cell vacuolization

In order to investigate the cell death mechanism activated by Jaspine B treatment, cells were characterized by phase contrast microscopy. Cells that were treated with JB were characterized by the accumulation of phase-lucent cytoplasmic vacuoles, that increased their size and number in a dose dependent manner (**Figure 5.13, A-D**). When cells were treated with 5 µM of JB, vacuoles were visible after 4 hours of treatment and increased their size in a time dependent manner. Lower concentration of JB (1 µM) needed up to 16 hours to show vacuole formation. Higher concentration of JB (12 µM) induced the formation of round shaped cells 1 hour after the treatment, making the observation of intracellular vacuoles formation difficult, and leading to cell detachment (not shown).

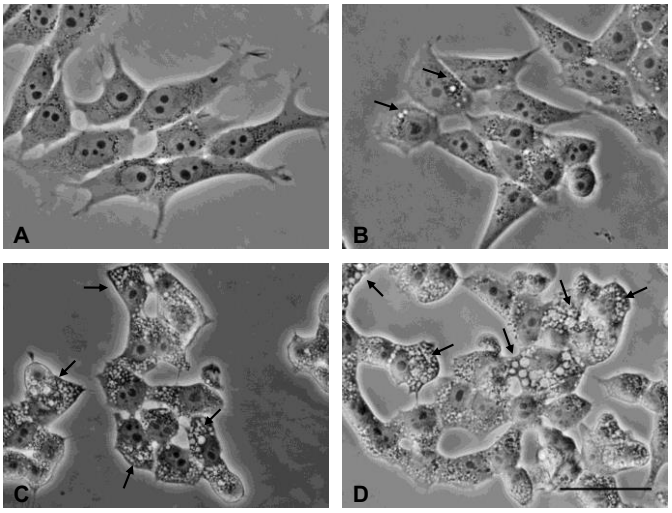

Figure 5.13: JB induces cell vacuolization in HGC-27 cells. Cells were treated with ethanol (**A**) as a control or Jaspine B 1 µ (**B**), 3 µM (**C**) and 5 µM (**D**). Phase-contrast images were taken after 24 hour of incubation. Images are representative of the phenotype observed in different experiments. Scale bar: 50 µm.

Cytoplasmic vacuolization induced after JB treatment was further analysed by transfer electron microscopy (TEM). TEM analysis revealed that the vesicles are multiple-size, low electron-dense areas that occupy broad cytoplasmic sections. Moreover higher

image magnification showed that in contrast to cytoplasmic alteration, cellular nucleus were intact, presenting similar features to the untreated sample (**Figure 5.14**).

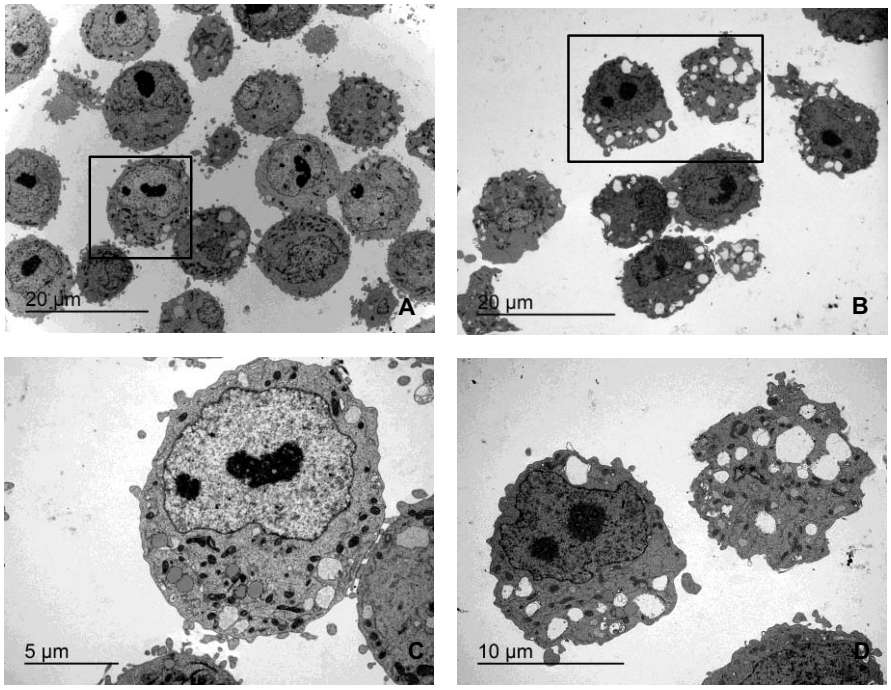

Figure 5.14: TEM analysis of JB induced cell vacuolization. HGC-27 cells were treated with ethanol as vehicle (**A**) or JB 5 µM (**B**) during 16 hours. After fixation, cells were analyzed by TEM. **B** and **C** are higher magnification of the selected areas of images **A** and **B**. The experiment was run in triplicate; images are representative of the observed phenotypes.

In order to check if JB induces the same phenotype in other cancer cell lines, A549, T98 and U87 cells were treated with 5 µM JB and then were analyzed after different times of incubation by phase contrast microscopy. This analysis showed that cell vacuolization was produced in all cell lines short time after the incubation with 5 µM JB (**Figure 5.15**), which lead to cell death and detachment. Interestingly, JB treatment up to 24 hours lead to variable phenotypes in the different cell lines (not shown).

The role of SLs in cell membrane structure and properties, as well as their involvement in different signaling pathways[1] prompt us to investigate the connection between alteration of sphingolipid metabolism by JB with JB-induced cytotoxicity and cell vacuolization.

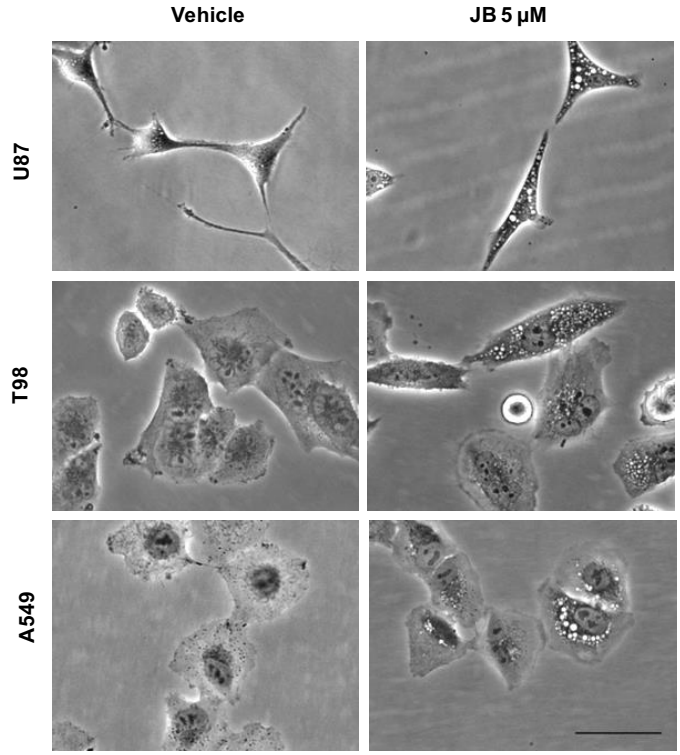

Figure 5.15: JB induces cell vacuolization in a panel of cancer cells. U87, T98, and A549 cells were incubated with JB 5 µM or ethanol as a vehicle. Phase contrast images were taken after 4 hours (U87), 6 hours (T98) and 8 hours (A549). Images are representative of the cell phenotype observed in two different experiments for each cell line. Scale bar: 50 µm.

For this end, cells were treated with myriocin (Myr), the *de novo* inhibitor of SLs synthesis, to counteract the accumulation of sphingoid bases and dhCer. First a sphingolipidomic analysis was carried out after culturing cells with Myr for 8 hours and then adding JB for additional 16 hours. As shown in **Figure 5.16, A** Myr caused a decrease in the amounts of dhCer and its metabolite dhSM; the effect was more evident when the accumulation of dhCer and dhSM induced by JB significantly dropped in presence of Myr. DhSo and dhSoP were undetectable in both control and Myr treated samples because of their low levels. Conversely, dhSo and dhSoP accumulated after JB treatment, and their levels were strongly reduced when JB was combined with Myr. These results confirmed that the use of Myr, alone or in combination with the natural sphingolipid analogue JB cause a blockage in the *de novo* synthesis. However changes in the

sphingolipidome were not paralleled by differences in JB cytotoxicity (**Figure 5.16, B**) or in cytoplasmic vacuolization (**Figure 5.16, C**), suggesting that SLs *de novo* synthesis is probably not involved in these processes.

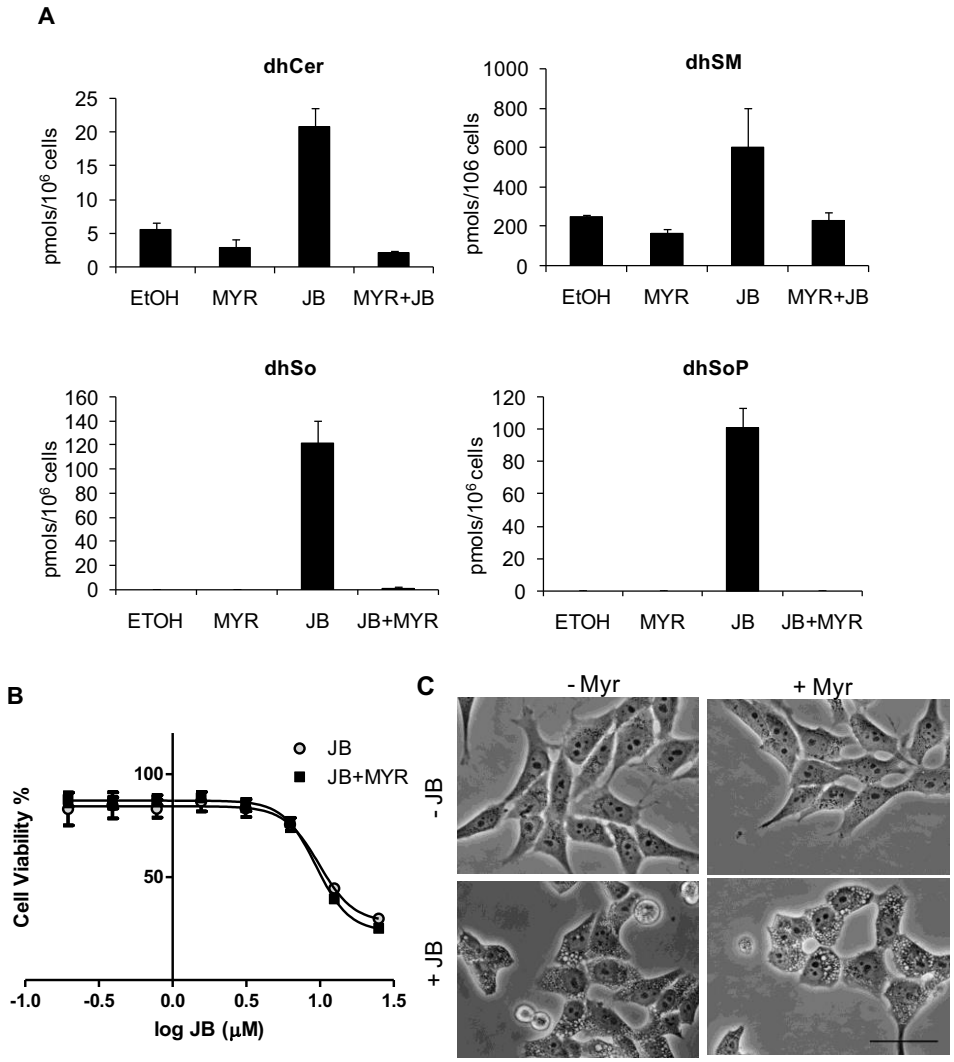

Figure 5.16: Myriocin blocks SL *de novo* synthesis without altering JB cytotoxicity: **A,C.** HGC-27 cells were cultured with 0,1 µM of myriocin (Myr) or ethanol as vehicle during 8 hours and then incubated with JB 3 µM during 16 hours. Phase contrast pictures were taken before cell collection. **C.** Images are representative of the phenotype observed in two independent experiments in triplicates. Scale bar: 50 µM. **A.** Cells were collected, and sphingolipids were analysed as described in Materials and Methods. Results are means ± SD of a typical experiment repeated two times in triplicates. **B.** HGC-27 cell were treated with 0,1 µM of Myr (or EtOH as vehicle) and then incubated with different concentrations of JB for 16 hours. Cell viability was determined by MTT test. Results are means ± SD of two experiments in triplicates.

5.3.2. Apoptosis is not activated by JB

The formation of cytoplasmic vacuoles is a feature shared by different forms of cell death that are collectively known as non-apoptotic cell death mechanisms. We therefore checked if JB induced cell death is a non-apoptotic cell death. JB cytotoxicity was evaluated in presence of the pan-caspase inhibitor z-VAD, showing no changes in cell viability (**Figure 5.17, B**).

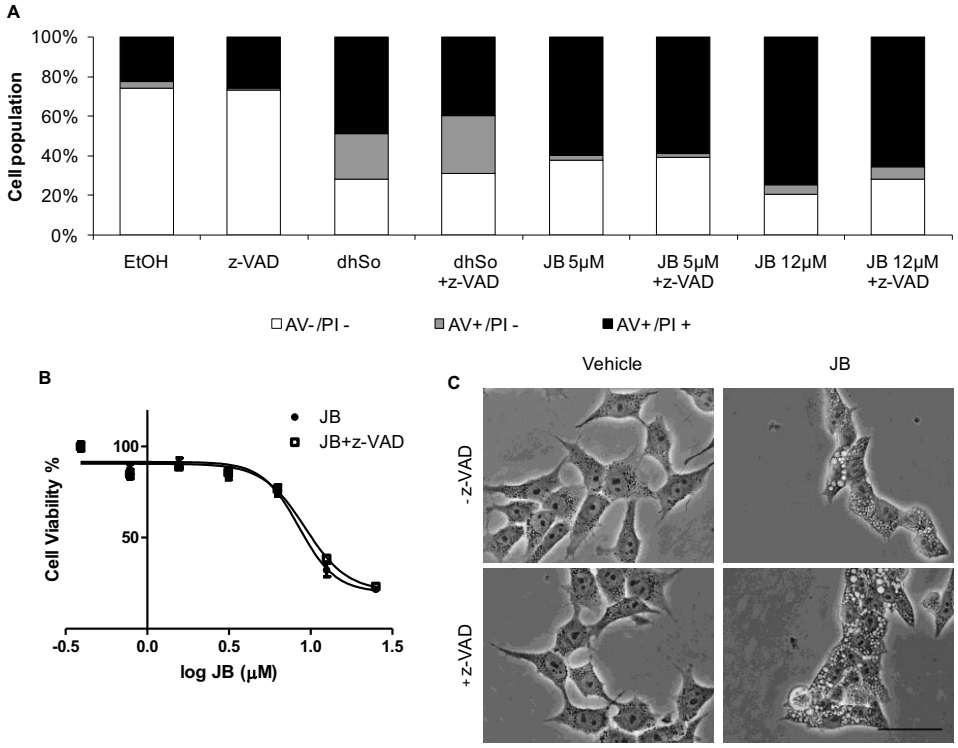

Figure 5.17: JB cause non apoptotic cell death in HGC-27 cells. **A.** Cells were incubated with the indicated concentrations of JB or dhSo 12 µM (or ethanol 0.1% as a control) for 16 hours in presence of 20 µM of z-VAD (or DMSO 0.2% as a control). Cells were stained with Annexin V/PI and fluorescence was analyzed by flow cytometry. Percentages of cell populations stained with AV, PI or both are reported in the histogram. Data are the representative of tree experiments that gave similar results. **B**. Cells were treated with the indicated concentrations of Jaspine B for 16 hours in presence of 20 µM of z-VAD (or DMSO as a control). Cell viability was assessed by MTT assay. Data are expressed as percentage of cell viability over control (n=2). **C.** Phase-contrast images of cells incubated with Jaspine B 5 µM or ethanol as a vehicle for 16 h in presence of z-VAD 20 µM (+z-VAD) or DMSO as a vehicle (-z-VAD). Images are representative of the phenotype observed in three independent experiments. Scale bar: 50 µM.

With the same aim cells treated with different concentration of JB were analyzed by flow cytometry after double labeling with annexin-V (AV), that stains apoptotic cells, and propidium iodide (PI) that is not permeable to live cells and bind DNA. Results showed that AV-positive cells presence was not increased upon treatment with 5 μM of JB (2% of AV positive cells) over the control (3% of AV positive cells). The same was observed also when HGC-27 were treated with 12 μM of JB (4% of AV positive cells). On the contrary, a built up of AV and PI double positive cells was observed while increasing JB concentration. Moreover cells treated with the pro-apoptotic molecule dhSo (that showed a LD_{50} of 12 μM after 16 hours treatment in HGC-27 cells, not shown) resulted in around 20% of cells positive for AV (**Figure 5.17, A**).

These results showed that dhSo induced apoptotic cell death, while almost no signs of apoptosis were detected in presence of JB. The pan-caspase inhibitor z-VAD did not change the AV/PI staining obtained for JB treatment, confirming that apoptosis is not involved in JB-induced cell death. Remarkably, the addition of z-VAD to dhSo treated cells did not rescue cells from dhSo induced apoptosis, suggesting that the sphingoid base probably activates a caspase-independent apoptotic mechanism in this cell line (**Figure 5.17, A**). In addition phase contrast microscope analysis showed that z-VAD did not prevent cytoplasmic vacuolization, confirming that this is not an apoptotic phenotype (**Figure 5.17, C**).

Apoptosis and necrosis give a characteristic pattern of DNA degradation: in apoptosis DNA is enzymatically cut in fragments that are visible in agarose gel as defined bands, while during necrosis DNA is highly degraded and it appears as a smear in the agarose gel[346]. To further confirm that apoptosis was not involved in JB cell death, DNA pattern was analyzed. The electrophoresis results showed that JB did not produce neither DNA laddering nor smearing, finding out that DNA content is not degraded (**Figure 5.18**).

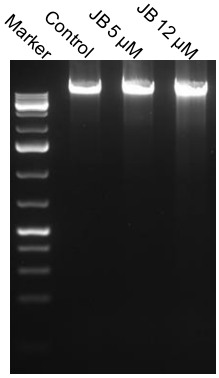

Figure 5.18: JB does not induce DNA degradation. HGC-27 cells were treated with, JB 5 μM or 12 μM or ethanol (0.12%) as a control for 16 hours. After extraction, DNA was run on agarose gel containing SYBR green. 100 Kb DNA standard was used as a marker. Image represent a typical experiment repeated two times that give similar results.

All together this findings suggest that caspase-dependent apoptosis is not involved in JB induced cell death and that cytoplasmic vacuolization is not related to this process. Although AV/PI staining might give an indication for apoptotic or necrotic cell death, DNA analysis showed that even though the cells were permeable to PI, a necrotic mechanism is not activated.

Moreover HGC-27 cells showed to be resistant to caspase-dependent apoptosis even upon treatment with the apoptosis inducer dhSo. It has been extensively reported that many cancers harbor mutations in genes that are essential to promote apoptotic cell death, between them PTEN and p53[347]. HGC-27 cells are characterized by mutated PI3KCA[348] with high level of AKT activity and Akt phosphorylation; moreover they show very low levels of PTEN expression[341]. Since activation of Akt has been suggested to associate with chemoresistance[349], it is not surprising that HGC-27 cells respond with mechanism that differs from the caspase-dependent apoptotic cell death. Alternative mechanisms that can execute programmed cell death involve several cellular organelles, including mitochondria, ER and lysosomes[322]. For instance the latter strategy has been reported by Ullio *et al*., describing sphingosine as an inducer of lysosomal membrane permeabilization and responsible for apoptotic-like cell death in hepatoma cells[99].

5.3.3. JB causes autophagy-independent LC3-II elevation

Autophagic cell death, one of the most widely studied alternatives to apoptosis, is characterized by the formation of small vesicles called autophagosomes and autolysosomes[350]. Autophagy can be activated to trigger cell death or as a protective mechanism to overcome stressful conditions in cancer cells[326]. The activation of the autophagic machinery after treatment with JB was investigated. For this end the autophagic marker LC3-II was quantified to confirm the activation of autophagy. Results showed increase of LC3-II levels in JB treated samples over the control, that was enhanced by protease inhibitors (**Figure 5.19**).

Since SLs such as dhCer and S1P are involved in autophagy regulation[351,352], we wondered if increased levels of LC3-II were related to the alteration of the SLs metabolism induced by JB. To check this hypothesis, cells were treated with JB in presence or absence of myriocin that was already shown to reduce dhCer, dhSM, dhSo and dhSoP levels (**Figure 5.16, A**) and LC3-II levels were determined by immunoblotting. Myriocin treatment resulted in the reduction of JB induced LC3-II levels. Nevertheless, also the levels of basal autophagy decreased with myriocin, suggesting that the inhibition of the

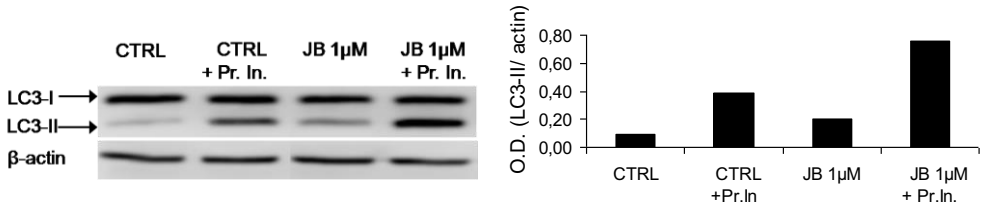

Figure 5.19: JB induces LC3-II accumulation. HGC-27 cells were treated with JB 1 µM for 1 hour in presence or absence of protease inhibitors (Pr.In.: Pepstatin-A 5 µgr/ml and E64-d 10 µgr/ml) that were preincubated during 2 hours. LC3-I and LC3-II level were detected by western blot form cell lysates. Bands intensity was determined by densitometry analysis using LI-COR Image Studio Lite Software. LC3-II levels were normalized with β-actin as a loading control. Reported results are an example of three different experiments that gave similar results.

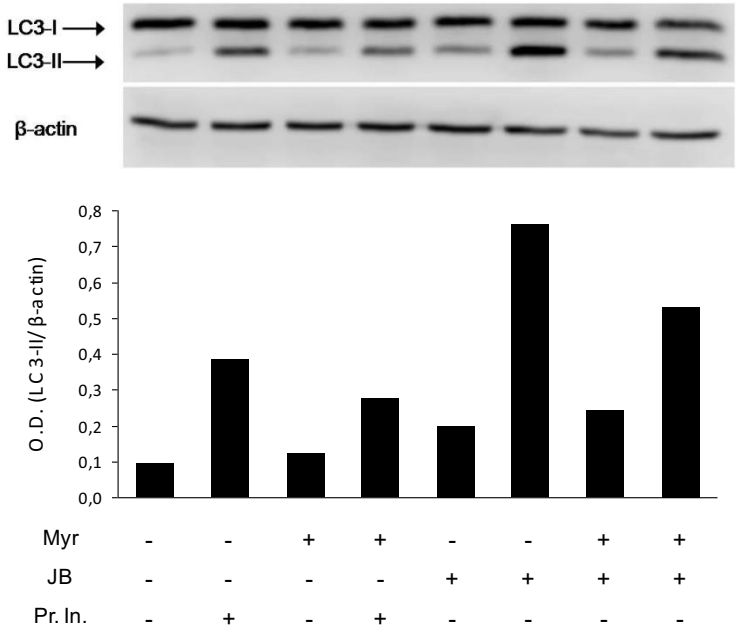

Figure 5.20: Effect of myriocin on LC3-II production. HGC-27 cells were treated with myriocin (Myr) 0.1 µM or ethanol as vehicle for 8 h and then with JB 1µM for 16 h. In the indicated cases (Pr. In.) a pre-treatment with protease inhibitors (E64d 10 µgr/ml, Pepstatin A 5 µgr/ml) was supplied 2 h before myr treatment. LC3-I and LC3-II were detected by western blot as autophagic markers in cell lysates. Bands intensity was determined by densitometry analysis using LI-COR Image Studio Lite Software. LC3-II levels were normalized with β-actin as a loading control. Data are representative of two separated experiments that gave similar results.

synthesis *de novo* of sphingolipids has the same effect on LC3-II levels also in basal conditions (**Figure 5.20**). Increased levels of LC3-II in presence of protease inhibitors show that LC3-II accumulation is not due to altered protein degradation and accumulation.

The activation of autophagy by JB treatment was further investigated by using the autophagy inhibitor wortmannin (Wt), a class III PI3K inhibitor[353] that actuates at the beginning of the autophagic process. First cell viability was evaluated after JB treatment in presence of Wt, showing that 100 nM Wt had no effect on JB cytotoxicity, while 500 nM Wt decreased cell viability, with a LD_{50} of 4.2 μM compared to 9.3 μM given by JB alone (**Figure 5.21**).

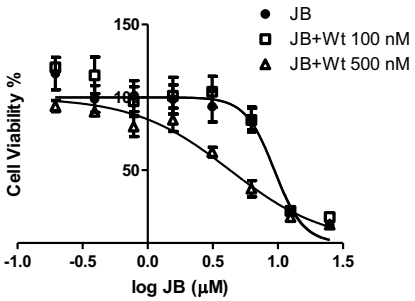

Figure 5.21: Wortmannin increase JB cytotoxicity. Cells were treated with different concentrations of JB for 16 hours after a preincubation of 1 hour with wortmannin (Wt) 100 nM or 500 nM or DMSO as a vehicle. Cell viability was assessed by MTT assay. Data are expressed as percentage of cell viability over control and are representative of three independent experiment that gave similar results.

In order to confirm that the increased cell death caused by Wt was due to the inhibition of autophagy, LC3-II was quantified in cells treated with JB together with wortmannin. Western blotting analysis showed that JB produced a concentration dependent LC3-II accumulation. Unexpectedly neither 100 nM, nor 500 nM of wortmannin showed a decrease of LC3-II levels (**Figure 5.22**).

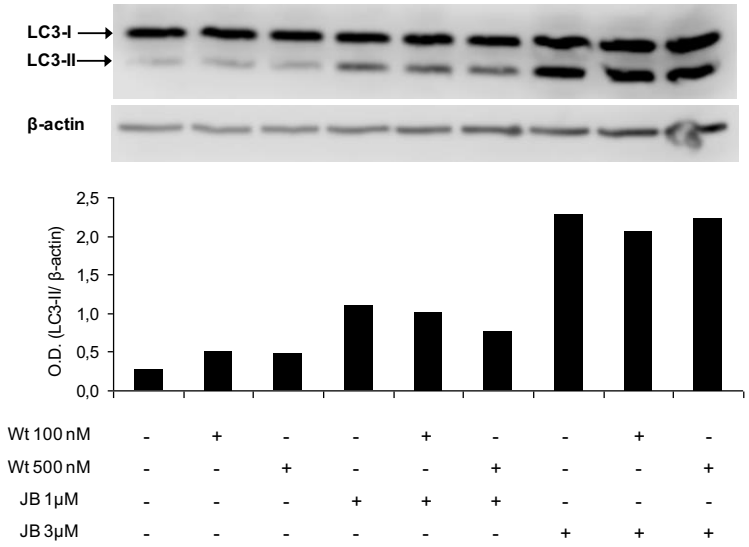

Figure 5.22: JB does not induce autophagy in HGC-27 cells. Cells were previously incubated with wortmannin (Wt) 100 nM or 500 nM (or DMSO as vehicle) during 1h and then with Jaspine B 1 μM or 3 μM (or ethanol as vehicle) for 16 h. LC3-I and LC3-II were detected by western blot as autophagic markers in cell lysates. Bands intensity was determined by densitometry analysis using LI-COR Image Studio Lite Software. LC3-II levels were normalized with β-actin as a loading control. Reported results are an example of three different experiments that gave similar results.

Autophagy activation was further investigated by the quantification of p62, an ubiquitin-binding scaffold protein that is degraded during the autophagic process[354]. Results showed no difference in p62 levels between samples treated with ethanol as a control or JB 1 and 3 μM (**Figure 5.23**).

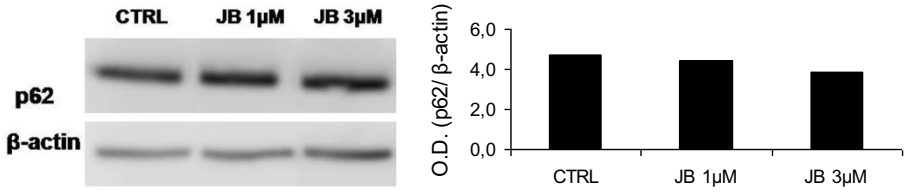

Figure 5.23: JB does not change p62 levels. HGC-27 cells were treated with the reported concentrations of Jaspine B for 16 hours (or ethanol as a control). p62 was detected by western blot in cell lysates. Bands intensity was determined by densitometry analysis using LI-COR Image Studio Lite Software. LC3-II levels were normalized with β-actin as a loading control. Reported results are an example of two different experiments that gave similar results.

In addition the effect of the activation of the autophagy kinase regulator mTOR[355] was investigated in JB treated cells. For this end cell viability was assessed in presence of the inhibitor of mTOR, rapamycin. Results showed that autophagy induction did not change cell viability (**Figure 5.24**).

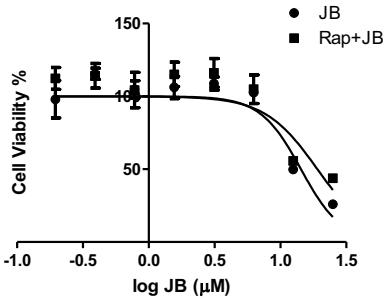

Figure 5.24: Rapamycin does not change Jaspine B cytotoxicity. HGC-27 cells were incubated with the reported concentrations of Jaspine B after a preincubation of 6 hours with rapamycin (Rap, 1μM). Cell viability was assessed by MTT assay. Data are expressed as mean ± SD (n=3)

Finally the involvement of autophagy was investigated trough electron microscopy analysis. As shown in **Figure 5.25, A-B** vacuoles induced after JB treatment appeared as single membrane structures that are no compatible with the double membrane structures that characterize autofagosomes[356]. Moreover comparison with XM462 treatment, a molecule that causes autophagy in this cell line[80], clearly showed that vesicles produced by this treatment had different shape, contain electron-dense particles, and in some case a double membrane can be identified, confirming the different nature of JB vacuoles from the autophagic structures produced by XM462 treatment (**Figure 5.25, C-D**). Moreover vesicles produced by XM462 were not visible by phase contrast microscopy (not shown), underlining the difference with JB induced cell vacuolization.

All together these findings suggest that autophagy is not activated as a cell death mechanism in HGC-27 cells by JB. Despite the increased levels of LC3-II in presence of protease inhibitors indicate the presence of an autophagic flux, the use of Wt did not confirm this evidence. Therefore the increased toxicity observed when Wt was added to JB treatment was not paralleled in a decrease of LC3-II, suggesting that autophagy is not involved in the process. Accordingly unchanged levels of p62 also exclude the activation of autophagic machinery. Moreover the lack of effect of rapamycin on JB cytotoxicity suggests mTOR independence from the cytotoxic effect of JB. In addition the inhibition of SLs *de novo* synthesis by myriocin reduced LC3-II levels in both JB-treated and control samples, suggesting that myriocin decrease basal autophagy. However alteration of the SL

metabolism induced by JB is not related to increased levels of LC3-II in HGC-27 cells. The different nature of JB induced vacuoles compared to the autophagic structures visible after cell treatment with XM462 further confirmed this evidence. The increase of JB cytotoxicity given by the addition of Wt is probably related to a mechanism that is independent from autophagic cell death. Yu *et al*. reported that pretreatment with Wt was able to attenuate cells resistance to etoposide and doxorubicine in two different gastric cancer cell lines[341]. Similarly increased cytotoxicity in HGC-27 cells might be due to the effect of Wt that by inhibiting class III-PI3K make cells more sensitive to JB.

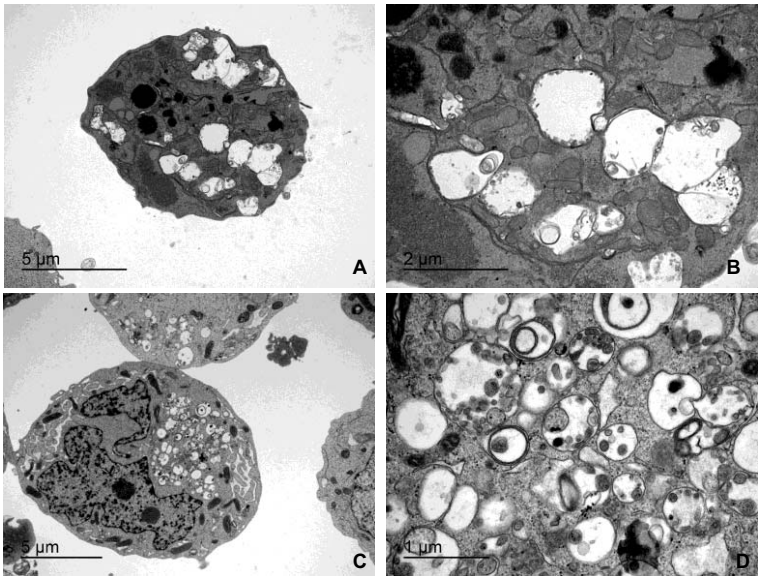

Figure 5.25: JB induced vacuoles are not autophagic structures. Transmission electron micropraphs of cells treated with JB 5µM (**A**) or XM462 8 µM (**C**) for 16 hours. **B** and **D** represents magnification of JB and XM462 treated cells respectively. Arrows indicate single (**B**) or double (**D**) membrane vesicles. The experiment was run in triplicate; images are representative of the observed phenotypes.

Although LC3-II is a widely used marker for autophagy detection, it has been recently described that different treatment can induce non-autophagic cell death with increased levels of LC3-II associated to cell vacuolization. For instance Manumycin A, a natural antibiotic, was reported to induce non-autophagic LC3-mediated cytoplasmic vacuolization and cell death in breast cancer cells[357]. In a different study increased levels

of LC3-II induced by lymphoma cells treatment with the cannabinoid receptor agonist WIN55,212-2 were shown to be unrelated to classical autophagy[358]. In addition Maltese group described a new form of non-apoptotic cell death, named methuosis, that is characterized by the same phenotype and can be associated to LC3-II elevation[335].

5.3.4. Is methuosis responsible for cell death?

The observation of the cell phenotype induced by JB treatment, the autophagic-independent elevation of LC3-II protein and the lack of apoptosis activation led us to investigate methuosis as JB-induced cell death mechanism. Methuosis is characterized by large fluid-filled vacuoles that originate from macropinocytosis, a clathrin-independent pathway of endocytosis[359], distinguished by the formation of protrusions that elongate from the plasma membrane and encapsulate extracellular fluids[336].

First the involvement of an endocytic process in cell vacuolization was investigated by using the H^+-ATPase inhibitor Bafilomycin A1 (Baf-A1) that was reported to impede the formation of vesicular intermediates between early and late endosomes[360], and to block endosomal vacuolization induced by *H. pylori*[361]. Cell treatment with Baf-A1 prior to the incubation with JB prevented cytoplasmic vacuolization, suggesting the involvement of the endocytic compartment (**Figure 5.26**).

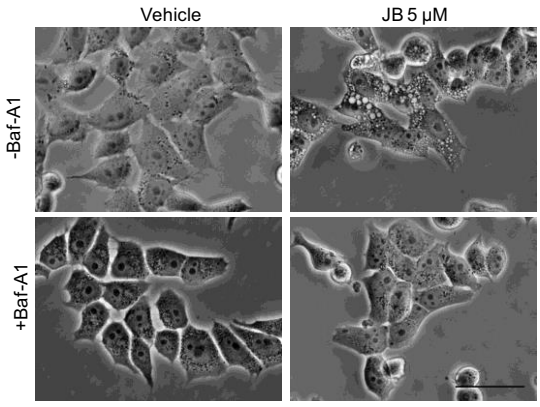

Figure 5.26: Bafilomycin-A1 impairs Jaspine B induced vacuolization. Phase-contrast images of HGC-27 cells treated with JB for 24 hours or ethanol as vehicle, after 1 hour of pre-incubation with Baf-A1 100 nM or ethanol (- Baf-A1). Pictures are representative of the phenotype, observed in two independent experiments. Scale bar: 50 µM.

The nature of the endocytic vacuoles was further investigated by treating cells with 5-(N-Ethyl-N-isopropyl)amiloride (EIPA), a Na^+/H^+ exchanger inhibitor that blocks

macropynocitosis[362,363]. As shown in **Figure 5.27, A** EIPA treatment prevented JB induced cell vacuolization. The origin of the cytoplasmic vacuoles was also confirmed by using Lucifer Yellow (LY), a fluid-phase tracer that has been reported to be incorporated inside cells during macropinocytosis[334,364]. Therefore cells were treated with JB in presence of LY and vacuoles formation was analyzed by fluorescence microscopy. Results showed that the cytoplasmic vacuoles that are visible in the contrast phase images, perfectly correspond to rounded-shaped vacuoles filled with the fluorescent tracer (**Figure 5.27, B**), confirming that vacuoles exhibit characteristics of micropinosomes.

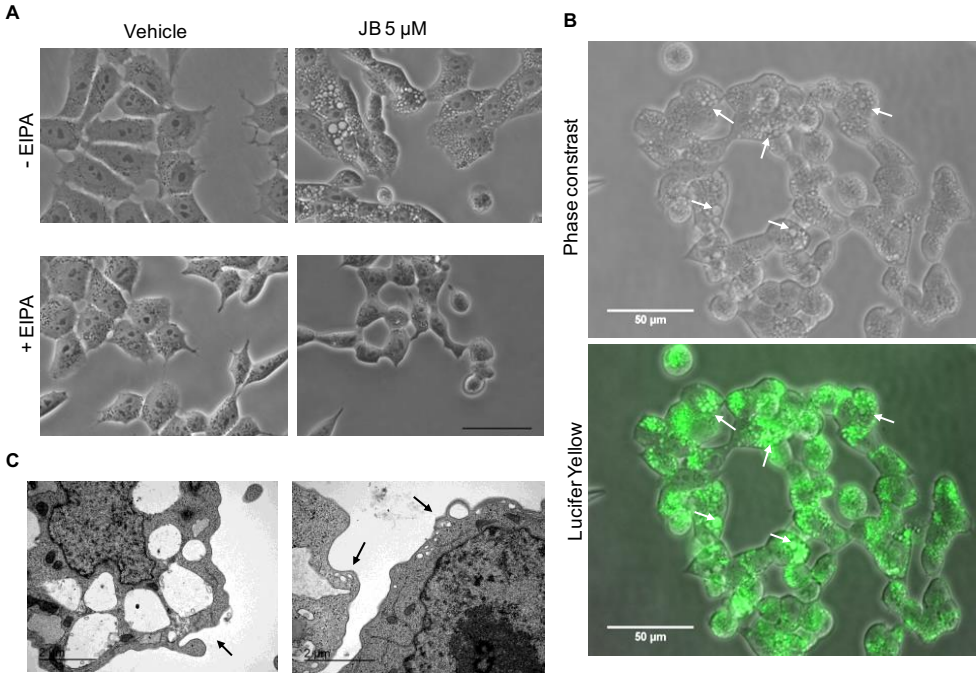

Figure 5.27: Vacuoles induced by JB exhibit characteristics of micropinosomes. A. HGC-27 cells were treated with JB 5 µM (or EtOH as a vehicle) after 1 hour of pretreatment with EIPA 25 µM (or MeOH) as vehicle. Phase-contrast images were taken after 24 hour of incubation and are representative of the phenotype, observed in three independent experiments. Scale bar: 50 µM. **B.** Phase contrast and fluorescence microscopy images of HGC-27 cells after 16 hours co-incubation with JB 5 µM and Lucifer Yellow (1 mg/ml). Images are representative of the results obtained in three independent experiments. **C.** Transmission electron micrograph of HGC-27 treated with 5 µM of JB. After 16 hours cell were fixed and analyzed. Arrows indicate membrane extension (left panel) and nascent micropinosomes (right panel).

Moreover TEM analysis of cells treated with JB showed the presence of extensions of the cell surface and small vesicles in the peripheral area (**Figure 5.27, C**), suggesting that vacuoles originate from cell membrane engulfment and then coalesce into bigger structures, in agreement with the mechanism described for macropinosomes formation.

Our results provide evidence for massive initiation of macropinocytosis by JB and suggest that macropinoytic bulk cytoplasmic vacuolization might be responsible for irreversible cell damage. Considering that macropynocitic vacuolization is the leading force of methuosis, this might be the postulate mechanism for JB-induced cell death.

All together our results showed that JB induces cell death in a gastric cancer model by activating a mechanism characterized by bulk cytoplasmic vacuolization. Cell vacuolization and cytotoxicity are independent from caspase activity; moreover annexin-V staining and lack of DNA laddering confirmed that apoptosis is not activated. Although JB treated cells were positive for PI, the absence of DNA degradation suggested that cells were not necrotic. PI probably entered because of membrane damage or permeabilization. JB-induced vacuoles does not share the features of autophagic vesicles, moreover LC3-II increase is not impaired by treatment with wortmannin, suggesting that autophagy is not involved in cell death. In agreement p62 levels did not change. The independence from mTOR was also demonstrated, confirming that autophagy is not responsible for cell death.

Methuosis has been recently reported as a novel non-apoptotic cell death mechanism[333]. The current understanding of methuosis specifies that this form of cell death, characterized by large fluid-filled cytoplasmic vacuoles[335], involves the stimulation of macropinocytosis, combined with defects in clathrin-independent endocytic vesicle trafficking, ultimately leading to extreme vacuolization and rupture of the cell[338].

The peculiar phenotype induced by JB treatment in gastric cancer cells prompt us to investigate the nature of the cytoplasmic vacuolization. First the involvement of the endosomal compartment was investigated by using the H^+-ATPase inhibitor Baf-A1. A deeper characterization of the JB-induced vacuoles was achieved by using the macropinocytosis inhibitor EIPA and the intracellular tracer Lucifer Yellow, and led to define endosomal vesicles as macropinosomes. Electron micrographs clearly confirmed this evidence, showing protrusion and nascent vesicles on cell surface, in agreement with the macropinocytic mechanism[365]. These results suggest that JB-induced cell vacuolization is related to hyperstimulation of macropinocytosis and may play an important role in cytotoxicity. Moreover the presence of lucent vacuoles in glioblastoma and alveolar adenocarcinoma cells, after JB treatment indicates that the natural sphingolipid activate this process also in other cell lines.

The presence of different-sized vesicles in cells, some with small dimension and closely localized to the external margin of the cell, others with greater extension and occupying a wide area in the cytoplasm, indicates that macropinosomes might coalesce into wider structures. This observation suggests that micropinosomes probably do not undergo a maturation or recycling process as usually happens in regulated macropinocytosis[366], pointing out a possible alteration in the endocytic trafficking. The characterizing features of methuosis induced by different mechanism and molecules have been recently defined by Maltese[335]. In one of the reported studies caspase activation, although strictly related to apoptosis, was detected. However treatment with the broad-spectrum caspase inhibitor z-VAD did not prevent loss of viability[338]. In agreement with this model JB induced both cell death and cytoplasmic vacuolization were independent from z-VAD treatment. In the first report of methuosis, Ras induced vacuolization in gastric cancer and glioma cells was connected to autophagy[367]. Further studies confirmed an increase of LC3-II levels, nevertheless immunofluorescence staining showed that cytoplasmic vacuoles were separated by LC3-II positive autophagososmes[334], pointing out that vacuoles were not autophagic structures. As above mentioned, high levels of LC3-II were associated with JB treatment, nevertheless also in this case vacuoles were shown to be different from autophagosomes. Another reported feature of methuosis is the lack of alteration of cell nucleus[334]; in line with this observation, vacuolization in HGC-27 cells perturbed mainly the cytoplasm, without altering nucleus in the cells. All together our findings strongly suggest that methuosis might be the activated as cell death mechanism in JB treated cells. Although the stimulation of macropinocytosis was proved in the present study, further investigation is necessary to better identify defects in macropinosomes recycling or maturation process. In this contest the involvement of GTPase as Arf6[368] and Rab5[369] that regulate those events, has been reported in methuosis[337,338], thus representing a eligible mechanism to be explored. It is worth noting that compared to other well-know mechanism, as apoptosis or autophagy, methuosis represents a newly reported form of cell death that is still not completely characterized and lacks well established molecular markers, making its clear identification difficult.

Recent studies have reported that various genetic or pharmacological manipulation induce non-apoptotic cell death with the involvement of macropinocytosis in a broad spectrum of cancer cells[370–372], including those that are resistant to conventional apoptosis-inducing drugs. Thus it is not surprising that HGC-27 cells, that present genetic mutations related to chemoresistance[341], might activate an alternative response to JB treatment. Recently the screening of a library compound through multidisciplinary and multisystem studies revealed a new molecule that induces cell death in glioblastoma cells

through "catastrophic vacuolization"[371], generating considerable interest in this new cell death mechanism[373].

In summary the investigation on JB induced cell death showed that is it characterized by non-apoptotic, non-autophagic cytoplasmic vacuolization. Vacuoles originating from bulk macropinocytosis might be responsible for JB cytotoxity and suggest the involvement of methuosis as cell death mechanism.

6. Inhibition of dihydroceramide desaturase activity by the sphingosine kinase inhibitor SKI II

Sphingosine kinase is a central enzyme in the sphingolipids metabolism that controls the balance between pro-apoptotic ceramide and sphingosine and mitogenic sphingosine-1-phosphate[124]. SK1 is widely characterized as a pro-survival and proliferating molecule[263], while SK2 has not been as well characterized and data about its involvement in physiological functions and in disease is controversory[253].

In light of SKs role in cell fate control, they became attractive targets in the development of cancer therapeutics. Many SK inhibitors with different selectivity against the two isoforms have been developed in the last years[374]. Among them SKI II has been widely used as a pharmacological tool to prove the involvement of sphingosine kinase and sphingosine-1-phosphate in cancer disease[375,376]. In a study published by Illuzzi *et al.*[377] SKI II was used to investigate the role of SK on A2780/4-HPR cells resistance to the antineoplasic drug fenretinide (4-HPR), a dihydroceramide desaturase inhibitor. This clone was obtained by culturing A2780 human ovarian cancer cells, that were shown to undergo apoptosis by treatment with 4-HPR, with increasing concentrations of this molecule. A2780/4-HPR cells are characterized by a 10-fold increase in resistance respect to parental sensible cells, moreover they are less responsive to 4-HPR in terms of dihydroceramide production. In this work authors found that SK activity was remarkably augmented in these cells, producing high levels of S1P, and leading to a lower dhCer/S1P ratio. Pharmacological inhibition of SK reduced S1P levels and was able to rescue cell sensitivity to 4-HPR treatment. Lipidomic analysis showed that 4-HPR treatment provoked an increase in intracellular dhCer levels, which was dramatically enhanced by the co-incubation with SKI-II. Interestingly, treatment with SKI II alone also caused a significant increase in dhCer, however this result was not further investigated by the same authors.

Likewise, in our work with JB we found that SKI II also increased dhCer levels in HGC-27 cells (not shown). These data prompted us to investigate the possibility of SKI II inhibiting Des1. The inhibition of Des1 by using chemical molecules[85] or its ablation by genetic manipulation[243] already showed that dhCer accumulation trigger a variety of cellular signalling and cellular responses, underlining its role as bioactive molecule.

In this section we aimed to investigate a new role of SKI II as dihydroceramide desaturase inhibitor. The alteration of the SL metabolism and the related biological effects is reported. Results are part of the following publication:

Cingolani F., Casasampere M., Sanllehí P., Casas J., Bujons J., Fabrias G. *Inhibition of dihydroceramide desaturase activity by the sphingosine kinase inhibitor SKI II.* J Lipid Res. 2014 May 29;55(8):1711-1720

6.1. SKI II inhibits both SK and Des1

6.1.1. SKI II inhibits Des1 activity in both intact and cell lysates

First SKI II cytotoxicity was determined in HGC-27 cells, showing a LD_{50} value of 84 μM (**Figure 6.1**). Therefore the standard concentration used to inhibit SK (10 μM) was not cytotoxic in these cells and was used to perform the inhibition assays.

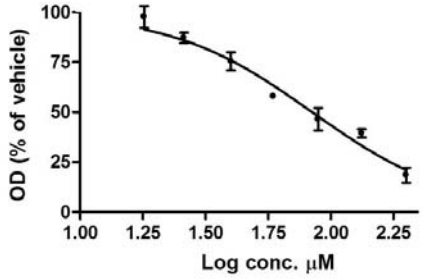

Figure 6.1: Effect of SKI II on cell viability. HGC-27 cells were treated with different concentrations of SKI II for 24 h and the number of viable cells was determined by the MTT test. Data correspond to the average ± SD of two independent experiments with triplicates.

The inhibition of Des1 by SKI II was investigated in both HGC-27 intact and cell lysates. For this end the conversion of the fluorescent dihydroceramide analogue *N*-[6-[(7-nitro-2-1,3-benzoxadiazol-4-yl)amino]hexanoyl]-D-*erythro* dihydrosphingosine (dhCerC6NBD) to the ceramide analogue *N*-[6-[(7-nitro-2-1,3-benzoxadiazol-4-yl)amino]hexanoyl]-D-*erythro* sphingosine (CerC6NBD) in presence of SKI II was evaluated. Results showed that SKI II produced significantly lower amounts of CerC6NBD and consequently of its metabolite NBD-labelled sphingomyelin in intact cells compared to the control after 4 hours of incubation (**Figure 6.2, A**). Des1 inhibition also occurred in cell lysates for the same time of treatment (**Figure 6.2, B**). In both cases SKI II inhibition was similar to that observed with XM462, a dhCer desaturase inhibitor included as a positive control[250].

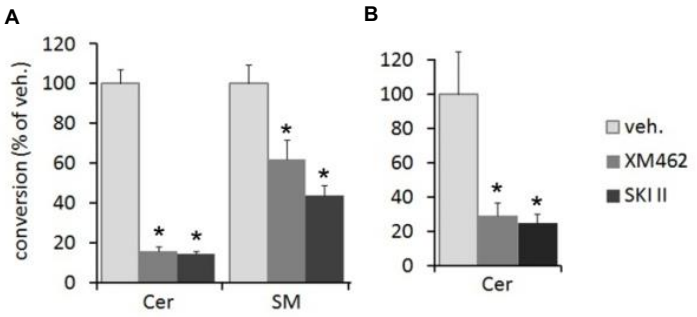

Figure 6.2: Inhibitory activity of Des1 by SKI II. Intact cells (**A**) or cell lysates (**B**) were treated with either vehicle (ethanol), SKI II (10 µM) or XM462 (8 µM) and incubated with the Des1 reaction substrate (dhCerC6NBD, 10 µM). After 4 h, cells were collected (**A**) or the reaction was stopped by adding methanol (**B**). Samples were processed as described in the experimental section for analysis by HPLC coupled to a fluorimetric detector. Data correspond to the average ± SD of three experiments with triplicates. Asterisks indicate statistical significance ($p \leq 0.05$, unpaired two - tail *t* test).

6.1.2. Determination of kinetic parameters for SKI II as Des1 inhibitor

First the IC_{50} of SKI II against Des1 was evaluated by incubating cell lysates with dhCerC6NBD as substrate in presence of different concentrations of SKI II. Results showed an IC_{50} of 0.6 µM after 4 hours of incubation (**Figure 6.3**).

Then the potency of SKI II as a Des1 inhibitor was investigated. For this end cell lysates were incubated with various amounts of the compound and different substrate concentrations during 4 hours. Results showed that concentration-dependent inhibition was observed at all doses. Moreover, while K_m did not change, V_{max} decreased with increasing SKI II concentrations, which is in accordance with non-competitive type of inhibition, with a calculated K_i of 0.3 µM (**Figure 6.4**).

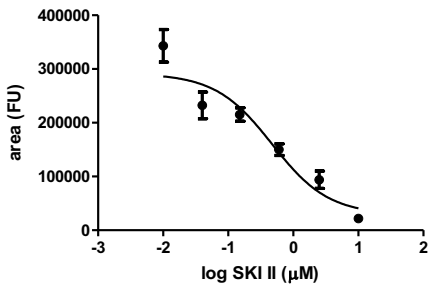

Figure 6.3: IC_{50} of SKI II against Des1. HGC-27 cell lysates were incubated with either SKI II at the reported concentrations, or ethanol as a vehicle, for 4 hours. Reaction was stopped by adding methanol. Samples were processed as described in the experimental section for analysis by HPLC coupled to a fluorimetric detector. Data correspond to the average ± SD of three independent experiments with triplicates.

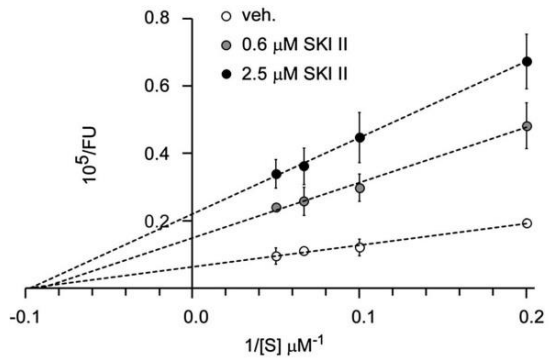

Figure 6.4: SKI II is a non-competitive inhibitor of Des1. HGC-27 cell lysates were treated with either vehicle (ethanol) or the reported concentrations of SKI II and 5 μM, 10 μM, 15 μM or 20 μM of dhCerC6NBD as substrate during 4 hours. Des1 activity was assessed as reported in Materials and Methods section. Data correspond to the average ± SD of three independent experiments with triplicates.

6.1.3. Des1 is not degraded after SKI II treatment

A part from the inhibition of SK enzymatic activity, it has been reported that SKI II induce SK1 degradation by either lysosomal[255] or proteosomal pathway[256]. In order to check if the inhibition of the catalytic activity of Des1 by SKI II was also combined with the protein degradation, Des1 levels were examined. Western blot analysis showed that Des1 exhibited similar protein levels in comparison to the control in presence of SKI II (**Figure 6.5, A**). Conversely SK1 protein levels were substantially reduced in cells exposed to SKI II at the same concentration, which agrees with published reports in other cell models[256] (**Figure 6.5, B**).

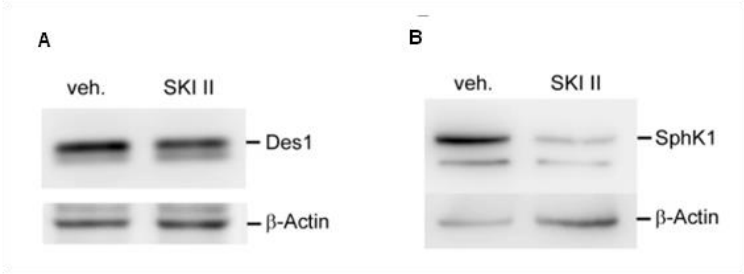

Figure 6.5: SKI II cause SK 1 but not Des1 degradation. HGC-27 cells were incubated with SKI II 10 μM or ethanol as a vehicle for 3 hours. Des1 and SphK1 proteins were detected by Western blot in cell lysates as detailed in Materials and Methods. β-actin was used as a loading control. Images are representative of three to five independent experiments with similar results.

Altogether these results describe SKI II as a non-competitive inhibitor of Des1 with an IC_{50} of 0.6 μM and a K_i if 0.3 μM. The inhibitory effect of SKI II was not paralleled by a degradation of Des1, while a reduction in SK1 protein was evident.

Since SKI II is not a structural analogue of Des1 substrate, a direct interaction with the desaturase protein is probably not responsible for the inhibition. SKI II might affect Des1 activity by modifying the redox status of the enzyme environment, which has been reported to affect Des1 activity[245]. Although SKI II has been shown to induce oxidative stress[378], in line with the hypothesis of an altered redox status of the cell, the occurrence of inhibition in cell lysates is against this theory. Thus, Des1 inhibition by SKI II is more likely related to SKI II action on other components of the electron transport chain associated to the enzyme.

This hypothesis was investigated by Dr. Jordi Bujons and Pol Sanllehí as a part of this work[379], by molecular modelling studies. Comparison of the structure of SKI II with those of flavonoids which are known to inhibit NADH-cytochrome b5 reductase (CB5R)[380,381], such as luteolin, showed a significant shape and electrostatic character coincidence. Since it has been proposed that this flavonoid and other related compounds could bind to the NADH binding site of CB5R[382], the potential binding of SKI II at that site was examined using an *in silico* docking method. Results showed that SKI II could interfere with the binding of different parts of the NADH molecules. Analogue docking experiments ran with the known CB5R inhibitors luteolin, quercetin and (+)- taxifolin showed similar results, supporting the supposed mechanism.

6.2. Sphingolipidome analysis

The effect of SKI II treatment on the sphingolipidome was evaluated after treating HGC-27 cells with a concentration of 10 μM of the inhibitor for 0.5, 4, 8, 24 and 48 hours. Levels of dhCer exhibited a 20-fold increase over controls at 4 hours after treatment and then decreased slowly to reach a constant level that was maintained up to the latest time point determined (48 hours). DhCer metabolites, namely dihydrosphingomyelin (dhSM) and dihydroceramide dihexosides (dhCDH, or lactosyldihydroceramide), also increased over controls at 4, 8, 24 and 48 h. Although similar levels of dhSM were found at all these time points, higher amounts of dhCDH occurred at 24 and 48 hours than at 4 and 8 hours. Dihydroceramide monohexosides (glucosyldihydroceramide and galactosyldihydroceramide) have never been detected in

HGC-27 cells under any treatment. As expected from its SK inhibitory activity, S1P was reduced in cells treated with SKI II to almost undetectable levels at all time points sampled. Moreover, inhibition of SK brought about a two-fold increase of the natural substrate So over controls at 4 hours, while ceramide and CMH (ceramide monohexoside, or glucosylceramide and galactosylceramide) and ceramide dihexoside (CDH, or lactosylceramide) increased over controls at 4, 8 and 24 h. In contrast, SM was not remarkably affected by SKI II treatment (**Figure 6.6**).

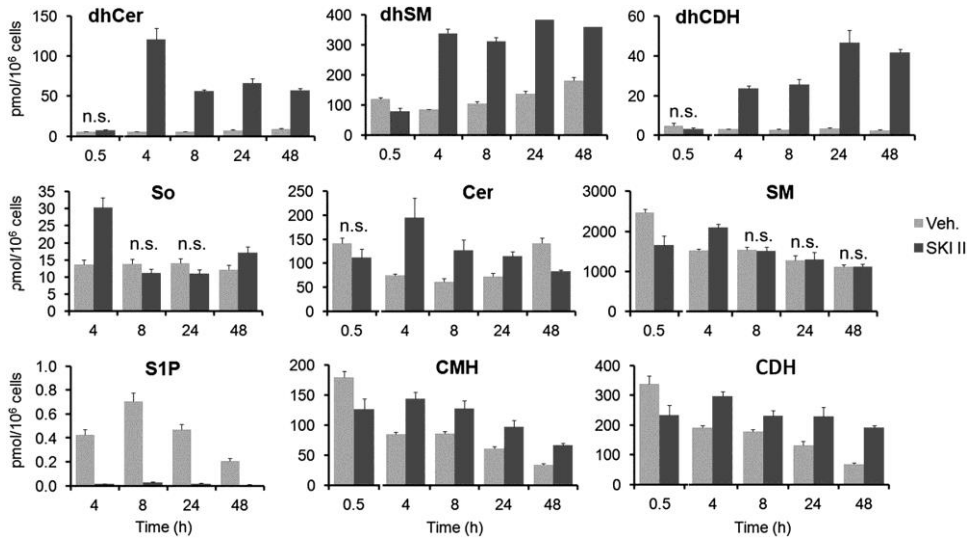

Figure 6.6: Effect of SKI II on the sphingolipid content. HGC-27 cells were treated with either ethanol (vehicle, veh.) or SKI II (10 μM) for the indicated times. Cells were collected and processed for UPLC/TOFMS analysis as described under *Material and Methods*. Data are the average ± SD of three experiments with triplicates. In all cases, except for those indicated with n.s., the differences between means corresponding to control and treated cells are statistically significant ($p \leq 0.05$, unpaired two-tail *t* test). dhCer, dihydroceramide; dhSM, dihydrosphingomyelin; dhCDH, dihydroceramide dihexoside (or lactosyldihydroceramide); So, sphingosine, Cer, ceramide, SM, sphingomyelin; S1P, sphingosine‐1‐phosphate; CMH, ceramide monohexoside (glucosyl and galactosylceramide); CDH, ceramide dihexoside (lactosylceramide).

A parallel study of the sphingolipidome was carried out using PF-543 that has been reported to inhibit SK1[286]. Similarly to SKI II, PF-543 caused S1P reduction to undetectable levels after 8 and 24 hours of treatment and represented the most important effect on the sphingolipidome. Other significant alterations were observed at 8 hours, but

not at 24 hours after treatment. These effects were slight and included a 1.5 fold increase in dhCers and 1.3 and 1.4 fold increase in CMH and ceramide dihexoside CDH respectively (**Figure 6.7**).

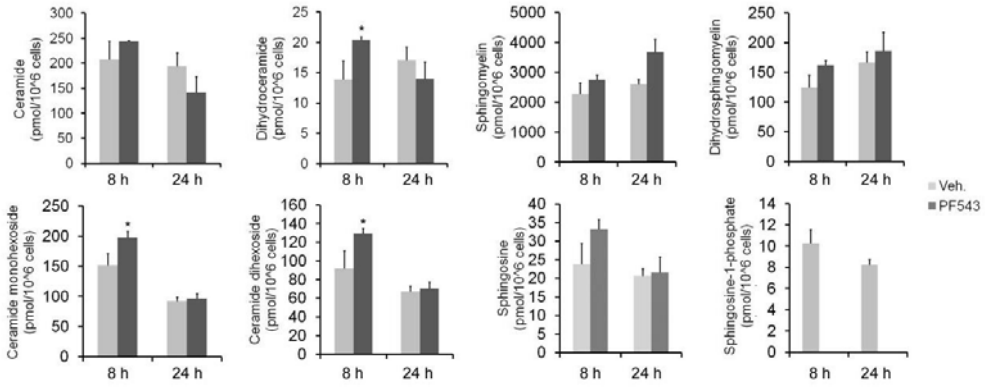

Figure 6.7: Effect of PF-543 on the sphingolipid composition of HGC27 cells. Cells were treated with either ethanol as a vehicle or 1 µM PF-543 for the indicated times. Cells were collected, and lipids were extracted and analyzed as detailed in *Material and Methods*. Data correspond to the average ± SD of two experiments with triplicates. The asterisk denotes statistical significance of treatments *versus* control at $p \leq 0.05$ (unpaired, two-tail *t* test)

Collectively results of sphingolipid analysis are in agreement with the role of SKI II as dual SK and Des1 inhibitor. The main sign of Des1 inhibition was the remarkable accumulation of dhCer for all times of treatment, that was in turn metabolized to dhSM and dhCDH. As expected from its SK inhibitory activity, S1P was reduced to almost undetectable levels in presence of SKI II at all time-points sampled, causing a two-fold increase of the natural SK substrate sphingosine after 4 hours of treatment. The increase in Cer after 4, 8 and 24 hours of treatment is the result of So metabolism by ceramide synthase. Downstream metabolites of Cer, namely SM, CHMs and CDHs also augmented in presence of SKI II. While SM increased over control only at 4 hours time point, CMH and CDH remained higher in SKI II treated cells than in vehicle-treated cells at all time points. These results suggest that conversion into SM is a first response of cells to the deleterious increase in cytotoxic So, while glycosilation is activated as a sustained response. Similar effects were observed by Gao *et al*[374] for SKI-II in A498 kidney adenocarcinoma cells. In this study levels of intracellular S1P were decreased by over 90% after treatment with SKI

II compared to the control group, while total Cer levels increased and amounts of sphingosine were dramatically decreased. These findings agree with the metabolism of the accumulated long chain base into Cer. Of note, also C16-dhCer levels were found to be elevated in SKI-II treated cells. Other SK inhibitors such as DMS and the SK2-selective inhibitor ABC294640 augmented dhCer, although not as much as SKI II[374]. Additional sphingolipids analysis were carried out as part of this work in T98 and HeLa cells, showing inhibition of Des1 also in these cells, thus indicating that inhibition of Des1 by SKI II is not cell line specific.

The sphingolipids analysis of cells treated with the specific SK1 inhibitor PF-543 clearly show that it also causes a decrease of S1P to undetectable levels as SKI II but produces minor alterations for some of the sphingolipid metabolites analysed, mainly dhCer, CMH and CDH.

6.3. Biological effects of SKI II treatment in HGC-27 cells

6.3.1. Decrease of cell proliferation and accumulation of cells at G1 phase

The mitogenic effect of S1P[383] prompt us to investigate the effect of SKI II on cell growth. The inhibitor produced a reduction in cell proliferation after 8 hours of treatment, that was maintained up to the latest time point checked (**Figure 6.8 A**). This effect was not observed when cells were exposed to PF-543 (8 hours: control, 6.11±0.36 10^{-5} cells; PF-543, 5.04 ±0.52 10^{-5} cells; 24 h: control, 0.97±0.78 10^{-5} cells; PF-543, 1.19±1.8 10^{-5} cells).

Examination of the cell cycle of HGC-27 treated for 24 hours with 10 μM of SKI II showed an increase in the number of cells at G1 phase (**Figure 6.8 B,C**) as compared to vehicle treated control cells.

6.3.2. Autophagy induction

Both Des1 and SK have been implicated in autophagy[352]. To check the activation of this mechanism after SKI II treatment, levels of the autophagic marker LC3-II were detected. As shown in **Figure 6.8, D** levels of LC3-II in cells exposed to 40 μM of SKI II for 24 hours were higher than in control cells treated with vehicle and similar to those in

cells treated with XM462 (10 μM, 24 hours), previously shown to induce autophagy in these cells[85]. On the contrary PF-543 treatment did not show LC3-II increase compared to the control.

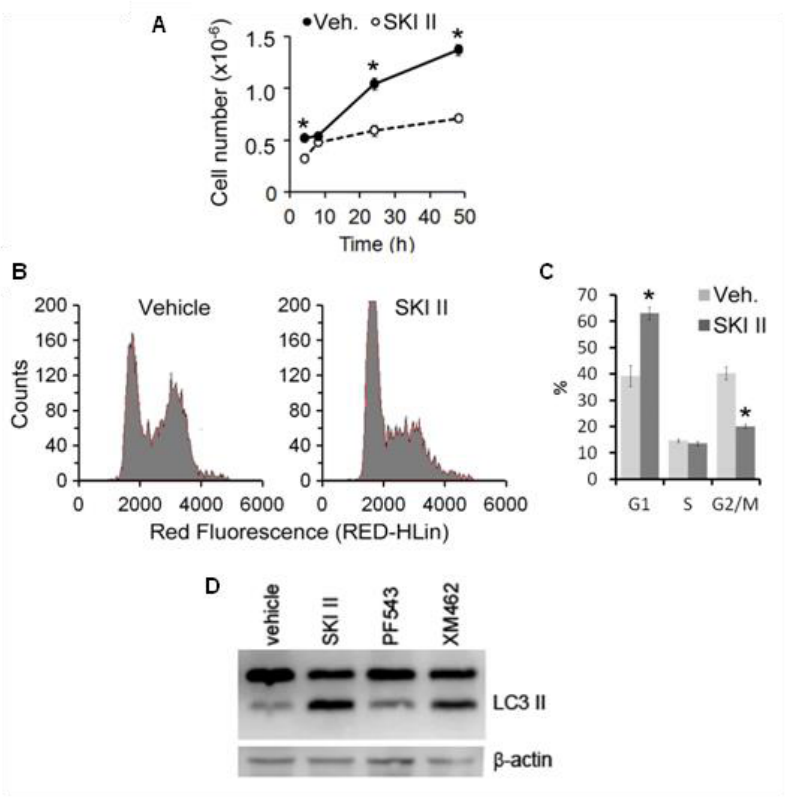

Figure 6.8: Effect of SKI II on proliferation, cell cycle and autophagy. A-C. HGC27 cells were treated with either ethanol as a vehicle or SKI II (10 μM) for 4, 8, 24 and 48 h. Then cells were collected, counted and processed for cell cycle analysis. **A**, Cell proliferation as the number of cells counted with a Countess Automated Cell Counter. **B**, Representative cell cycle histograms obtained from HGC-27 cells after 24 h exposure to vehicle or SKI II. **C**, quantification of the relative number of cells in each stage of the cell cycle (Multicycle AV software). Data are the average ± SD of three experiments with triplicates. Asterisks denote statistical significance ($p \leq 0.05$, unpaired two-tail *t* test). **D**, HGC-27 cells were exposed to SKI-II (40 μM), PF-543 (1 μM) or XM462 (8 μM) for 24 h. Levels of LC3-II were assessed by Western blotting of cell lysates as described under Materials and Methods. β-actin was used as a loading control. The images shown are representative of three independent experiments with similar results.

Collectively this results show that SKI II treatment impair HGC-27 cell proliferation. This is in accordance with the lack of the mitogenic S1P: it has been widely reported that overexpression of SK promotes growth, while decreasing SK activity by either genetic or pharmacological means reduces cell proliferation[267]. Cell cycle analysis showed cell accumulation in G1 phase after SKI II treatment, in agreement with a previous report in leukaemia K562 cells[384]. Similar effects on cell cycle were found with DMS in rat intestinal epithelial cells[385] and by SK1 silencing in breast[386], ovarian[272] and glioblastoma cell lines[387]. In apparent contrast Gao *et al*.[374] reported that SKI II arrested A498 cells in S phase with a concomitant decrease in the G2/M phase, while downregulation of SK1 or SK2 in U87MG cells under hypoxia arrests the cell cycle at G2/M[388]. Even though is not completely clear whether the effect on cell cycle is due to SK or Des1 inhibition, the latter possibility is supported by two experimental evidence. First, the SK1 specific inhibitor PF-543 did not affect HGC-27 cell proliferation, although it avoided S1P production with no remarkable changes in other sphingolipid species. Second, the effect of dihydroceramides at slowing or arresting the cell cycle with accumulation of cells in the G0/G1 phase is well documented[79,80,389]. Therefore, all these elements suggest that the effect of SKI II on cell cycle may be due to the accumulation of dhCer resulting from its Des1 inhibitory activity. SKI II was also able to induce autophagy in HGC-27 cells as shown by the increase in LC3-II levels, while SK1 inhibition by PF-543 did not produce the same effect. This result suggests that autophagy induced by SKI II is due to increases in dhCer rather than to decreased levels of S1P, which occurs with both SKI II and PF-543. It was previously reported by our group that the accumulation of dhCer after Des1 inhibition with XM462 induced autophagy in HGC-27 cell line[85]. In agreement, several studies have reported on the induction of autophagy by treatment with drugs that increase dhCer, such as fenretinide, resveratrol and gamma-tocopherol[236].

All together these results show that SKI II inhibits Des1 with a consequent accumulation of dhCer and its metabolites, thus some of the effects attributed to decreased S1P may be actually caused by elevated levels of these molecules. These findings should be taken into account when using SKI II as a pharmacological tool.

7. Use of chemical tools for ceramidases investigation

Ceramide is hydrolyzed to sphingosine by ceramidases, a family of amidohydrolases characterized by acid, neutral or alkaline optimal pH[176]. Given the opposite role of apoptotic ceramide and proliferating S1P, that is biosynthesized from sphingosine[11], ceramidase activity represents a nodal point in cell fate. The upregulation of AC activity in different types of cancer and its involvement in chemotherapy resistance has been widely studied[196]. Moreover AC deficiency is responsible for Farber disease development[390]. ACER and NC activity have also been related to different biological processes and cellular responses[202], as already reported in the introduction (see Chapter 2, paragraphs 2.2.2.2. and 2.2.2.3.).

The increasing interest on ceramidases involvement in cell physiopathology led us to the develop of chemical tools in our laboratory. With this aim coumarinic analogues of ceramide were synthesized in order to measure ceramidases activity by a high throughput assay. The first analogue named RBM14C16, characterized by C16-fatty acid chain, was described by Bedia *et al.* in 2007[224]. The molecule carries a 2-oxo-2H-chromen-7-yloxy moiety in CH_3-terminal part of the sphingoid chain and releases fluorescent umbelliferone after hydrolysis by ceramidase (**Figure 7.1, A**). Several analogues of the original substrate that differ by their fatty acid chain length were further synthesized (**Figure 7.1, B**), finding that C12-analogue was the best substrate for AC, thus a suitable tool in Farber disease diagnosis[225].

In a more recent study carried out in collaboration with Dr. Timothy Thomson, the development of ceramide analogues as new AC inhibitors, and their effect on prostate cancer cells was reported[228]. Among them two α-bromoamides named SABRAC and RBM1-12 (**Figure 7.1, C**) were the most potent inhibitors. They were shown to inhibit AC both in intact and in cell lysates, whereas they did not alter NC activity.

In this section the ability of NC and ACER to hydrolyze the coumarinic ceramide analogues, is investigated. Moreover the study of the inhibitory features of SABRAC and RBM1-12 is reported. The last part of the results is dedicated to a brief study that describes the use of RBM14C12 substrate together with SABRAC as a combined method for AC detection in intact cells.

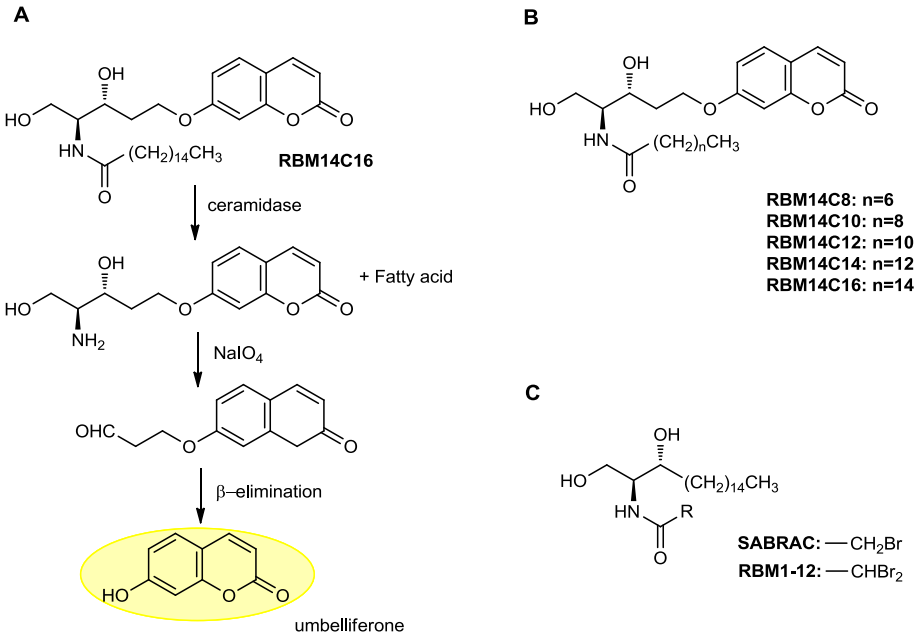

Figure 7.1: Chemical tools for ceramidases investigation. A. Transformation of RBM14C16 into fluorescent umbelliferone. Ceramidases hydrolyze the ceramide amide bond to yield a fatty acid and a sphingoid base. As 2-amino-1,3-diols, sphingoid bases can be converted to fatty aldehydes by periodate oxidation. The resulting aldehyde undergoes a ß-elimination reaction to release the fluorescent product umbelliferone. From *Bedia et at., Chembiochem, (2007)*[225] **B.** Structure of RBM14 analogues that differ by the fatty acyl-chain. **C**. Structure of SABRAC and RBM1-12.

7.1. RBM14 ceramide analogues are hydrolyzed by neutral and alkaline ceramidases

7.1.1. Hydrolysis by neutral ceramidase

The ability of NC to hydrolyze the coumarinic substrates was investigated by using a bacterial enzyme originating from *Pseudomonas aeruginosa* (pCDase), that was produced and purified in our laboratory as previously describeded[391]. In this report Wu *et al.* assessed pCDase activity by using D-*erythro*-C12-NBD-ceramide (CerC12NBD) in the presence of Tris buffer containing Ca^{2+} and Triton X-100. Since the use of coumarinic substrate in the enzymatic reaction determines the formation of an aldehyde[224] (**Figure**

7.1, A), the presence of primary amines in the solution must be avoided. Therefore Tris was substituted with HEPES that is also compatible with the presence of Ca^{2+} in the reaction mix. Moreover it was already reported that Triton X-100 decreases RBM14C12 hydrolysis when the latter is used as AC substrate[225]. It was hypothesized that the effect was related to the low partition coefficient of the substrate that might be engulfed into micelles, rather than a direct inhibitory effect of the detergent on the enzyme.

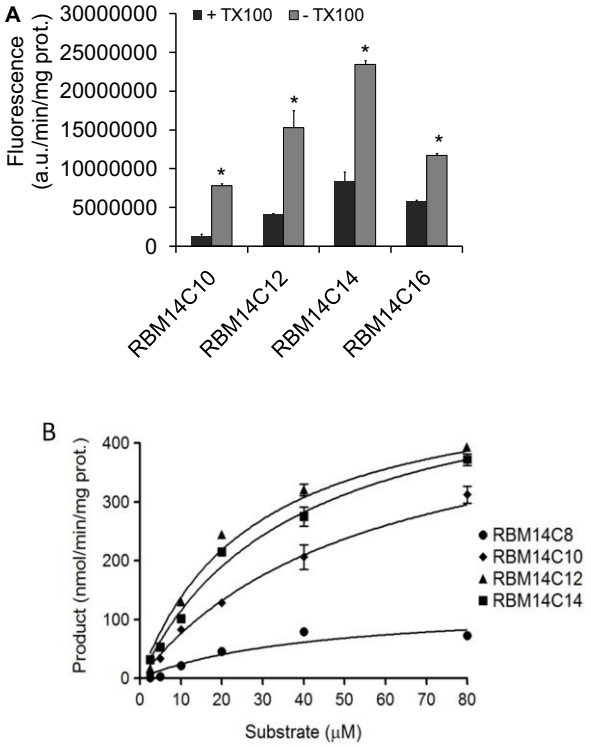

Figure 7.2: Hydrolysis of RBM14 compounds by pCDase. A. Effect of Triton X-100 on the hydrolysis of RBM14C14 compounds**.** Enzymatic activity was carried out in presence or absence of 0.3% w/v of Triton X-100 (TX100) by using 40 μM of RBM14 substrates and 10 ng of protein, as detailed in Material and Methods. **B.** Determination of kinetic parameters for RBM14 compounds. Enzymatic activity was carried out in absence of Triton 100-X by using different concentration of RBM14 substrates and 50 ng of protein, as detailed in Material and Methods. Data are mean ± SD of three to five independent experiments with triplicates. In A, asterisks indicate significant difference between samples with and without Triton X-100 ($p< 0.001$, unpaired, two tail *t*-test)

To check if Triton X-100 might alter substrates hydrolysis also in the case of NC, activity measurement was carried out in presence or absence of the detergent. Results in **Figure 7.2, A** showed that NC activity was higher in absence of Triton X-100 for all the substrates tested, therefore it was omitted from then on.

Next, determination of the kinetic parameters for the RBM14 coumarinic analogues was carried out by using pCDase and a human recombinant NC (hNC). As concluded from the kinetic parameters, the best substrates of pCDase are RBM14C14≈RBM14C12>RBM14C10>>RBM14C8 (**Figure 7.2 and Table 7.1**). RBM14C16, that in the previous assay was hydrolyzed similarly to C10-analogue, was not included in the study. The affinity appeared to directly increase with increasing *N*-acyl chain length in the substrate also for the human enzyme. Indeed, the K_m/V_{max} ratios for hNC indicate that substrate preferences is RBM14C16≈RBM14C14>>RBM14C12>>RBM14C10>>RBM14C8 (**Figure 7.3 and Table 7.1**).

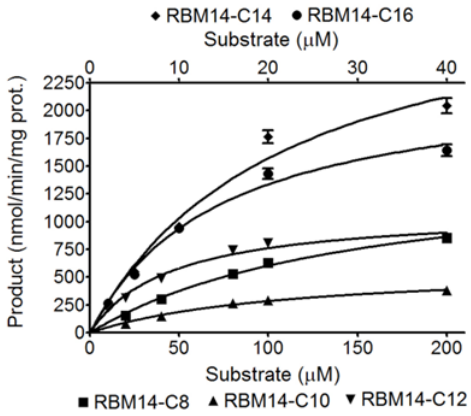

Figure 7.3: Kinetic parameters for human NC. Determination of kinetic parameters for neutral ceramidase. Substrates were incubated at different concentrations with the human recombinant NC (5 ng). Measurements were carried out as detailed in Materials and Methods. Results are mean of three experiments in triplicates.

Table 7.1 RBM14 hydrolysis by neutral ceramidases: kinetic parameters[a]

	pCDase			Human NC		
	K_m	V_{max}	K_m/V_{max}	K_m	V_{max}	K_m/V_{max}
RBM14C8	45.9±18.1	101.3±20.4	0.45	262±32.1	2201±321	0.119
RBM14C10	32.7±4.2	408.1±22.6	0.080	181±21.2	807±82	0.225
RBM14C12	15.2±3.0	469.9±35.9	0.032	55±4.8	1186±122	0.047
RBM14C14	22.5±2.9	469.3±24.5	0.048	39±4.9	4716±453	0.0083
RBM14C16	N.D	N.D		16±3.3	2372±298	0.00069

[a] K_m is given in μM and V_{max} as nmol/min/mg protein. Data are mean ± SD of three to five experiments with triplicates for pCDase and three experiments with triplicated for human NC. Protein amounts were: pCDase 50 ng; hNC, 5 ng. Experiments were carried out as detailed in Materials and Methods.

These results showed that RBM14s are suitable substrates for NC, with C14-analogue and C12-analogue preferred by the bacterial enzyme and C16-analogue and C14–analogues as best substrates for the human recombinant protein. In both cases, the substrate affinity increases directly with increasing the *N*-acyl chain length, as concluded from the decrease of the K_m values. This correlation is particularly evident with the human enzyme, which has, in general, less affinity for the coumarinic substrates than the bacterial enzyme. In contrast the latter hydrolyzes RBM14 with lower reaction rates than the human enzymes. In a previous study carried out in our group, the measurement of NC activity in both lysates and intact Farber disease cells transfected with murine NC, showed that the enzyme hydrolyzed preferentially RBM14C10, followed by C12- and C14-analogues (Luz Camacho, PhD Thesis). The preferential trend for the short acyl chain substrates is not in agreement with the results obtained with bacterial and human NC and contradicts a previous report that described long-chain ceramides (C16- and C18-) as highly favored by murine NC[178]. However it is worth noticing that in that report the activity measurement was carried out with radioactively labeled ceramides. Moreover in the same study the fluorescent substrate CerC12NBD was highly hydrolyzed by NC and the reaction was much faster than native ceramide. These observations suggest that a difference in the enzymatic substrate affinity can be due to the different polarity of the substrates. Moreover the different substrates preferences between bacterial, human and mouse NC are likely due to differences in their amino acid sequences that might impart different 3D-structures to the substrate binding pocket.

7.1.2. Hydrolysis by alkaline ceramidases

In order to investigate if RBM14 compounds are hydrolyzed by alkaline ceramidases, mouse embryonic fibroblasts (MEF) defective in ASAH2 gene codifying for neutral ceramidase (ASAH2$^{(-/-)}$) were used. As shown in **Figure 7.4, A**, all the analogues except for RBM14C8 were hydrolyzed in intact cells, with RBM14C14 and RBM14C16 producing the highest fluorescence values.

Hydrolysis of RBM14 compounds was also analyzed in ASAH2$^{(-/-)}$ MEF lysates at different pH. As shown in **Figure 7.4, B**, the highest activity occurred at basic pH, at which RBM14C14 and RBM14C16 gave the highest hydrolysis rates, while no activity was obtained at acid pH. In addition RBM14 compounds were also hydrolyzed at neutral pH. These results suggested that RBM14, were hydrolyzed by at least one of the alkaline ceramidases in ASAH2$^{(-/-)}$ MEF.

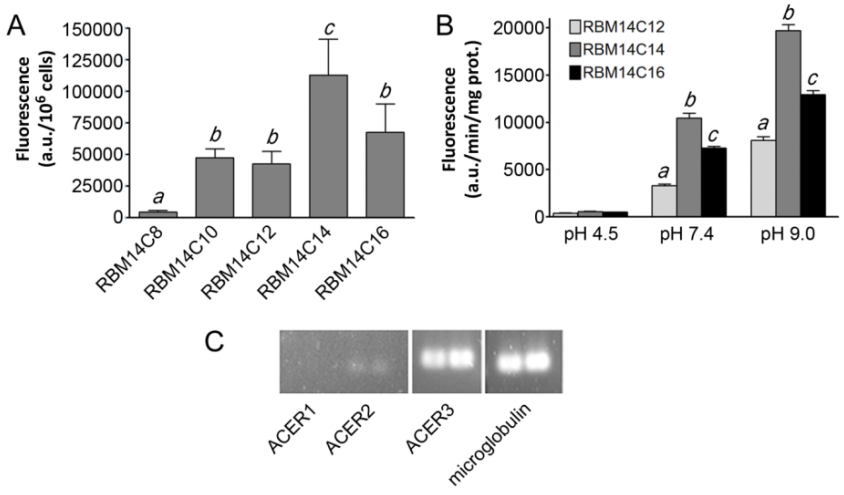

Figure 7.4. Hydrolysis of RBM14 compounds by alkaline ceramidases. Enzymatic activity was determined in (**A**) intact or (**B**) lysates ASAH2$^{(-/-)}$ MEF as detailed in Material and Methods. In **A** data, shown as mean ± SD were obtained from three different experiments with triplicates (final amount of cells:3.7, 5.1 and 6.5x10^4 cells/well). In **B** data correspond to the mean ± SD of 3 to 5 experiments with triplicates. Data were analyzed by one-way ANOVA test (A, P<0.0001; B/pH 7.4, P<0.0001; B/pH 9.0, P<0.0001) followed by Bonferroni's multiple comparison test. Different letters denote statistically significant difference between groups (p<0.05). **C**. Evaluation of ACER1, ACER2 and ACER3 mRNA content in ASAH2$^{(-/-)}$ MEF by RT-PCR. Result is representative of two experiments in duplicates.

In humans three different alkaline ceramidases have been reported (ACER1, ACER2 and ACER3) and they have the same counterpart in mouse[176]. Therefore we determined the levels of mRNA for the different alkaline ceramidases in order to find the responsible protein(s) for RBM14 hydrolysis. As shown in **Figure 7.4, C**, ASAH2 deficient MEF presented high levels of ACER3 transcript. In contrast, levels of ACER2 mRNA were very low and ACER1 mRNA was undetectable.

All together these results show that RBM14 analogues are substrates of alkaline ceramidase, with RBM14C14 and RBM14C16 as the best candidate. This result was confirmed also in cell lysates where the highest enzymatic activity was achieved at alkaline pH with this analogue. The activity observed at neutral pH is likely to correspond to residual activity of alkaline ceramidases that have been reported to have a range of pH between 7 and 9.5 (see Chapter 2, paragraph 2.2.2.3). Moreover the low activity showed at acid pH suggest that MEF contain few amount of acid ceramidase. Thus, these findings suggest that RBM14 are hydrolyzed by at least one of the three alkaline ceramidases. The determination of mRNA levels corresponding to the three alkaline ceramidases suggested that ACER3 is probably involved in the enzymatic cleavage of RBM14 at basic pH in ASAH2$^{(-/-)}$ MEF. These results are in agreement with reported data (http://biogps.org), confirming this theory. However mRNA analysis represented a qualitative method to check alkaline ceramidases in this cell line; a quantitative determination by using qRT-PCR or protein quantification must be performed in order to confirm that, among alkaline ceramidades, ACER3 is responsible for RBM14 hydrolysis. Moreover ACER3 knockdown HCT116 cells and HeLa cells that overexpress ACER1 and ACER2 are currently used in our lab to better characterize RBM14s hydrolysis by the different ACERs.

7.2. SABRAC and RBM1-12 as acid ceramidase inhibitors

Acid ceramidase is a cysteine protease characterized by the nucleofilic thiol residue Cys143 at the *N*-terminus of the ß-subunit, after cleavage of the precursor protein. Thus AC inhibitors design was inspired to reported irreversible cysteine protease inhibitors. Particularly SABRAC and RBM1-12 are ceramide analogues modified at the amide linkage with thiol reactive functions. The study of their inhibitory activity showed that AC was inhibited with an IC_{50} value of 52 nM and 0.53 µM for SABRAC and RBM1-12

respectively[228]. In order to better characterize these molecules as AC inhibitors, further experiments were carried out as a part of the same study.

First a time-dependent inhibition assay was performed to delineate the type of inhibition. Enzymatic activity assays carried out in Farber Disease fibroblasts transformed to stably overexpress AC (FD10X) cell lysates showed that activity presented an exponential decay versus incubation time at the two protein concentrations tested, suggesting an irreversible type of inhibition (**Figure 7.5)**. This was in line with the rational design of these molecules (ref. 51-53 from Camacho *et al.*[228]).

In order to exclude non-specific inhibition against other cysteine proteases, the inhibitory activity of these molecules was tested by using papain, being a member of this family of proteins[392]. Results showed that neither SABRAC nor RBM1-12 inhibited the enzyme, whereas chymostatin, a described cysteine protease inhibitor[393], completely blocked its activity (**Figure 7.6**).

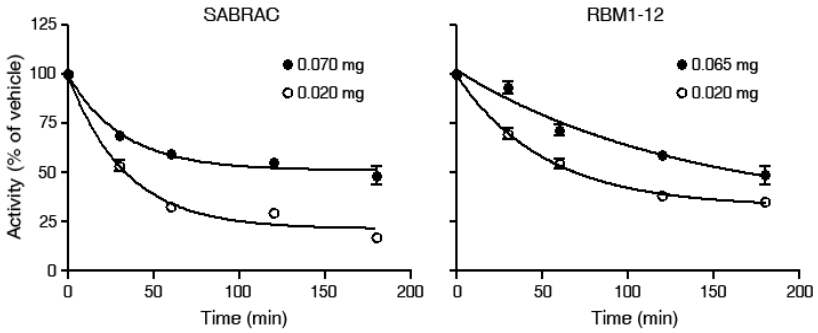

Figure 7.5: Time-dependence curves of acid ceramidase activity in presence of inhibitors. Reaction mixtures containing the specified amounts of protein (FD10X cell lysates), substrate (40 uM) and either vehicle or test compounds (SABRAC: 0.020 uM; RBM1-12: 0.5 uM) were incubated for 0.5, 1,2 and 3 hours in 96-well plates. Reaction were stopped and the formation of umbelliferone was measured as detailed in Materials and Methods. Experiments were carried out twice with triplicates. Curves were fitted to the one phase exponential decay equation (Y=Span*e(-K*X)+Plateau) without constraints.

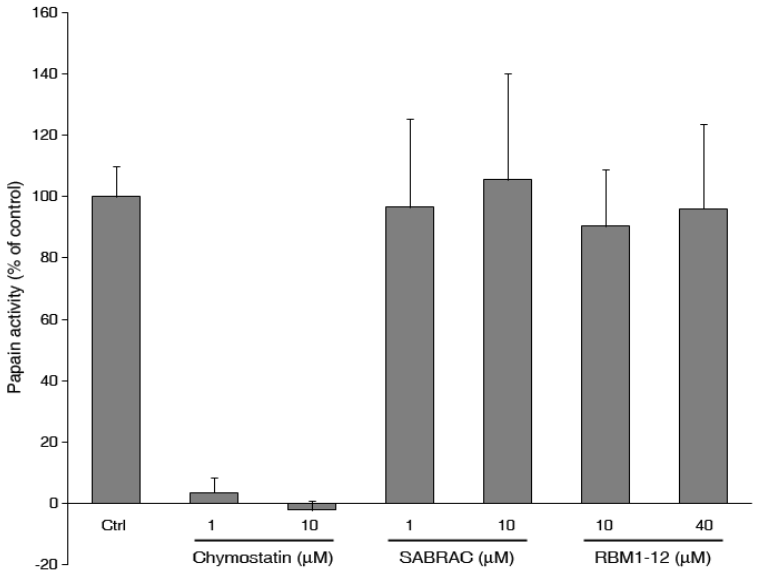

Figure 7.6: Effect of SABRAC and RBM1-12 on papain activity. The enzyme (0.6 ug) was incubated with the substrate (0.22 mM) in the absence (Ctrl) or presence of test compounds at the specified concentrations. Absorbance was determined at 410 nm after 30 min. Chymostatin was used as a positive control of inhibition of papain activity. Data correspond to the mean ± SD of a representative experiment with triplicates.

This results showed that SABRAC and RBM1-12 are specific inhibitors of acid ceramidase. Moreover they appear to block AC irreversibly. Different attempts were done to confirm this result. AC activity was measured in FD10X cells after different times of pre-incubation with the inhibitor and subsequent dilution in the reaction mix containing the substrate in order to calculate K_i (constant of inhibition) and k_i (velocity of inactivation). However, no conclusive results were obtained. The difficulties related to the use of cell lysates in the biochemical characterization of AC prompt us to continue this work by using the human recombinant purified enzyme that is now commercially available. The irreversible inhibition of AC and the kinetic parameters of SABRAC are currently being investigated in our laboratory.

7.3. Use of RBM14C12 and SABRAC for AC determination in intact cells

Previous experiments carried out in our group by using RBM14C12 substrate for the screening of AC in different cancer cells lines pointed out a correlation between the AC enzymatic activity and p53 genetic alteration, or metastatic ability, in colon and prostate cancer cell lines respectively (Luz Camacho, PhD Thesis). Further studies in prostate cancer cells revealed that the highly tumorigenic and metastatic clone PC-3/Mc expressed higher levels of ASAH1 compared to the non-metastatic clone PC-3/S[228]. Thus RBM14C12 substrate might be a potential tool to screen cancer cells for AC content and its possible correlation with genetic alterations or tumorigenic properties of the cells. However RBM14C12 can be hydrolyzed also by neutral and alkaline ceramidases as described above. Therefore the use of this ceramide analogue for ceramidase activity determination in intact cells cannot be considered exclusively representative for AC content.

For this reason SABRAC was used in combination with RBM14C12 substrate in a study aimed to determine AC activity in intact cells. Gastric cancer cells (HGC-27) and breast cancer cells (MDA-MB 231) were chosen as cellular models. Ceramidase activity in intact cells was similar in both cell lines, and was deeply decreased by SABRAC, suggesting that AC was the main responsible for the substrate hydrolysis (**Figure 7.7, A**). To asses these results, enzymatic activity was measured in cell lysates in acidic conditions. Results showed that AC activity was highly reduced (HGC-27 cells) or even completely abolished (MDA-MB 231 cells) in the presence of SABRAC (**Figure 7.7, B**), supporting the result obtained in intact cells.

This brief study represents an example of the possible use of RBM14C12 and SABRAC as a combined method to check AC content in different cell lines. The use of SABRAC as acid ceramidase inhibitor allows to exclude the contribution of other ceramidases to the hydrolysis of RBM14C12 substrate. Apart from prostate cancer, AC was shown to be upregulated in melanomas and head and neck cancer, which leads to the hypothesis that AC could be a tumour marker. Moreover, AC in tumour cells confers resistance to chemo- and radiotherapy thus making the inhibition of this enzyme a potential target for cancer therapy[394]. This method allows the analysis of AC content in intact cells, avoiding the more time-wasting methods in cell lysates, thus representing a suitable tool for a primary screening of cells.

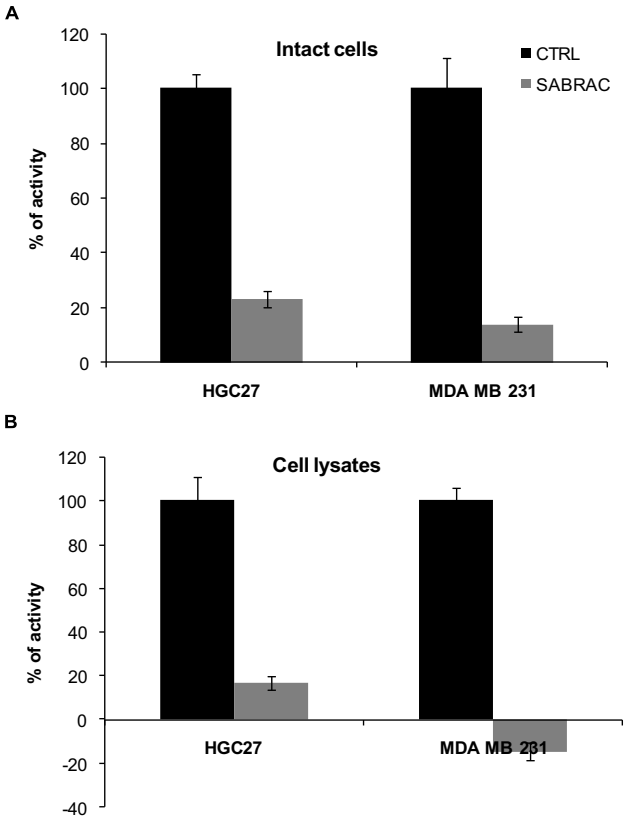

Figure 7.7: AC activity determination by using RBM14C12 and SABRAC. A. HGC-27 and MDA-MB 231 cells were incubated with SABRAC (1 μM) or ethanol (0.2%) as a control for 1 hour; then RBM14C12 substrate (40 μM) was added to the medium. Ceramidase activity assay was carried out as detailed in Materials and Methods. **B.** Cell lysates were incubated with RBM14C12 (40 μM) in presence (SABRAC, 1 μM) or absence (CTRL, 1% ethanol) of the inhibitor for 3 hours. The assay was carried out in 100 mM acetate buffer pH 4.5, as described in Materials and Methods. Results represent mean of two different experiments in triplicates.

In summary RBM14 ceramide analogues and the AC inhibitors SABRAC and RBM1-12 are chemical tools that might be used in the investigation of ceramidases. Besides acid ceramidase, NC and ACER also hydrolyze fluorogenic RBM14 compounds. Although the different enzymes tested preferentially hydrolyzed some of the substrates, (RBM14C14 and C12 for pCDase, RBM14C14 and C16 for human NC) none of them is specific for a particular enzyme. Despite the lack of specificity, these substrates should prove useful in library screening programs aimed to identify potent and selective inhibitors of NC and ACER, which are currently unknown.

SABRAC and RBM1-12 inhibit the cysteine protease AC without showing inhibition against papain that belong to the same protein family. Moreover preliminary results suggest an irreversible inhibition. The use of SABRAC in combination with the RBM14C12 substrate represents a suitable tool for the specific determination of AC activity in intact cancer cells.

GENERAL DISCUSSION

For many years after their identification, SLs were believed to be only structural components of cell membranes. Their metabolism was little known, and the available techniques at the time did not make it easy to differentiate among the many different members of the SL extended family. This changed radically over the past decades and now SL metabolism is well known and established. These progresses are mainly due to the development of a variety of techniques and tools that allowed to characterize the intricate pathway of reactions that regulates the SL metabolism. Thanks to the use of synthetic radioactive labelled and fluorescent SLs analogues, the metabolic pathways were elucidated two decades ago[395]. More recent advances in liquid chromatography and mass spectrometry analyses have allowed us to detect and quantify individual SLs, their intermediates and metabolites[396]. Moreover enzyme inhibitors, cross-linking probes and artificial membrane models have been developed to address questions like detailed enzyme mechanisms, topology and trafficking of individual lipids, lipid–lipid and lipid–protein interactions[395]. The growing body of information collected during the last years by using different strategies made it possible to delineate a more defined picture of SLs and their role in cell biology. Cell growth, and differentiation, senescence and cell death are some of the cellular processes that are regulated by different classes of SLs, that indeed represent important targets in biomedical investigation. The interest in the SL metabolism also inhabit in its involvement in pathological processes: sphingolipid dysregulations are responsible for the development of sphingolipidosis, with Gaucher, Fabry, Niemann-Pick, and Farber diseases, among other[12]. Moreover SLs are involved in initiation and progression of cancer, development of resistance to chemotherapy agents, neurodegenerative disease and immunological disorders[12,13,15,16]. For this reason, therapeutic strategies based on the design of small molecules to restore sphingolipid levels to their physiological condition have rapidly emerged in the last years. In addition, some of these new chemical entities, even if they fail to succeed along the pipeline, become valuable pharmacological tools for the study of sphingolipid function[397]. Although incredible progresses have been done since the firsts pioneering studies on SL metabolism and function, many efforts are still needed to better characterize their involvement in physiopathological processes. Thus the finding of new chemical molecules that might be used as a pharmacological tool could improve our knowledge in this field. In this PhD Thesis sphingolipid enzymatic inhibitors and sphingolipid analogues have been used as an investigation-tool in cancer cells, thus representing an example of this kind of approach in biomedical investigation.

The leading character of the first study reported in this Thesis was Jaspine B, a natural sphingolipid analogue that already catch the attention of our group for its cytotoxic properties in cancer cells, and for its effects on the sphingolipid metabolism. Here we investigated the effects of JB on HGC-27 gastric cancer cells to better understand the bases of the SL metabolism alteration and the cytotoxic effect induced by JB treatment.

Our results revealed that JB is a new CerS inhibitor. The accumulation of CerS natural substrates, dhSo and So, is a consequence of the enzymatic inhibition and it is an effect shared with other described CerS inhibitors such as FB1 and AAL-toxin[173]. From a structural point of view both FB1 and AAL present structural similarity with the sphingoid backbone. FB1 is characterized by a linear amino pentahydroxyeicosane chain in which two of the hydroxyl groups are each ester bound to a tricarballylic acid molecule (**Figure 2.2**). AAL-toxin has a similar structure, however it is lacking one of the tricarballylic acid molecule, and the terminal methyl group is also absent. In JB, where the sphingoid base can be recognized as a part of a heterocyclic system, the terminal amino-alcohol is part of the ring system (**Figure 5.1**). These observations of the structure of different CerS inhibitors are consistent with the apparent low structural demanding effects of CerS towards the terminal amino portion in this kind of compounds. Interestingly the use of JB stereosisomers (2-*epi*-, 3-*epi*- and 2,3-*epi*-JB), that vary for C2 and C3 configuration, in CerS inhibition studies suggests that the *S* configuration of the secondary alcohol (C3), present in JB and 2-*epi*-JB but not in 3-*epi*-JB and 2,3-*epi*-JB, is necessary for the inhibitory activity. This is in agreement with the stereochemistry of FB1 that has the same configuration on this position. On the other hand the *S* configuration does not match that present in natural sphingoid bases at this level. These observations suggest that CerS exhibit low stereo selectivity toward linear sphingoid bases, while the *S* configuration at C3 appears to be fundamental when the secondary alcohol is a part of a closed and more rigid system, like the JB heterocycle. However, further studies focused on CerS stereoselectivity are necessary to confirm this assumption. FB1 is largely used in basic research as pharmacological tool for CerS inhibition. FB1 inhibits fungal CerS in vitro, but its activity in whole cells is very weak, probably due to deficient internalization[398]. The effect of JB on CerS was not evaluated in intact cells, however in a parallel study in our laboratory (Maria Garrido, PhD) it was reported that JB was able to inhibit Cer formation after one hour of incubation in HGC-27 cells, while FB1 needed a longer incubation time (24 hours) to get the same result (not published), making the use of the natural sphingolipid useful for the inhibition of CerS in intact cells. Thus JB represent a new suitable enzymatic inhibitor to block SL metabolism at the CerS level.

The investigation of JB induced cytotoxicity on HGC-27 cells showed the activation a non-apoptotic non-autophagic cell death mechanism characterized by bulk cytoplasmic vacuolization. We hypothesized that cell death is triggered by methuosis, a mechanism based on the formation of macropinosomes originating from the cell membrane. Considering that JB was shown to induce apoptosis or autophagy in different cancer cell lines, this result was unexpected. However it is well established that pharmacological treatments can activate a variety of signals and cell death mechanisms in different cancer cells. The perturbation of cell homeostasis with a pharmacological treatment activate different pathways and the effect on the cell fate represents the final result coming out from the interaction of activated/inactivated molecules and their downstream signals, and the genetic background of the treated cells. For instance fenretinide has to be shown to induce apoptotic cell death in a wide range of tumour cell types. However it induces autophagic cell death in caspase-defective breast cancer cells, suggesting that fenretinide does not invariably elicit an apoptotic response but it is able to induce autophagy when apoptotic pathway is deregulated[399]. Similarly manumycin A, that exhibits antitumour effects by inducing apoptosis in thyroid, leukemia and prostate cancer cells[400], was shown to reduce cell viability through the induction of non-apoptotic, non-autophagic cytoplasmic vacuolization in therapy-resistant triple-negative breast cancer cells[401]. The latter report reminds of the effect of JB in gastric cancer cells, which harbor genetic alterations that confer chemo-resistance and undergo cell death through an alternative pathway characterized by bulk cytoplasmic vacuolization. Further studies are necessary to define the molecular mechanism that trigger to JB induce vacuolization and cell death. Even though SLs have been extensively described as regulators of membrane structure and modeling[1,5], our results does not suggest a connection between the alteration of the *de novo* SL pathway alteration and induction of cell death. Indeed, the use of the myriocin, that counteracted JB induced elevation of dhSo and dhSoP, did not alter neither cytotoxicity nor cell vacuolization. JB-induced LC3-II elevation also appears independent from sphingoid bases elevation. However the involvement of other SL species should be investigated before completely discarding involvement of SLs alteration in JB-induced biological effects.

The second study reported in this Thesis was focused on SKI II, a well known sphingosine kinase inhibitor that is currently used as a pharmacological tool to block the production of phosphorylated sphingoid bases in the SLs pathway. However the increased levels of dhCer after treating cells with SKI II in different cell models suggested a simultaneous inhibition of dihydroceramide desaturase[377]. Our results confirmed this

hypothesis, showing that SKI II inhibits Des1 both *in vitro* and in intact gastric cancer cells. Moreover SKI II treatment provoked cell cycle alteration and autophagy induction in the same cellular model. We speculated that these effects can be related to dhCer accumulation rather than S1P reduction.

There is a plenty of example in scientific literature that show how a molecule first described as having a specific action on a certain target, may actually play multiple roles. In the SLs field for instance, the tricyclic anti-depressant desipramine was reported to induce intracellular proteolytic degradation of mature aSMSase but not other lysosomal enzymes, and accordingly it has been widely used in the literature as a specific aSMase inhibitor[402]. However further investigation revealed that desipramine can also inhibit AC[403], which has an opposite action on ceramide compared to aSMase. Thus the use of desipramine can alter the SL metabolism, generating multiple overlapping effects. Similarly SKI II shows a double inhibitory action on both SK and Des1. Although these enzymes are part of the same metabolic pathway, in this case they do not have an opposite action on a specific metabolite. However both S1P and dhCer are bioactive molecules that can trigger a variety of molecular signals, as discussed in the introduction. Thus the biological effects observed in cells treated with SKI II can be due to the multiple effects of this molecule on sphingolipid modulating enzymes and their sphingolipid products. Therefore, based on the above, care has to be exercised in using SKI II in intact cells as SK inhibitor.

In the third studies reported in this Thesis we focused on ceramide analogues as chemical tools for ceramidase investigation. Previous works from our laboratory described a family of coumarinic analogue of ceramide, named RBM14 compounds, as CDases substrates, with RBM14C12 as the best substrate for acid ceramidase[224,225]. This work was undertaken with the aim of determining the capacity of neutral and alkaline ceramidases to hydrolyze RBM14. Results show that both enzymes use RBM14 compounds as substrates. Although the different enzymes tested in this work preferentially hydrolyzed some of the substrates, no absolute specificity was found for any of the enzymes. Thus RBM14 represents suitable tools for CDases investigation, however enzymatic activities have to be measured with some restrictions. For instance the use of specific inhibitors to block other CDases activities, as well as the control of pH conditions might help to measure the activity of different ceramidases. Ceramidases are key molecule in the SL metabolism because of their role in regulating ceramide and sphingosine levels, thus the availability of chemical substrates that allow their study and biochemical characterization will be useful to extend our knowledge in this field.

Among CDases, AC is expressed at high levels in several tumor types and has been proposed as a cancer therapeutic target. In a recent study published in collaboration with Dr. Timothy Thomson we show that AC is required for self-renewal and growth factor signaling in drug-resistant and metastatic PC-3/Mc prostate cancer cells[228]. SABRAC and RBM1-12 were developed as AC inhibitors for the treatment of these cells. The studies reported in this Thesis show that these molecules represent a helpful tool to determine acid ceramidase activity in intact cancer cells. The hydrolysis of RBM14C12, a AC substrate in presence of SABRAC or RBM1-12 might help to discriminate acid ceramidase from other ceramidases activities, revealing those cell lines where AC can be a biomarker for carcinogenicity and a possible target for therapy.

The reported studies show how the perturbation of cells homeostasis and metabolic pathways with chemical compounds represents a strategy for sphingolipid investigation in biological processes. JB and SKI II are sphingolipid enzymatic inhibitors that lead to specific changes in the sphingolipid metabolism depending on their targets. In the case of cell treatment with SKI II, it emerged that there is a direct connection between the changes produced in the SL metabolism and the biological effects observed. In the case of JB the enzymatic inhibition of CerS appears to be an independent event from the cytotoxic effect of the natural sphingolipid. However the study of JB induced cytotoxicity led to the identification of a novel cell death mechanism. It will be interesting to investigate the mechanism of cell vacuolization in other cell models to establish if it represents a suitable strategy of cell death in a wide variety of cancer types. The use of enzymatic inhibitors together with the NC and ACER substrates RBM14 will shed light on the role of this CDases in cancer and other diseases, while acid ceramidase inhibitors SABRAC and RBM1-12 represent promising molecules for cancer investigation and treatment. The irreversible inhibitory nature of SABRAC towards AC led us to develop an azide-derivative, named ωN_3-SABRAC that is currently the subject of a promising project in our laboratory. ωN_3-SABRAC has the same cytotoxic properties of SABRAC (not shown) and is suitable for conjugation by click-reaction with an fluorescent alkine, giving a fluorescent acid ceramidase-SABRAC adduct. Therefore ωN_3-SABRAC represents a suitable tool to study the localization and trafficking of AC in cells.

CONCLUSIONS

Sphingolipid metabolism represents a complex and highly regulated pathway that is involved in biological and pathological processes. The use of chemical molecules such as enzymatic inhibitors (SKI II) and sphingolipid analogues (Jaspine B, RBM14 compounds) allows to investigate different aspects of sphingolipid-related processes in cells. Considering the involvement of sphingolipid dysregulation in different diseases, particularly in cancer, the use of these molecules represents a suitable tool to investigate the effects of SLs on cellular processes and to find potential treatments. Here the end points that come out from the different studies that have been presented in this work are summarized.

Alterations of sphingolipid metabolism and cytotoxic effects of Jaspine B in gastric cancer cells

I. JB is cytotoxic in gastric cancer cells, glioblastoma cells and breast cancer cells in low micromolar concentrations. In HGC-27 gastric cancer cells JB shows a LD_{50} of 7.3±0.7 μM after 24 hours of treatment.

II. JB alters the sphingolipid metabolism in HGC-27 cells, mainly increasing dhSo and dhSoP levels after 4, 8 and 24 hours of treatment. Importantly, So and SoP levels also increase their levels after short time of JB treatment, while dhCer and dhSM levels show lower accumulation.

III. JB (5 μM) inhibits CerS with a percentage of inhibition between 66% and 44% for the tested isoforms (CerS1, CerS2, CerS4, CerS5 and Cer6), showing that JB inhibition of CerS inhibition is not specific for any of the isoforms.

IV. 2-*epi* JB slightly inhibits CerS6, while 3-*epi* JB, 2,3-*epi* JB, C8-acyl JB, C16-acyl JB and N_3-JB are not CerS inhibitors at the tested concentrations (5 μM).

V. JB is CerS substrate, showing 50% of acylation by CerS5 compared to dhSo acylation. JB acylation in HGC-27 results in acyl-JBs formation with C-16, C-24 and C-24:1 as the most abundant species.

VI. Acid and neutral ceramidases are not inhibited by JB.

VII. JB treatment induces the formation of phase-lucent cytoplasmic vacuoles in different cancer cells lines.

VIII. JB-induced cytotoxicity and vacuolization in HGC-27 cells are not impaired by SLs *de novo* synthesis inhibition, suggesting that JB induced SLs alteration in not involved these processes.

IX. Apoptosis is not responsible for JB-induced cell death and vacuolization. Moreover JB treatment does not induce DNA degradation, excluding necrotic cell death.

X. JB induces LC3-II elevation, which is not impaired by SLs *de novo* synthesis inhibition, showing that SLs alteration is not connected to LC3-II accumulation.

XI. HGC-27 cells treatment with 500 nM wortamannin decreases JB cytotoxicity, without decreasing LC3-II levels. Moreover JB does not change p62 levels, and mTOR inhibition has no effect on JB-induced cytotoxicity. All these findings suggest that JB does not induce autophagy.

XII. In agreement, TEM analysis shows that single membrane low electron-dense JB-induced vacuoles are different from electron-dense and doubled-membrane vacuoles produced by the autophagy inducer XM462 in HGC-27 cells.

XIII. Bafilomycin-A1 treatment prevents JB-induced cell vacuolization in HGC-27 cells, indicating the involvement of the endocytic compartment in cell vacuolization.

XIV. JB-induced vacuoles originate from macropinocytosis, suggesting the involvement of methuosis in JB-induced cell death mechanism.

Inhibition of dihydroceramide desaturase activity by the sphingosine kinase inhibitor SKI II

I. SKI II has a LD_{50} of 84 μM in HGC-27 cells.

II. SKI II inhibits Des1 in both intact and lysate HGC-27 cells, showing an IC_{50} of 0.6 μM after 4 hours of incubation in cell lysates.

III. SKI II is a non-competitive inhibitor of Des1 with a calculated K_i of 0.3 μM.

IV. SKI II treatment induces SK1 degradation, whereas Des1 levels are not altered, showing that the inhibition of Des1 activity by SKI II is not paralleled by protein degradation. Molecular modeling studies suggest that SKI II might interfere with the binding of the NADH molecule at the NADH binding site of CB5R, indicating that the inhibitory effect of SKI II on Des1 arises from an effect on an upstream target.

V. Sphingolipids analysis shows that SKI II treatment results in a remarkable accumulation of dhCer and its metabolites (dhSM and dhCDH) for all treatment time-points. S1P is reduced to undetectable levels. So augments after 4 hours of treatment, while Cer and its metabolites (CMH and CDH) increase after 4, 8 and 24 hours. These results are in agreement with the role of SKI II as dual SK and Des1 inhibitor.

VI. PF-543 treatment reduces S1P to undetectable levels, while dhCer and CMH and CDH are slightly reduced.

VII. SKI II impairs HGC-27 cell proliferation and alters cell cycle with the accumulation of cells in G1 phase.

VIII. SKI II treatment causes accumulation of LC3-II marker, suggesting the activation of autophagy.

IX. Since PF-543 treatment in HGC-27 does not change neither cell proliferation nor LC3-II levels, biological effects on this cell line appear to be related to dhCer accumulation rather than to S1P depletion.

Use of chemical tools for ceramidases investigation

I. RBM14 coumarinic ceramide analogues are hydrolyzed by NC. Higher fluorescence is obtained when the activity assay is carried out in absence of Triton X-100.

II. RBM14C14 and RBM14C12 are the best substrates for the bacterial NC with a K_m/V_{max} ratio of 0.048 and 0.032 respectively.

III. Human NC better hydrolyzes RBM14C16 and RMB14C14 substrates with a K_m/V_{max} ratio of 0.00069 and 0.0083 respectively.

IV. Human NC has, in general, less affinity for the coumarinic substrates but higher reaction rate than the bacterial NC.

V. RBM14C10, C12, C14 and C16 are hydrolyzed by ASAH2$^{(-/-)}$ MEF intact cells, with C16-analogue and C-14 analogue giving the highest values of fluorescence.

VI. Experiments in ASAH2$^{(-/-)}$ MEF cell lysates with different pH show higher enzymatic activity at basic conditions, suggesting that RBM14s are hydrolyzed by alkaline ceramidases.

VII. mRNA levels analysis suggests that, among alkaline ceramidases, ACER3 might be the responsible for RBM14s hydrolysis.

VIII. SABRAC and RBM1-12 show an exponential decay in a time-dependent inhibition assay in FD10X cell lysates, suggesting an irreversible inhibition of AC.

IX. SABRAC and RBM1-12 do not inhibit the cysteine protease papain.

X. The combined use of SABRAC and RBM14C12 allows to discriminate between acid ceramidase from other ceramidases activity in intact cells.

MATERIALS AND METHODS

MATERIALS

Minimum Essential Media (MEM) , Dulbecco's modified Eagle's medium (DMEM), Fetal bovine serum (FBS), non-essential aminoacids, penicillin/streptomycin, trypsin-EDTA, polyethylenimine (PEI), 3-(4,5-dimethylthiazol-2-yl)-2,5-diphenyl tetrazolium bromide (MTT), BSA (Bovine Serum Albumin), NADH, Tween-20, protease inhibitors (aprotinin, leupeptin, phenylmethylsulfonyl fluoride-PMSF), umbelliferone, agarose, Fumonisin B1, EIPA, Papain, Chymostatin, GenElute™ Mammalian Genomic DNA Miniprep Kit, HEPES buffer were from Sigma-Aldrich. SKI II (CAS registry number 312636-16-1) and PF-543 (CAS registry number 1415562-82-1) were from Calbiochem (Merk Millipore). z-VAD and Bafilomycin-A were from Enzo Life Sciences. Compounds *N*-[6-[(7-nitro-2-1,3-benzoxadiazol-4-yl)amino]hexanoyl]-D-*erythro* dihydrosphingosine (dhCerC6NBD), RBM14 ceramide analogues (RBM14C8, RBM14C10, RBM14C12, RBM14C14, RBM14C16^{225}, RMB2-40^{343} and XM462^{250} were synthesized in our laboratories. Recombinant Human ASAH2 (N-acylsphingosine Amidohydrolase-2) was purchased from R&D Systems. Annexin V-FITC Early Apoptosis Detection Kit was from Cell Signaling. RNeasy Mini Kit was pursued from Qiagen. Laemmli buffer and acrylamide were from BioRad. SDS was from Fluka. MicroBCA Protein Assay Kit was from Thermo Scientific. One Step RT-PCR kit, SYBR® Safe DNA Gel Stain, Lucifer Yellow, Forward and reverse primers for ACER1, ACER2, ACER3 and microglobulin were from Life Technologies. RNase and PDVF membrane were from Roche. Internal standards for lipidomics and NBD-sphinganine were from Avanti Polar Lipids. Radioactive labelled acyl-CoAs were from American Radiolabeled Chemicals. TAE was from GIBCO. Glass bottom dishes were from MaTtek Corporation. Methanol gradient grade for liquid chromatography, water for chromatography, and silica gel 60 TLC plates were from Merck (Darmstadt, Germany). Antibodies: anti-SK1 (rabbit) was from Cell Signaling, anti-Des1 (rabbit), LC3-II (rabbit) and p62 (mouse) from Abcam and β-actin (mouse) from Sigma. HRP-secondary antibodies and ECL were from GE Healthcare.

METHODS

I. Cell cultures

HGC-27 (human gastric cancer cells), kindly provided by Prof. Riccardo Ghidoni (Lab. Biochemistry and Molecular Biology, San Paolo University Hospital, Medical School, University of Milan, Italy), were maintained in MEM supplemented with 10% FBS, 1% non-essential amino acids, 100 IU/ml penicillin and 100 µgr/ml streptomycin. Cells were routinely growth without reaching high confluence.

HEK293T (human embryonic kidney cells), ASAH2$^{(-/-)}$ MEF (mouse embryonic fibroblasts lacking *ASAH2* gene, kindly provided by Dr. Richard Proia, National Institutes of Health, Bethesda, MD, USA), MDA-MB 231 and MDA-MB 468 (human breast cancer cells, kindly given by Dr. Timothy Thomson,), T98 and U87 (human glioblastoma cells, kindly provided by Dr. Guillermo Velasco, Complutense University, Madrid,) and FD10X (Farber Disease fibroblasts transformed to stably overexpress AC, kindly provided by Dr. Jeffrey A. Medin, Ontario Cancer Institute, Canada) and A549 (adenocarcinomic human alveolar basal epithelial cells) were cultured in DMEM supplemented with 10% FBS, 100 IU/ml penicillin and 100 µgr/ml streptomycin.

All cells were kept at 37°C in humidified atmosphere, 95% air-5% CO_2.

II. Cell transfection

HEK293T cells were growth in 10 cm dishes until 60-70% of confluence. Human CerS genes were cloned in pCMV-Tag2B vector with a N-terminal FLAG tag, or in pcDNA3 vector containing an HA tag as reported[344]. Transfection mix was prepared by adding 6 µgr of plasmid and 15 µl of PEI to a final volume of 1375 µl of incomplete DMEM (DMEM without FBS and antibiotics) for each well. After mixing, the transfection mix was incubated 20 minutes at RT. Cells were washed twice, medium was replaced with 8 ml of incomplete DMEM and the transfection mix was added. After incubating cells for 5-6 hours, 5 ml of DMEM complemented with FBS and antibiotics were added. Cells were collected by trypsinization after 36-48 hours. Ectopic protein expression was evaluated by Western Blot analysis.

III. Microscope analysis

Phase contrast microscopy

Phase contrast pictures were taken by using a Nikon Eclipse TS100 inverted microscope with an objective 40X, connected to a Digital Sight DS-2Mv camera and acquired with Nis Element F 3.0 software.

Transmission electron microscopy (TEM)

Cells were seeded at $0.1x10^6$ cells/ml, 1 ml/well, in 6 wells plates and allowed to grow overnight. Medium was replaced with fresh medium containing JB (5 μM), XM462 (8 μM) or ethanol (0.14%) as a control. After 16 hours of treatment cells were collected with 400 μl trypsin-EDTA and 600 μl MEM and pellet was washed twice with PBS 1%. Cells were fixed in 2% paraformaldehide, 2.5% glutaraldehide in 0.1 M phosphate buffer (PB) pH 7.4 for 30 minutes at 4°C. Samples were centrifuged (1 minute, 1500 rpm) and resuspended in the same fixation mix overnight. After PB washing, cells were treated with 1% OsO_4, 0.8% $K_3Fe(CN)_6$ in 0.1 M PB pH 7.4. Cells were then dehydrated through an ethanol series (90%, 96% and 100%). Cells were included in Spurr resine by polimerization at 60°C during 48 hours. Ultrathin sections were obtained with ULTRACUT ultramicrotome and examined with a JEOL 1010 transmission electron microscope connected to a CCD Orius camera (Gatan) and acquired with Digital Micrograph software (Gatan). Cell fixation and analysis were carried out in collaboration with Scientific and Technological Centers, University of Barcelona.

IV. Biological assays in intact cells

Cell viability

Cell viability was determined by the colorimetric 3-(4,5-dimethylthiazol-2-yl)-2,5-diphenyl tetrazolium bromide (MTT) assay. Cells were seeded in 96-well plates by adding 100 μl/well of cell suspension ($0.1x10^6$ cells/ml for HGC-27, MDA-MB 231 and MDA-MB 468 cells; $0.25x10^6$ cells/ml for T98 and U87 cells) and allowed to grow overnight. Medium

was replaced with fresh medium and the specific treatments were added. In case of co-treatment after a pre-incubation time, medium was not replaced again. All compounds were dissolved in ethanol or DMSO and control experiments were performed with the correspondent solvent. Plates were incubated for the reported times; after that 10 µl of MTT reactive (5 mg/ml) was added and incubated during 1 to 3 hours. Subsequently the medium was removed and the formazan precipitate was solubilized in 100 µl of DMSO. Absorbance was measured at 570 nm with a Spectramax Plus Reader (Molecular Device Corporation).

Uptake of fluid-phase tracer Lucifer yellow

Cells were seeded at $0.85x10^6$ cells/ml, 1 ml/ well in 35 mm glass bottom dishes (14 mm microwell), and allowed to grow overnight. Medium was replaced with 1 ml/well of fresh medium containing LY (1 mg/ml) and cells were incubated with JB (5 µM) or ethanol (0.1%) as a control for 16 hours at 37°C, 5% CO_2. Medium was removed, cells were washed 3 times with 1 ml PBS 1% and 1,5 ml/well of fresh MEM was added. Fluorescent images of live cells were taken using Leica DMIRB microscope, in collaboration with Scientific and Technological Centers, University of Barcelona .

Annexin V-FITC staining

Cells were seeded at $0.1x10^6$ cells/ml, 1 ml/ well, in 6 wells plates and allowed to grow overnight. Medium was replaced with fresh medium and cells were treated with JB (5 or 12 µM), dhSo (12 µM) or ethanol (0.1%) as a control for 16 hours in presence of z-VAD (20 µM)or DMSO (0.2%) as a control. After incubation, the medium was collected together with 400 µl of 50 mM PBS-EDTA, 1% BSA used to wash each well. Cells were collected with 400 µl of trypsin-EDTA, 1% BSA (37 °C, 5% CO_2/2 min); reaction was stopped by adding 600 µl of fresh medium and the resulting suspension was added to the falcon tube containing the medium previously collected for each sample. Cells were centrifuged at 1300 rpm for 3 minutes at 4°C and pellets were washed two times with 200 µl of 50 mM PBS-EDTA, 1% BSA. For cell staining Annexin V-FITC kit was used. Dry pellets were resuspended in 96 µl of 1X Annexing binding buffer and incubated with 1 µl of V-FITC Annexin V and 12.5 µl of propidium iodide for 10 minutes in the dark. 140 µl of 1X Annexing-binding buffer were added and pellets were resuspend before the analysis.

Samples were kept on ice until the moment of the analysis. Stained cells were analyzed by using a Guava EasyCyte™ Flow Cytometer (Merck Millipore, Billerica, MA). Data analysis was performed using the Multicycle AV program (Phoenix Flow Systems, San Diego, CA).

Cell cycle analysis

Cells were seeded at 150.000 cells/ml into 6-wells plates (1 ml/well). Cells were allowed to adhere for 24 h, and then they were treated with vehicle (0.1 % ethanol) or SKI II (10 μM in 0.1 % ethanol in medium). After exposure for 24 h, cell media was discarded; cells were washed with 400 μL PBS-EDTA 1 % BSA, and harvested with 400 μL Trypsin-EDTA 1% BSA (37°C/2 min) and 600 μL of MEM. Cells were pulled down by centrifugation at 1300 rpm/3 min; cell pellet was washed once with 400 μL PBS-EDTA 1% BSA and again centrifuged at the same speed/time. Cells were fixed at -20°C overnight incubation with a 70% ethanol (9.5 ml) in 1X PBS solution (0.5 mL). Fixed cells were pulled down, washed once with PBS-EDTA 1% BSA and stained at 37 °C for 2 hours with propidium iodide solution (0,1 mg/ml in PBS) and RNAsa (10 μgr/mL). Stained cells were analyzed by using a guava easyCyte™ Flow Cytometer (Merck Millipore, MA, USA). Data analysis was performed using the Multicycle AV program (Phoenix Flow Systems, CA, USA).

V. Enzymatic activity assays

Des1 activity assay

Cell lysates

To prepare the cell lysate for Des1 activity determination *in vitro*, a suspension of 10^6cells/ml per sample was centrifuged (1400 *rpm*/3 min), the pellets were washed twice with PBS and resuspended in 0.1 ml of 0.2 M phosphate buffer pH 7.4. The ice cooled suspension was submitted to 1 round of bath sonication (30 sec.)/rest on ice (30 sec.), 5 rounds of bath sonication (15 sec.)/rest on ice (15 sec.) and 1 final round of bath sonication (30 sec.)/rest on ice (30 sec.). A 3.5 % (v/v) solution of the required amount of stock substrate solution (0.5, 1.0, 1.5 and 2 mM in EtOH) in a BSA solution (3.3 mg/ml in

0.2 M phosphate buffer pH 7.4) was prepared to have the needed substrate concentrations (inhibition experiments, 35 µM; kinetics experiment: 17.5, 35, 52 and 70 µM). To each tube containing lysate from 10^6 cells was added: 85 µL of BSA-substrate mix (final substrate concentrations: inhibition experiments, 10 µM; kinetics experiment: 5 µM, 10 µM, 15 µM and 20 µM), 3 µL of SKI II stock solution in EtOH (final concentrations: inhibition experiments, 10 µM; kinetics experiment: 2.5 µM and 0.6 µM), 3 µl of XM462 stock solution in ethanol (10 µM final concentration) or 3 µl ethanol (vehicle control). Then were added 30 µL of NADH (20 mg/ml in 0.2 M phosphate buffer pH 7.4) and 82 µL of 0.2 M phosphate buffer pH 7.4 to have a final volume of 300 µL. The reaction mixture was incubated at 37°C for 4 h. To stop the reaction, 0.7 ml/sample of methanol was added to each tube, mixed by vortex and kept at 4°C overnight. The mixture was centrifuged (10.000 *rpm*/3 min), the clear supernatants were transferred to HPLC vials and 25 µL were injected. HPLC analyses were performed with an Alliance apparatus coupled to a fluorescence detector using a C18 column (Kromasil, 100 C18, 5µm, 15x0.40 cm, Tracer) precolumn equipped (precolumn ODS, Tracer). Compounds were eluted with 20% H_2O and 80% acetonitrile, both with a 0.1% of trifluoroacetic acid, flowing at 1 mL/min. The detector was set at an excitation wavelength of 465 nm and measure the emission wavelength at 530 nm. Each sample was run for up to 15 minutes.

Intact cells

To determine the compounds activity on Des1 in intact cells, cells were seeded in 24 well plates (10^6cell/ml, 0.4 ml/well). Twenty four hours after seeding, the medium was replaced by fresh complete medium containing substrate and either SKI II or XM462, which was used as a positive control (vehicle in controls) (0.4 ml/well). This solution was prepared as follows: 8 µL each of substrate and test compound solutions (10 mM in EtOH) were taken and diluted with medium to 1 ml and then 50 µL each of substrate and test compound solutions were added to each well (Substrate = SKI II = XM462 = 10 µM) prior addition of 0.3 ml/well of medium. After incubation at 37°C for 4h, the media was collected, cells were washed with PBS (0.2 ml/well) and the washing solution was mixed with the collected media. Cells were harvested by trypsinization (trypsin/EDTA, 0.2 ml/well), washed with PBS and the pellet was resuspended in H2O (0.1 ml) and sonicated (water bath) for 30 sec. MeOH (media, 0.4 ml; cell lysate, 0.9 ml) was added to each tube and the mixture was stirred and kept at 4°C overnight. Then the suspension was centrifuged (10,000 *rpm* for 3 min), the solution was transferred to HPLC vials and either

25 µL (media) or 0.1 ml (cells) was injected. HPLC analysis was carried out as described above.

Ceramide synthase activity assay

HEK293T cells expressing ectopic CerS were homogenated in 20 mM HEPES-KOH, pH 7.2, 25 mM KCl, 250 mM sucrose, and 2 mM $MgCl_2$ containing a protease inhibitor cocktail (Sigma-Aldrich). Protein content was determined using the Bradford reagent (Bio-Rad, Hercules, CA). The assay was carried out as reported[152]. Cell homogenates were incubated for different times at 37°C with 15 µM NBD-sphinganine, 20 µM defatted BSA, and 50 µM acyl-CoA, in a 20 µl reaction volume. Alternatively, the direct acylation produced by CerS was measured by incubating cells homogenates with 15 µM sphinganine (or Jaspine B), 20 µM defatted BSA and 50 µM of hot/cold acyl-CoA containing 0.05 ^{14}C-acyl-CoA in a final volume of 250 µl. Reactions were terminated by the addition of 750 µl of chloroform-methanol (1:2, v/v), and lipids were extracted by adding 500 µl of chloroform and 750 µl of deuterium-depleted water (DDW). After centrifugation (2000 rpm, 10 minutes) the water phase was removed. Lipids in the organic phase were then dried under N_2, resuspended in 110 µl chloroform-methanol (9:1, v/v), and separated by TLC using chloroform-methanol-2M NH_4OH (40:10:1, v/v/v) as the developing solvent. NBD-labelled lipids were visualized using a Typhoon 9410 variable mode imager and quantified by ImageQuantTL (GE Healthcare, Chalfont St. Giles, UK). Radioactively-labelled sphingolipids were visualized using a phosphorimaging screen (Fuji, Tokyo, Japan), recovered from TLC plates by scraping the silica directly into scintillation vials, and quantified by liquid scintillation counting.

Ceramidase activity assay

<u>Intact cells</u>

To measure CDase activity in intact cells, cells were seeded in 96-well plates by adding 100 µl/well of a $0.2x10^6$ cells/ml cell suspension and allowed to grow for 24 hours. Medium was replaced with fresh medium containing the RBM14 substrate (40 µM as final concentration) and plates were incubated for 3 hours at 37°C, 5% CO_2. In case of pre-treatment, medium was replaced with fresh medium containing the indicated treatment

and RBM14C12 substrate was added after the preincubation time. The enzymatic reaction was stopped by adding 25 µl of methanol and 100 µl of a 2.5 mg/ml $NaIO_4$ freshly prepared solution in 100 mM glycine/NaOH buffer pH 10.6 to each well. After incubation at 37°C 1 hour in the dark, 100 µl of 100 mM glycine/NaOH buffer pH 10.6 were added and fluorescence was detected at 355/460 nm excitation/emission wavelengths on a Spectramax Plus Reader (Molecular Device Corporation). For negative control samples (blank) the experimental procedure was carried out in wells containing free-cell medium.

In vitro analysis

The assay was based on a previous report[225]. For ceramidases activity investigation *in vitro* different enzymatic sources were used:

(i) Bacterial pCDase was obtained following the reported procedure[391]. The protein was obtained at a 0.33 mg/ml final concentration and it was stored at -80°C. Once thawed, the enzyme solution was kept at 4°C until activity loss. For pCDase activity determinations, the reaction buffer contained 50 mM HEPES buffer, 1mM $CaCl_2$ pH 7.4 in the presence or absence of 0.3% (w/v) Triton X-100. RBM14 substrates were tested at the final concentration of 40 µM in a total volume of 100 µL. For the assay, pCDase was diluted from 0.33 mg/ml to 0.01 mg/ml. Substrates and protein were dissolved in the reaction buffer and the assay was carried out at 37ºC for 1 hour in a 96 wells/plate using 10 µl/well of pCDase 0.01 mg/ml (10 ng/well), 15 µL/well of reaction buffer and 75 µL/well of substrate. Reaction was stopped with 25 µl/well of MeOH and next step were carried out as described above. Determination of K_m and V_{max} was conducted in 96 well/plates, which contained 5 µl/well of 0.01 mg/ml pCDase (50 ng protein/well), 20 µl/well of 50 mM HEPES buffer, 1 mM $CaCl_2$ pH 7.4 and 75 µl/well of substrate at different concentrations (from 2.5 uM to 80-120 uM in 50 mM HEPES buffer, 1 mM $CaCl_2$, pH 7.4 in a total volume of 100 µl). The reaction mixture was incubated at 37 ºC for 30 minutes. The reaction was stopped with 25 µl/well MeOH and next steps were carried out as described above

(ii) Determination of K_m and V_{max} of human recombinant neutral ceramidase activity was determined in 96 wells/plate by dissolving 20 µl/well of the enzyme (0.25 ng/µl, 5 ng/well) and 40 µl of RBM14 substrates (20, 40, 80, 100, 200 µM for RBM14C8, C10 and C12; 2, 5, 10, 20, 40 µM for RBM14C14 and C16) in 50 mM HEPES buffer, 150 mM NaCl, 1% sodium cholate, pH 7.5. Final reaction volume was 100 µl/well. The reaction was carried out at 37 ºC for 30 minutes and stopped with 25 µl/well MeOH. Next steps were carried out as described above.

(iii) For ceramidase activity determination in cell lysates, cells were trypsinized, washed with PBS 1% and resuspended in 0.25 M sucrose. Cell lysis was carried out by sonication with an ultrasonic probe (10 W; 3 cycles of 5 seconds sonication/5 seconds pause in an ice-cold bath). Samples were centrifuged (3 minutes, 5000 rpm), and supernatant were collected. Protein concentration was determined with Micro BCA Protein Kit according to the manufacturer's protocol. Ceramidases activity assays were carried out in 96 wells/plates by adding 25 µl of cell lysates (~1 mg/ml) and 75 µl of buffer (100 mM acetate buffer pH 4.5, or 50 mM HEPES buffer, 1mM $CaCl_2$ pH 7.4; or 50 mM HEPES buffer, 1mM $CaCl_2$ pH 9 for activity determination in $ASAH2^{(-/-)}$ MEF cells. 100 mM acetate buffer pH 4.5; or 100 mM phosphate buffer pH 7.4 for activity determination in FD10X, HGC-27 and MDA-MB 231 cell lysates) containing RBM14 substrates (final concentration of 40 µM in 100 µl/well). In the indicated cases, specific treatments were added to the reaction mix. Plates were incubated for 3 hours at 37°C. Reaction was stopped with 25 µl/well MeOH and next steps were carried out as described above. Free-lysates samples were used as negative control (blank). The amount of umbelliferone released was calculated from the fluorescence intensity by using calibration curves of umbelliferone, in the range from 0 to 3000 pmol.

Papain activity assay

Papain activity was determined in 96-well plates by a modification of the reported procedure[404]. The reaction mixture contained 250 µl of 0.1 M phosphate buffer (pH 6.5) with 0.3 M KCl, 0.1 mM EDTA, and 3 mM DTT; 30 µl of substrate solution (L-pyroglutamyl-L-phenylalanyl-L-leucine- p -nitroanilide; 2.2 mM in DMSO, 0.22 mM final concentration); 20 µl of enzyme solution (30 µg/ml in reaction buffer); and 3 µl of inhibitor solution or vehicle. Chymostatin at 1 µM and 10 µM was used as positive control of inhibition of papain activity. The reaction was stopped by the addition of 20 µl of 1 N HCl, and the OD wasmeasured at 410 nm. on a Spectramax Plus Reader (Molecular Device Corporation).

VI. Protein and DNA analysis

Western Blotting

For protein analysis $0.1x10^6$ HGC-27 cells were plated in 6 wells plates and were allowed to grow for 24 h. Cells were treated with either the reported treatment or the

corresponding vehicles for the indicated times and collected with trypsin-EDTA, keeping the samples on ice. Pellets were washed two times with cold PBS. Cell lysis was performed with 30-40 µl of lysis buffer (150 mM NaCl, 1% Igepal-CA630, 50 mM Tris-HCl pH 8, aprotinin 2 µgr/ml, leupeptin 5 µgr/ml and 1mM PMSF): cells were lysed in a sonication bath during 5 seconds and kept on ice during 10 seconds, for tree cycles. Then samples were kept on ice for 30 minutes and centrifuged for 3 minutes at 10000 rpm. Supernatants were collected and protein determination was performed using the Micro BCA™ Protein Assay Kit according to the manufacturer's protocol. Supernatants were combined with Laemmli sample buffer and boiled for 5 minutes. Equal amount of proteins (30 µgr for Des1 and SK, 20 µgr for LC3 and p62) were loaded onto a 12% polyacrylamide gel, separated by electrophoresis at 100 V/90 minutes and transferred onto a PVDF membrane (100 V/1 hour). Unspecific binding sites were then blocked in 5% milk in TBS-T 0.1% for 1 hour at RT. Alternatively, membrane blocking was carried out with 3% BSA in TBS-T 0.1% before incubation with anti-β-actin antibody. Anti-Des1 antibody was diluted 1:1000 in 5% milk PBS-T 0.1%; anti-LC3, anti-SK and anti-p62 1:1000 in 5% milk TBS-T 0.1%,:anti β-actin in 3% BSA TBS-T 0.1%. Membranes were incubated during 1 hour at room temperature or overnight at 4°C under gentle agitation. After washing with TBS-T 0.1%, membranes were probed with the correspondent secondary antibody for 1 hour at room temperature (for Des1: anti-rabbit 1:2000 in 5% PBS-T; for SK: anti rabbit 1:3000 in 5% milk TBS-T 0.1%; for LC3: anti rabbit 1:1000 3% BSA TBS-T 0.1%; for p62: anti-mouse 1:5000 in 5% milk TBS-T 0.1%;. for β-actin anti-mouse 1:10000 in 5% milk TBS-T 0.1%). Antibody excess was eliminated washing with TBS-T 0.1% and protein detection was carried out using ECL and scanning the membrane with LI-COR C-DiGit® Blot Scanner. Band intensity was quantified by LI-COR Image Studio Lite Software.

DNA agarose gel electrophoresis

Cells were seeded at $0.1x10^6$ cells/ml, 1 ml/ well in 6 wells plates and allowed to grow overnight. Medium was replaced with fresh medium containing JB (5 and 12 µM) or ethanol (0.12%) as a vehicle. After 16 hours medium and cells were collected. Cells were trypsinized with 400 µl trypsin-EDTA and 600 µl MEM and washed with PSB 1%. DNA was purified with GenElute™ Mammalian Genomic DNA Miniprep Kit according to the manufacturer's instructions. DNA concentration was determined by NanoDrop 8000 Spectrofotomer (Thermo Scientific). DNA (10-20 µgr) was loaded in 1% agarose gel containing 0.0001% of SYBR® Safe DNA Gel Stain in TAE. Agarose gel electrophoresis was

carried out for 30 minutes at 100 V and fluorescence was revealed with Gel Logic 200 Imaging System in combination with KODAK Molecular Imaging Software.

Reverse transcription-polymerase chain reaction (RT-PRC)

ASAH2$^{(-/-)}$ MEF cells were harvested, and RNA was extracted with RNeasy kit according to the manufacturer's protocol and treated with DNase I to remove genomic DNA contamination. RNA concentration was determined by NanoDrop 8000 Spectrofotomer (Thermo Scientific). RNA was reverse-transcribed using One Step RT-PCR kit and cDNA was used as a template for PCR. . Primers were: mACER1, 5´-TTGCAGCTTCTGGCAGCGGA-3´ (F) and ACTTTGCATCCACCAGGGCCA-3´ (R); mACER2,5´-GCTGGATCAGCGACCAAGCCT-3´ (F) and AGGCGAAGCACACACAGCCC-3´ (R); mACER3, 5´-ACTGGAGAAGCGGTACATTGCTG-3´ (F) and 5´-GGGAGCTCATCCAACAGCTGCATT(R), andmicroglobulin,5'-GCTATCCAGAAAACCCCTCAA-3' (F) and 5'-CATGTCTCGATCCCAGTAGACGGT-3' (R). Forward and reverse primers were added to the PCR reaction mix containing 1.5 mM $MgCl_2$, 0.2 mM dNTPs and 5u/µl of Go Taq polymerase in 24 µl of final volume. 1 µl containing 1 µgr of cDNA was added before starting the RT-PCR. RT-PCR conditions were as follows: initial denaturation for 2 min at 94 °C, followed by 30 cycles of 30 s at 94 °C, 30 s at 57 °C, and 20 s at 72 °C. A final elongation step followed for 5 min at 72 °C. PCR products were separated by electrophoresis in 1% (w/v) agarose gels containing 0.0001% of SYBR® Safe DNA Gel Stain in TAE. Agarose gel electrophoresis was carried out for 30 minutes at 100 V and fluorescence was revealed with Gel Logic 200 Imaging System in combination with KODAK Molecular Imaging Software.

VII. Lipidomic analysis

Cells were seeded at 200.000-250.000 cells/ml into 6-wells plates (1 ml/well) and allowed to grow overnight. After treatment, cells were collected with 400 µl trypsin-EDTA and 600 µl MEM. Wells were washed again with 400 µl MEM and residual cells were collected. Cell concentration was determined by Trypan Blue staining. Samples were centrifuged 3 min at 10000 rpm, washed with 200 µl of cold PBS 1% and resuspended in 100 µl of purified water. Sphingolipids extracts, fortified with internal standards [N-

dodecanoylsphingosine, N-dodecanoylglucosylsphingosine, N-dodecanoyl sphingosyl phosphorylcholine , C17-sphinganine (0.2 nmol each), and C17-sphinganine-1-phosphate, (0.1 nmol)] were prepared as described[63] and analyzed by ultraperformance LC (UPLC)-TOFMS or HPLC-MS/MS.

The liquid chromatography-mass spectrometer consisted of a Waters Aquity UPLC system connected to a Waters LCT Premier orthogonal accelerated time of flight mass spectrometer (Waters, Millford, MA), operated in positive electrospray ionisation mode. Full scan spectra from 50 to 1500 Da were acquired and individual spectra were summed to produce data points each 0.2 s. Mass accuracy and reproducibility were maintained by using an independent reference spray by the LockSpray interference. The analytical column was a 100 mm x 2.1mm i.d., 1.7 mm C8 Acquity UPLC BEH (Waters). The two mobile phases were phase A: methanol/water/formic acid (74/25/1 v/v/v); phase B: methanol/formic acid (99/1 v/v), both also contained 5mM ammonium formate. A linear gradient was programmed— 0.0 min: 80% B; 3 min: 90% B; 6 min: 90% B; 15 min: 99% B; 18 min: 99% B; 20 min: 80% B. The flow rate was 0.3 ml min^{-1}.The column was held at 30°C. Quantification was carried out using the extracted ion chromatogram of each compound, using 50 mDa. windows. The linear dynamic range was determined by injecting standard mixtures. Positive identification of compounds was based on the accurate mass measurement with an error <5 ppm and its LC retention time, compared to that of a standard (±2%).

Alternatively, analysis of the extracts was performed by LC/MS/MS with a system consisting of a Waters Alliance 2690 LC pump equipped with an autosampler and connected to a Quattro LC triple-quadrupole mass spectrometer from Micromass (Manchester, UK). Separation was achieved ona Purospher STAR-RP-18 column (125 × 2 mm, 5 µm) (Merck, Darmstadt). The two mobile phases were phase A and phase B as described above. A gradient was programmed: 0.0 min, 50% B; 2 min, 50% B; 7 min, 100% B; 17 min, 100% B; 19 min, 50% B; and 26 min, 50% B. The flow rate was 0.3 ml min^{-1}. MS/MS detection was performed with an electrospray interface operating in the positive ion mode acquiring the following selected reaction monitoring transitions: C17 d-*erythro*-dihydrosphingosine-1-phosphate, 368–252, collision energy 18 eV; and S1P, 380–264 Da, collision energy 16 eV.

VIII. Statistic analysis

Data were analysed by Student's *t* test or one-way ANOVA test followed by Bonferroni's multiple comparison test.

REFERENCES

1. Futerman, A. H. & Hannun, Y. a. The complex life of simple sphingolipids. *EMBO Rep.* **5,** 777–82 (2004).

2. Simons, K. & Ikonen, E. Functional rafts in cell membranes. *Nature* **387,** 569–72 (1997).

3. Munro, S. Lipid Rafts: Elusive or Illusive? Review. *Cell* **115,** 377–388 (2003).

4. Shaw, A. S. Lipid rafts: now you see them, now you don't. *Nat. Immunol.* **7,** 1139–42 (2006).

5. Simons, K. & Gerl, M. J. Revitalizing membrane rafts: new tools and insights. *Nat. Rev. Mol. Cell Biol.* **11,** 688–99 (2010).

6. Hannun, Y. a & Obeid, L. M. Principles of bioactive lipid signalling: lessons from sphingolipids. *Nat. Rev. Mol. Cell Biol.* **9,** 139–50 (2008).

7. Saddoughi, S. A., Song, P. & Ogretmen, B. Roles of bioactive sphingolipids in cancer biology and therapeutics. *Subcell. Biochem.* **49,** 413–40 (2008).

8. Lépine, S. *et al.* Involvement of sphingosine in dexamethasone-induced thymocyte apoptosis. *Ann. N. Y. Acad. Sci.* **973,** 190–3 (2002).

9. Cuvillier, O. *et al.* Sphingosine generation, cytochrome c release, and activation of caspase-7 in doxorubicin-induced apoptosis of MCF7 breast adenocarcinoma cells. *Cell Death Differ.* **8,** 162–71 (2001).

10. Cuvillier, O. Enzymes of sphingosine metabolism as potential pharmacological targets for therapeutic intervention in cancer. *Pharmacol. Res.* **47,** 439–445 (2003).

11. Spiegel, S. & Milstien, S. Sphingosine-1-phosphate: an enigmatic signalling lipid. *Nat. Rev. Mol. Cell Biol.* **4,** 397–407 (2003).

12. Kolter, T. A view on sphingolipids and disease. *Chem. Phys. Lipids* **164,** 590–606 (2011).

13. Ogretmen, B. & Hannun, Y. A. Biologically active sphingolipids in cancer pathogenesis and treatment. *Nat. Rev. Cancer* **4,** 604–16 (2004).

14. Ryland, L. K., Fox, T. E., Liu, X., Loughran, T. P. & Kester, M. Dysregulation of sphingolipid metabolism in cancer. *Cancer Biol. Ther.* **11,** 138–49 (2011).

15. Maceyka, M. & Spiegel, S. Sphingolipid metabolites in inflammatory disease. *Nature* **510,** 58–67 (2014).

16. Sabourdy, F. *et al.* Monogenic neurological disorders of sphingolipid metabolism. *Biochim. Biophys. Acta* (2015).

17. Van Echten-Deckert, G. & Walter, J. Sphingolipids: critical players in Alzheimer's disease. *Prog. Lipid Res.* **51,** 378–93 (2012).

18. Merrill, A. H. *et al.* Sphingolipids--the enigmatic lipid class: biochemistry, physiology, and pathophysiology. *Toxicol. Appl. Pharmacol.* **142,** 208–25 (1997).

19. Dickson, R. C. & Lester, R. L. Yeast sphingolipids. *Biochim. Biophys. Acta* **1426,** 347–57 (1999).

20. Gault, C., Obeid, L. & Hannun, Y. A. An overview of sphingolipid metabolism: from synthesis to breakdown. *Adv Exp Med Biol* **688,** 1–23 (2010).

21. Mandon, E. C., Ehses, I., Rother, J., van Echten, G. & Sandhoff, K. Subcellular localization and membrane topology of serine palmitoyltransferase, 3-dehydrosphinganine reductase, and sphinganine N-acyltransferase in mouse liver. *J. Biol. Chem.* **267,** 11144–8 (1992).

22. Pewzner-Jung, Y., Ben-Dor, S. & Futerman, A. H. When do Lasses (longevity assurance genes) become CerS (ceramide synthases)?: Insights into the regulation of ceramide synthesis. *J. Biol. Chem.* **281,** 25001–5 (2006).

23. Merrill, A. H. & Wang, E. Biosynthesis of long-chain (sphingoid) bases from serine by LM cells. Evidence for introduction of the 4-trans-double bond after de novo biosynthesis of N-acylsphinganine(s). *J. Biol. Chem.* **261,** 3764–9 (1986).

24. Yamaji, T., Kumagai, K., Tomishige, N. & Hanada, K. Two sphingolipid transfer proteins, CERT and FAPP2: their roles in sphingolipid metabolism. *IUBMB Life* **60,** 511–8 (2008).

25. Tafesse, F. G., Ternes, P. & Holthuis, J. C. M. The multigenic sphingomyelin synthase family. *J. Biol. Chem.* **281,** 29421–5 (2006).

26. Bornancin, F. Ceramide kinase: the first decade. *Cell. Signal.* **23,** 999–1008 (2011).

27. Stahl, N., Jurevics, H., Morell, P., Suzuki, K. & Popko, B. Isolation, characterization, and expression of cDNA clones that encode rat UDP-galactose: ceramide galactosyltransferase. *J. Neurosci. Res.* **38,** 234–42 (1994).

28. Wattenberg, B. W., Pitson, S. M. & Raben, D. M. The sphingosine and diacylglycerol kinase superfamily of signaling kinases: localization as a key to signaling function. *J. Lipid Res.* **47,** 1128–39 (2006).

29. Johnson, K. R. *et al.* Role of human sphingosine-1-phosphate phosphatase 1 in the regulation of intra- and extracellular sphingosine-1-phosphate levels and cell viability. *J. Biol. Chem.* **278,** 34541–7 (2003).

30. Marchesini, N. & Hannun, Y. A. Acid and neutral sphingomyelinases: roles and mechanisms of regulation. *Biochem. Cell Biol.* **82,** 27–44 (2004).

31. Kitatani, K., Idkowiak-Baldys, J. & Hannun, Y. A. The sphingolipid salvage pathway in ceramide metabolism and signaling. *Cell. Signal.* **20,** 1010–8 (2008).

32. Michel, C. & van Echten-Deckert, G. Conversion of dihydroceramide to ceramide occurs at the cytosolic face of the endoplasmic reticulum. *FEBS Lett.* **416,** 153–155 (1997).

33. D'Angelo, G. *et al.* Glycosphingolipid synthesis requires FAPP2 transfer of glucosylceramide. *Nature* **449,** 62–7 (2007).

34. Lannert, H., Gorgas, K., Meissner, I., Wieland, F. T. & Jeckel, D. Functional organization of the Golgi apparatus in glycosphingolipid biosynthesis. Lactosylceramide and subsequent glycosphingolipids are formed in the lumen of the late Golgi. *J. Biol. Chem.* **273,** 2939–46 (1998).

35. Riboni, L. *et al.* Metabolic fate of exogenous sphingosine in neuroblastoma neuro2A cells. Dose-dependence and biological effects. *Ann. N. Y. Acad. Sci.* **845,** 46–56 (1998).

36. Hait, N. C. *et al.* Regulation of histone acetylation in the nucleus by sphingosine-1-phosphate. *Science* **325,** 1254–7 (2009).

37. Shimeno, H., Soeda, S., Yasukouchi, M., Okamura, N. & Nagamatsu, A. Fatty acyl-Co A: sphingosine acyltransferase in bovine brain mitochondria: its solubilization and reconstitution onto the membrane lipid liposomes. *Biol. Pharm. Bull.* **18,** 1335–9 (1995).

38. Novgorodov, S. A. *et al.* Novel pathway of ceramide production in mitochondria: thioesterase and neutral ceramidase produce ceramide from sphingosine and acyl-CoA. *J. Biol. Chem.* **286,** 25352–62 (2011).

39. Colombaioni, L., Frago, L. M., Varela-Nieto, I., Pesi, R. & Garcia-Gil, M. Serum deprivation increases ceramide levels and induces apoptosis in undifferentiated HN9.10e cells. *Neurochem. Int.* **40,** 327–36 (2002).

40. Jaffrézou, J. P., Bruno, A. P., Moisand, A., Levade, T. & Laurent, G. Activation of a nuclear sphingomyelinase in radiation-induced apoptosis. *FASEB J.* **15,** 123–133 (2001).

41. Bektas, M., Orfanos, C. E. & Geilen, C. C. Different vitamin D analogues induce sphingomyelin hydrolysis and apoptosis in the human keratinocyte cell line HaCaT. *Cell. Mol. Biol. (Noisy-le-grand).* **46,** 111–9 (2000).

42. Charles, A. G. *et al.* Taxol-induced ceramide generation and apoptosis in human breast cancer cells. *Cancer Chemother. Pharmacol.* **47,** 444–50 (2001).

43. Bose, R. *et al.* Ceramide synthase mediates daunorubicin-induced apoptosis: an alternative mechanism for generating death signals. *Cell* **82,** 405–14 (1995).

44. Gómez del Pulgar, T., Velasco, G., Sánchez, C., Haro, A. & Guzmán, M. De novo-synthesized ceramide is involved in cannabinoid-induced apoptosis. *Biochem. J.* **363,** 183–8 (2002).

45. Obeid, L. M., Linardic, C. M., Karolak, L. A. & Hannun, Y. A. Programmed cell death induced by ceramide. *Science* **259,** 1769–71 (1993).

46. Cremesti, A. *et al.* Ceramide enables fas to cap and kill. *J. Biol. Chem.* **276,** 23954–61 (2001).

47. Lee, H. *et al.* Mitochondrial ceramide-rich macrodomains functionalize Bax upon irradiation. *PLoS One* **6,** e19783 (2011).

48. Charles, R. *et al.* Ceramide-coated balloon catheters limit neointimal hyperplasia after stretch injury in carotid arteries. *Circ. Res.* **87,** 282–8 (2000).

49. Dobrowsky, R. T., Werner, M. H., Castellino, A. M., Chao, M. V & Hannun, Y. A. Activation of the sphingomyelin cycle through the low-affinity neurotrophin receptor. *Science* **265,** 1596–9 (1994).

50. Venable, M. E., Lee, J. Y., Smyth, M. J., Bielawska, A. & Obeid, L. M. Role of ceramide in cellular senescence. *J. Biol. Chem.* **270,** 30701–8 (1995).

51. Sundararaj, K. P. *et al.* Rapid shortening of telomere length in response to ceramide involves the inhibition of telomere binding activity of nuclear glyceraldehyde-3-phosphate dehydrogenase. *J. Biol. Chem.* **279,** 6152–62 (2004).

52. Ogretmen, B. *et al.* Molecular mechanisms of ceramide-mediated telomerase inhibition in the A549 human lung adenocarcinoma cell line. *J. Biol. Chem.* **276,** 32506–14 (2001).

53. Riedl, S. J. & Shi, Y. Molecular mechanisms of caspase regulation during apoptosis. *Nat. Rev. Mol. Cell Biol.* **5,** 897–907 (2004).

54. Hochegger, H., Takeda, S. & Hunt, T. Cyclin-dependent kinases and cell-cycle transitions: does one fit all? *Nat. Rev. Mol. Cell Biol.* **9,** 910–6 (2008).

55. Scarlatti, F. *et al.* Ceramide-mediated macroautophagy involves inhibition of protein kinase B and up-regulation of beclin 1. *J. Biol. Chem.* **279,** 18384–91 (2004).

56. Daido, S. *et al.* Pivotal role of the cell death factor BNIP3 in ceramide-induced autophagic cell death in malignant glioma cells. *Cancer Res.* **64,** 4286–93 (2004).

57. Riboni, L. *et al.* Ceramide levels are inversely associated with malignant progression of human glial tumors. *Glia* **39,** 105–13 (2002).

58. Selzner, M. *et al.* Induction of apoptotic cell death and prevention of tumor growth by ceramide analogues in metastatic human colon cancer. *Cancer Res.* **61,** 1233–40 (2001).

59. Seelan, R. S. *et al.* Human acid ceramidase is overexpressed but not mutated in prostate cancer. *Genes. Chromosomes Cancer* **29,** 137–46 (2000).

60. Beckham, T. H. *et al.* Acid Ceramidase Promotes Nuclear Export of PTEN through Sphingosine 1-Phosphate Mediated Akt Signaling. **8,** 1–14 (2013).

61. Baran, Y. *et al.* Alterations of ceramide/sphingosine 1-phosphate rheostat involved in the regulation of resistance to imatinib-induced apoptosis in K562 human chronic myeloid leukemia cells. *J. Biol. Chem.* **282,** 10922–34 (2007).

62. Sobue, S. *et al.* Implications of sphingosine kinase 1 expression level for the cellular sphingolipid rheostat: relevance as a marker for daunorubicin sensitivity of leukemia cells. *Int. J. Hematol.* **87,** 266–75 (2008).

63. Merrill, A. H., Sullards, M. C., Allegood, J. C., Kelly, S. & Wang, E. Sphingolipidomics: high-throughput, structure-specific, and quantitative analysis of sphingolipids by liquid chromatography tandem mass spectrometry. *Methods* **36,** 207–24 (2005).

64. Haynes, C. A. *et al.* Quantitation of fatty acyl-coenzyme As in mammalian cells by liquid chromatography-electrospray ionization tandem mass spectrometry. *J. Lipid Res.* **49,** 1113–25 (2008).

65. Siskind, L. J. *et al.* The BCL-2 protein BAK is required for long-chain ceramide generation during apoptosis. *J. Biol. Chem.* **285,** 11818–26 (2010).

66. Ali, M. *et al.* Altering the sphingolipid acyl chain composition prevents LPS/GLN-mediated hepatic failure in mice by disrupting TNFR1 internalization. *Cell Death Dis.* **4,** e929 (2013).

67. Senkal, C. E., Ponnusamy, S., Bielawski, J., Hannun, Y. A. & Ogretmen, B. Antiapoptotic roles of ceramide-synthase-6-generated C16-ceramide via selective regulation of the ATF6/CHOP arm of ER-stress-response pathways. *FASEB J.* **24,** 296–308 (2010).

68. Mesicek, J. *et al.* Ceramide synthases 2, 5, and 6 confer distinct roles in radiation-induced apoptosis in HeLa cells. *Cell. Signal.* **22,** 1300–7 (2010).

69. Hartmann, D. *et al.* Long chain ceramides and very long chain ceramides have opposite effects on human breast and colon cancer cell growth. *Int. J. Biochem. Cell Biol.* **44,** 620–8 (2012).

70. Schiffmann, S. *et al.* Ceramide synthases and ceramide levels are increased in breast cancer tissue. *Carcinogenesis* **30,** 745–52 (2009).

71. Koybasi, S. *et al.* Defects in cell growth regulation by C18:0-ceramide and longevity assurance gene 1 in human head and neck squamous cell carcinomas. *J. Biol. Chem.* **279,** 44311–9 (2004).

72. Voelkel-Johnson, C., Hannun, Y. A. & El-Zawahry, A. Resistance to TRAIL is associated with defects in ceramide signaling that can be overcome by exogenous C6-ceramide without requiring down-regulation of cellular FLICE inhibitory protein. *Mol. Cancer Ther.* **4,** 1320–7 (2005).

73. Schiffmann, S. *et al.* Ceramide synthase 6 plays a critical role in the development of experimental autoimmune encephalomyelitis. *J. Immunol.* **188,** 5723–33 (2012).

74. Barthelmes, J. *et al.* Lack of ceramide synthase 2 suppresses the development of experimental autoimmune encephalomyelitis by impairing the migratory capacity of neutrophils. *Brain. Behav. Immun.* (2015).

75. Kolak, M. *et al.* Adipose tissue inflammation and increased ceramide content characterize subjects with high liver fat content independent of obesity. *Diabetes* **56,** 1960–8 (2007).

76. Kotronen, A. *et al.* Comparison of Lipid and Fatty Acid Composition of the Liver, Subcutaneous and Intra-abdominal Adipose Tissue, and Serum. *Obesity* **18,** 937–944 (2009).

77. Turpin, S. M. *et al.* Obesity-induced CerS6-dependent C16:0 ceramide production promotes weight gain and glucose intolerance. *Cell Metab.* **20,** 678–86 (2014).

78. Rodriguez-Cuenca, S., Barbarroja, N. & Vidal-Puig, A. Dihydroceramide desaturase 1, the gatekeeper of ceramide induced lipotoxicity. *Biochim. Biophys. Acta* **1851,** 40–50 (2015).

79. Kraveka, J. M. *et al.* Involvement of dihydroceramide desaturase in cell cycle progression in human neuroblastoma cells. *J. Biol. Chem.* **282,** 16718–28 (2007).

80. Gagliostro, V. *et al.* Dihydroceramide delays cell cycle G1/S transition via activation of ER stress and induction of autophagy. *Int. J. Biochem. Cell Biol.* **44,** 2135–43 (2012).

81. AHN, E. H. & SCHROEDER, J. J. Induction of Apoptosis by Sphingosine, Sphinganine, and C2-Ceramide in Human Colon Cancer Cells, but not by C2-Dihydroceramide. *Anticancer Res* **30,** 2881–2884 (2010).

82. Geley, S., Hartmann, B. L. & Kofler, R. Ceramides induce a form of apoptosis in human acute lymphoblastic leukemia cells that is inhibited by Bcl-2, but not by CrmA. *FEBS Lett.* **400,** 15–18 (1997).

83. Shikata, K., Niiro, H., Azuma, H., Ogino, K. & Tachibana, T. Apoptotic activities of C2-ceramide and C2-dihydroceramide homologues against HL-60 cells. *Bioorg. Med. Chem.* **11,** 2723–2728 (2003).

84. Noack, J., Choi, J., Richter, K., Kopp-Schneider, A. & Régnier-Vigouroux, A. A sphingosine kinase inhibitor combined with temozolomide induces glioblastoma cell death through accumulation of dihydrosphingosine and dihydroceramide, endoplasmic reticulum stress and autophagy. *Cell Death Dis.* **5,** e1425 (2014).

85. Signorelli, P. *et al.* Dihydroceramide intracellular increase in response to resveratrol treatment mediates autophagy in gastric cancer cells. *Cancer Lett.* **282,** 238–43 (2009).

86. Wang, H. *et al.* N-(4-Hydroxyphenyl)retinamide increases dihydroceramide and synergizes with dimethylsphingosine to enhance cancer cell killing. *Mol. Cancer Ther.* **7,** 2967–76 (2008).

87. Jiang, Q. *et al.* Gamma-tocotrienol induces apoptosis and autophagy in prostate cancer cells by increasing intracellular dihydrosphingosine and dihydroceramide. *Int. J. Cancer* **130,** 685–93 (2012).

88. Holliday, M. W., Cox, S. B., Kang, M. H. & Maurer, B. J. C22:0- and C24:0-dihydroceramides Confer Mixed Cytotoxicity in T-Cell Acute Lymphoblastic Leukemia Cell Lines. *PLoS One* **8,** e74768 (2013).

89. Schiffmann, S. *et al.* The selective COX-2 inhibitor celecoxib modulates sphingolipid synthesis. *J. Lipid Res.* **50,** 32–40 (2009).

90. Knapp, P. *et al.* Altered sphingolipid metabolism in human endometrial cancer. *Prostaglandins Other Lipid Mediat.* **92,** 62–6 (2010).

91. Yin, J., Miyazaki, K., Shaner, R. L., Merrill, A. H. & Kannagi, R. Altered sphingolipid metabolism induced by tumor hypoxia – New vistas in glycolipid tumor markers. *FEBS Lett.* **584,** 1872–1878 (2010).

92. Devlin, C. M. *et al.* Dihydroceramide-based response to hypoxia. *J. Biol. Chem.* **286,** 38069–78 (2011).

93. Suzuki, E., Handa, K., Toledo, M. S. & Hakomori, S. Sphingosine-dependent apoptosis: a unified concept based on multiple mechanisms operating in concert. *Proc. Natl. Acad. Sci. U. S. A.* **101,** 14788–93 (2004).

94. Hannun, Y. A. & Bell, R. M. Regulation of protein kinase C by sphingosine and lysosphingolipids. *Clin. Chim. Acta.* **185,** 333–45 (1989).

95. Smith, E. R., Jones, P. L., Boss, J. M. & Merrill, A. H. Changing J774A.1 cells to new medium perturbs multiple signaling pathways, including the modulation of protein kinase C by endogenous sphingoid bases. *J. Biol. Chem.* **272,** 5640–6 (1997).

96. Jarvis, W. D. *et al.* Coordinate regulation of stress- and mitogen-activated protein kinases in the apoptotic actions of ceramide and sphingosine. *Mol. Pharmacol.* **52,** 935–47 (1997).

97. Chang, H. C., Tsai, L. H., Chuang, L. Y. & Hung, W. C. Role of AKT kinase in sphingosine-induced apoptosis in human hepatoma cells. *J. Cell. Physiol.* **188,** 188–93 (2001).

98. Kågedal, K., Zhao, M., Svensson, I. & Brunk, U. T. Sphingosine-induced apoptosis is dependent on lysosomal proteases. *Biochem. J.* **359,** 335–43 (2001).

99. Ullio, C. *et al.* Sphingosine mediates TNFα-induced lysosomal membrane permeabilization and ensuing programmed cell death in hepatoma cells. *J. Lipid Res.* **53,** 1134–43 (2012).

100. Hu, W. *et al.* Golgi fragmentation is associated with ceramide-induced cellular effects. *Mol. Biol. Cell* **16,** 1555–67 (2005).

101. Ahn, E. H., Chang, C.-C. & Schroeder, J. J. Evaluation of sphinganine and sphingosine as human breast cancer chemotherapeutic and chemopreventive agents. *Exp. Biol. Med. (Maywood).* **231,** 1664–72 (2006).

102. Ahn, E. H. & Schroeder, J. J. Sphingoid bases and ceramide induce apoptosis in HT-29 and HCT-116 human colon cancer cells. *Exp. Biol. Med. (Maywood).* **227,** 345–53 (2002).

103. Solomon, J. C., Sharma, K., Wei, L. X., Fujita, T. & Shi, Y. F. A novel role for sphingolipid intermediates in activation-induced cell death in T cells. *Cell Death Differ.* **10,** 193–202 (2003).

104. Tolleson, W. H. *et al.* Fumonisin B1 induces apoptosis in cultured human keratinocytes through sphinganine accumulation and ceramide depletion. *Int. J. Oncol.* **14,** 833–43 (1999).

105. Mao, Z. *et al.* Alkaline ceramidase 2 (ACER2) and its product dihydrosphingosine mediate the cytotoxicity of N-(4-hydroxyphenyl)retinamide in tumor cells. *J. Biol. Chem.* **285,** 29078–90 (2010).

106. Chung, N., Mao, C., Heitman, J., Hannun, Y. A. & Obeid, L. M. Phytosphingosine as a Specific Inhibitor of Growth and Nutrient Import in Saccharomyces cerevisiae. *J. Biol. Chem.* **276,** 35614–35621 (2001).

107. Liu, K., Zhang, X., Lester, R. L. & Dickson, R. C. The Sphingoid Long Chain Base Phytosphingosine Activates AGC-type Protein Kinases in Saccharomyces cerevisiae Including Ypk1, Ypk2, and Sch9. *J. Biol. Chem.* **280,** 22679–22687 (2005).

108. Kim, S. *et al.* Phytosphingosine stimulates the differentiation of human keratinocytes and inhibits TPA-induced inflammatory epidermal hyperplasia in hairless mouse skin. *Mol. Med.* **12,** 17–24 (2006).

109. Nagahara, Y. *et al.* Phytosphingosine induced mitochondria-involved apoptosis. *Cancer Sci.* **96,** 83–92 (2005).

110. Choi, S.-Y., Kim, M.-J., Chung, H. Y., Lee, S.-J. & Jang, Y.-J. Phytosphingosine in combination with TRAIL sensitizes cancer cells to TRAIL through synergistic up-regulation of DR4 and DR5. *Oncol. Rep.* **17,** 175–84 (2007).

111. Ikeda, H. *et al.* Biological activities of novel lipid mediator sphingosine 1-phosphate in rat hepatic stellate cells. *Am. J. Physiol. Gastrointest. Liver Physiol.* **279,** G304–10 (2000).

112. Augé, N. *et al.* Role of sphingosine 1-phosphate in the mitogenesis induced by oxidized low density lipoprotein in smooth muscle cells via activation of sphingomyelinase, ceramidase, and sphingosine kinase. *J. Biol. Chem.* **274,** 21533–8 (1999).

113. Van Brocklyn, J., Letterle, C., Snyder, P. & Prior, T. Sphingosine-1-phosphate stimulates human glioma cell proliferation through Gi-coupled receptors: role of ERK MAP kinase and phosphatidylinositol 3-kinase beta. *Cancer Lett.* **181,** 195–204 (2002).

114. Cuvillier, O., Rosenthal, D. S., Smulson, M. E. & Spiegel, S. Sphingosine 1-phosphate inhibits activation of caspases that cleave poly(ADP-ribose) polymerase and lamins during Fas- and ceramide-mediated apoptosis in Jurkat T lymphocytes. *J. Biol. Chem.* **273,** 2910–6 (1998).

115. Kwon, Y. G. *et al.* Sphingosine 1-phosphate protects human umbilical vein endothelial cells from serum-deprived apoptosis by nitric oxide production. *J. Biol. Chem.* **276,** 10627–33 (2001).

116. Castillo, S. S. & Teegarden, D. Sphingosine-1-phosphate inhibition of apoptosis requires mitogen-activated protein kinase phosphatase-1 in mouse fibroblast C3H10T 1/2 cells. *J. Nutr.* **133,** 3343–9 (2003).

117. Lavieu, G. *et al.* Regulation of autophagy by sphingosine kinase 1 and its role in cell survival during nutrient starvation. *J. Biol. Chem.* **281,** 8518–27 (2006).

118. Chang, C.-L. *et al.* S1P(5) is required for sphingosine 1-phosphate-induced autophagy in human prostate cancer PC-3 cells. *Am. J. Physiol. Cell Physiol.* **297,** C451–8 (2009).

119. Paik, J. H., Chae Ss, Lee, M. J., Thangada, S. & Hla, T. Sphingosine 1-phosphate-induced endothelial cell migration requires the expression of EDG-1 and EDG-3 receptors and Rho-dependent activation of alpha vbeta3- and beta1-containing integrins. *J. Biol. Chem.* **276,** 11830–7 (2001).

120. Rosenfeldt, H. M. *et al.* EDG-1 links the PDGF receptor to Src and focal adhesion kinase activation leading to lamellipodia formation and cell migration. *FASEB J.* **15,** 2649–59 (2001).

121. LaMontagne, K. *et al.* Antagonism of sphingosine-1-phosphate receptors by FTY720 inhibits angiogenesis and tumor vascularization. *Cancer Res.* **66,** 221–31 (2006).

122. Takuwa, Y. *et al.* Roles of sphingosine-1-phosphate signaling in angiogenesis. *World J. Biol. Chem.* **1,** 298–306 (2010).

123. Mendelson, K., Evans, T. & Hla, T. Sphingosine 1-phosphate signalling. *Development* **141,** 5–9 (2014).

124. Pitson, S. M. Regulation of sphingosine kinase and sphingolipid signaling. *Trends Biochem. Sci.* **36,** 97–107 (2011).

125. Pyne, N. J. & Pyne, S. Sphingosine 1-phosphate and cancer. *Nat. Rev. Cancer* **10,** 489–503 (2010).

126. Rivera, J., Proia, R. L. & Olivera, A. The alliance of sphingosine-1-phosphate and its receptors in immunity. *Nat. Rev. Immunol.* **8,** 753–63 (2008).

127. Mullen, T. D., Hannun, Y. a & Obeid, L. M. Ceramide synthases at the centre of sphingolipid metabolism and biology. *Biochem. J.* **441,** 789–802 (2012).

128. Egilmez, N. K., Chen, J. B. & Jazwinski, S. M. Specific alterations in transcript prevalence during the yeast life span. *J. Biol. Chem.* **264,** 14312–7 (1989).

129. D'mello, N. P. *et al.* Cloning and characterization of LAG1, a longevity-assurance gene in yeast. *J. Biol. Chem.* **269,** 15451–9 (1994).

130. Guillas, I. *et al.* C26-CoA-dependent ceramide synthesis of Saccharomyces cerevisiae is operated by Lag1p and Lac1p. *EMBO J.* **20,** 2655–65 (2001).

131. Lee, S. J. Expression of growth/differentiation factor 1 in the nervous system: conservation of a bicistronic structure. *Proc. Natl. Acad. Sci. U. S. A.* **88,** 4250–4 (1991).

132. Jiang, J. C., Kirchman, P. A., Zagulski, M., Hunt, J. & Jazwinski, S. M. Homologs of the yeast longevity gene LAG1 in Caenorhabditis elegans and human. *Genome Res.* **8,** 1259–72 (1998).

133. Venkataraman, K. *et al.* Upstream of growth and differentiation factor 1 (uog1), a mammalian homolog of the yeast longevity assurance gene 1 (LAG1), regulates N-stearoyl-sphinganine (C18-(dihydro)ceramide) synthesis in a fumonisin B1-independent manner in mammalian cells. *J. Biol. Chem.* **277,** 35642–9 (2002).

134. Winter, E. & Ponting, C. P. TRAM, LAG1 and CLN8: members of a novel family of lipid-sensing domains? *Trends Biochem. Sci.* **27,** 381–3 (2002).

135. Venkataraman, K. & Futerman, A. H. Do longevity assurance genes containing Hox domains regulate cell development via ceramide synthesis? *FEBS Lett.* **528,** 3–4 (2002).

136. Riebeling, C., Allegood, J. C., Wang, E., Merrill, A. H. & Futerman, A. H. Two mammalian longevity assurance gene (LAG1) family members, trh1 and trh4, regulate dihydroceramide synthesis using different fatty acyl-CoA donors. *J. Biol. Chem.* **278,** 43452–9 (2003).

137. Pan, H. *et al.* Cloning, mapping, and characterization of a human homologue of the yeast longevity assurance gene LAG1. *Genomics* **77,** 58–64 (2001).

138. Weinmann, A., Galle, P. R. & Teufel, A. LASS6, an additional member of the longevity assurance gene family. *Int. J. Mol. Med.* **16,** 905–10 (2005).

139. Mizutani, Y., Kihara, A. & Igarashi, Y. LASS3 (longevity assurance homologue 3) is a mainly testis-specific (dihydro)ceramide synthase with relatively broad substrate specificity. *Biochem. J.* **398,** 531–8 (2006).

140. Hirschberg, K., Rodger, J. & Futerman, A. H. The long-chain sphingoid base of sphingolipids is acylated at the cytosolic surface of the endoplasmic reticulum in rat liver. *Biochem. J.* **290,** 751–7 (1993).

141. Shimeno, H. *et al.* Partial purification and characterization of sphingosine N-acyltransferase (ceramide synthase) from bovine liver mitochondrion-rich fraction. *Lipids* **33,** 601–5 (1998).

142. Kageyama-Yahara, N. & Riezman, H. Transmembrane topology of ceramide synthase in yeast. *Biochem. J.* **398,** 585–93 (2006).

143. Tidhar, R. *et al.* Acyl chain specificity of ceramide synthases is determined within a region of 150 residues in the Tram-Lag-CLN8 (TLC) domain. *J. Biol. Chem.* **287,** 3197–206 (2012).

144. Laviad, E. L., Kelly, S., Merrill, A. H. & Futerman, A. H. Modulation of ceramide synthase activity via dimerization. *J. Biol. Chem.* **287,** 21025–33 (2012).

145. Laviad, E. L. *et al.* Characterization of ceramide synthase 2: tissue distribution, substrate specificity, and inhibition by sphingosine 1-phosphate. *J. Biol. Chem.* **283,** 5677–84 (2008).

146. Becker, I., Wang-Eckhardt, L., Yaghootfam, A., Gieselmann, V. & Eckhardt, M. Differential expression of (dihydro)ceramide synthases in mouse brain: oligodendrocyte-specific expression of CerS2/Lass2. *Histochem. Cell Biol.* **129,** 233–41 (2008).

147. Cai, X.-F., Tao, Z., Yan, Z.-Q., Yang, S.-L. & Gong, Y. Molecular cloning, characterisation and tissue-specific expression of human LAG3, a member of the novel Lag1 protein family. *DNA Seq.* **14,** 79–86 (2003).

148. Mizutani, Y., Kihara, A., Chiba, H., Tojo, H. & Igarashi, Y. 2-Hydroxy-ceramide synthesis by ceramide synthase family: enzymatic basis for the preference of FA chain length. *J. Lipid Res.* **49,** 2356–64 (2008).

149. Xu, Z., Zhou, J., McCoy, D. M. & Mallampalli, R. K. LASS5 is the predominant ceramide synthase isoform involved in de novo sphingolipid synthesis in lung epithelia. *J. Lipid Res.* **46,** 1229–38 (2005).

150. Mesika, A., Ben-Dor, S., Laviad, E. L. & Futerman, A. H. A new functional motif in Hox domain-containing ceramide synthases: identification of a novel region flanking the Hox and TLC domains essential for activity. *J. Biol. Chem.* **282,** 27366–73 (2007).

151. Harrer, H., Laviad, E. L., Humpf, H. U. & Futerman, A. H. Identification of N-acyl-fumonisin B1 as new cytotoxic metabolites of fumonisin mycotoxins. *Mol. Nutr. Food Res.* **57,** 516–22 (2013).

152. Kim, H. J., Qiao, Q., Toop, H. D., Morris, J. C. & Don, A. S. A fluorescent assay for ceramide synthase activity. *J. Lipid Res.* **53,** 1701–7 (2012).

153. Lahiri, S. *et al.* Ceramide Synthesis Is Modulated by the Sphingosine Analog FTY720 via a Mixture of Uncompetitive an Noncompetitive Inhibition in a Acyl-CoA Chain Lenght-dependent Manner. *Jbc* (2009).

154. Kirin, M. *et al.* Genome-wide association study identifies genetic risk underlying primary rhegmatogenous retinal detachment. *Hum. Mol. Genet.* **22,** 3174–85 (2013).

155. Strettoi, E. *et al.* Inhibition of ceramide biosynthesis preserves photoreceptor structure and function in a mouse model of retinitis pigmentosa. *Proc. Natl. Acad. Sci. U. S. A.* **107,** 18706–11 (2010).

156. Chen, H. *et al.* Inhibition of de novo ceramide biosynthesis by FTY720 protects rat retina from light-induced degeneration. *J. Lipid Res.* **54,** 1616–29 (2013).

157. Eckl, K.-M. *et al.* Impaired epidermal ceramide synthesis causes autosomal recessive congenital ichthyosis and reveals the importance of ceramide acyl chain length. *J. Invest. Dermatol.* **133,** 2202–11 (2013).

158. Radner, F. P. W. *et al.* Mutations in CERS3 cause autosomal recessive congenital ichthyosis in humans. *PLoS Genet.* **9,** e1003536 (2013).

159. Park, J.-W., Park, W.-J. & Futerman, A. H. Ceramide synthases as potential targets for therapeutic intervention in human diseases. *Biochim. Biophys. Acta* **1841,** 671–81 (2014).

160. Ebel, P. *et al.* Ceramide synthase 4 deficiency in mice causes lipid alterations in sebum and results in alopecia. *Biochem. J.* **461,** 147–58 (2014).

161. Peters, F. *et al.* Ceramide Synthase 4 Regulates Stem Cell Homeostasis and Hair Follicle Cycling. *J. Invest. Dermatol.* (2015).

162. Marasas, W. F. Discovery and occurrence of the fumonisins: a historical perspective. *Environ. Health Perspect.* **109 Suppl ,** 239–43 (2001).

163. Thiel, P. G., Marasas, W. F., Sydenham, E. W., Shephard, G. S. & Gelderblom, W. C. The implications of naturally occurring levels of fumonisins in corn for human and animal health. *Mycopathologia* **117,** 3–9 (1992).

164. Denli, M. *et al.* Efficacy of AdiDetox™ in reducing the toxicity of fumonisin B1 in rats. *Food Chem. Toxicol.* **78,** 60–3 (2015).

165. Merrill, A. H., Sullards, M. C., Wang, E., Voss, K. A. & Riley, R. T. Sphingolipid metabolism: roles in signal transduction and disruption by fumonisins. *Environ. Health Perspect.* **109 Suppl ,** 283–9 (2001).

166. Riley, R. T. *et al.* Sphingolipid perturbations as mechanisms for fumonisin carcinogenesis. *Environ. Health Perspect.* **109 Suppl,** 301–8 (2001).

167. Merrill, A. H., van Echten, G., Wang, E. & Sandhoff, K. Fumonisin B1 inhibits sphingosine (sphinganine) N-acyltransferase and de novo sphingolipid biosynthesis in cultured neurons in situ. *J. Biol. Chem.* **268,** 27299–306 (1993).

168. Wang, E., Norred, W. P., Bacon, C. W., Riley, R. T. & Merrill, A. H. Inhibition of sphingolipid biosynthesis by fumonisins. Implications for diseases associated with Fusarium moniliforme. *J. Biol. Chem.* **266,** 14486–14490 (1991).

169. Ciacci-Zanella, J. R., Merrill, A. H., Wang, E. & Jones, C. Characterization of cell-cycle arrest by fumonisin B1 in CV-1 cells. *Food Chem. Toxicol.* **36,** 791–804

170. Ciacci-Zanella, J. R. & Jones, C. Fumonisin B1, a Mycotoxin Contaminant of Cereal Grains, and Inducer of Apoptosis Via the Tumour Necrosis Factor Pathway and Caspase Activation. *Food Chem. Toxicol.* **37,** 703–712 (1999).

171. Schmelz, E. M. *et al.* Induction of apoptosis by fumonisin B1 in HT29 cells is mediated by the accumulation of endogenous free sphingoid bases. *Toxicol. Appl. Pharmacol.* **148,** 252–60 (1998).

172. Smith, E. R. & Merrill, A. H. Differential roles of de novo sphingolipid biosynthesis and turnover in the "burst" of free sphingosine and sphinganine, and their 1-phosphates and N-acyl-derivatives, that occurs upon changing the medium of cells in culture. *J. Biol. Chem.* **270,** 18749–58 (1995).

173. Abbas, H. K. *et al.* Fumonisin- and AAL-Toxin-Induced Disruption of Sphingolipid Metabolism with Accumulation of Free Sphingoid Bases. *Plant Physiol.* **106,** 1085–1093 (1994).

174. Mandala, S. M. *et al.* The Discovery of Australifungin , a Novel Inhibitor of Sphinganine TV-Acyltransferase from Sporormiella australis Producing Organism , Fermentation , Isolation , and Biological Activity. **48,** (1995).

175. Gräler, M. H. & Goetzl, E. J. The immunosuppressant FTY720 down-regulates sphingosine 1-phosphate G-protein-coupled receptors. *FASEB J.* **18,** 551–3 (2004).

176. Mao, C. & Obeid, L. M. Ceramidases: regulators of cellular responses mediated by ceramide, sphingosine, and sphingosine-1-phosphate. *Biochim. Biophys. Acta* **1781,** 424–34 (2008).

177. Ito, M., Okino, N. & Tani, M. New insight into the structure, reaction mechanism, and biological functions of neutral ceramidase. *Biochim. Biophys. Acta - Mol. Cell Biol. Lipids* **1841,** 682–691 (2014).

178. Tani, M. *et al.* Purification and characterization of a neutral ceramidase from mouse liver. A single protein catalyzes the reversible reaction in which ceramide is both hydrolyzed and synthesized. *J. Biol. Chem.* **275,** 3462–8 (2000).

179. Mao, C., Xu, R., Bielawska, A. & Obeid, L. M. Cloning of an alkaline ceramidase from Saccharomyces cerevisiae. An enzyme with reverse (CoA-independent) ceramide synthase activity. *J. Biol. Chem.* **275,** 6876–84 (2000).

180. Okino, N. *et al.* The reverse activity of human acid ceramidase. *J. Biol. Chem.* **278,** 29948–53 (2003).

181. Gatt, S. Enzymic hydrolysis and synthesis of ceramides. *J. Biol. Chem.* **238,** 3131–3 (1963).

182. Bernardo, K. *et al.* Purification, characterization, and biosynthesis of human acid ceramidase. *J. Biol. Chem.* **270,** 11098–102 (1995).

183. Li, C. M. *et al.* Cloning and characterization of the full-length cDNA and genomic sequences encoding murine acid ceramidase. *Genomics* **50,** 267–74 (1998).

184. Koch, J. *et al.* Molecular cloning and characterization of a full-length complementary DNA encoding human acid ceramidase. Identification Of the first molecular lesion causing Farber disease. *J. Biol. Chem.* **271,** 33110–5 (1996).

185. Ferlinz, K. *et al.* Human acid ceramidase: processing, glycosylation, and lysosomal targeting. *J. Biol. Chem.* **276,** 35352–60 (2001).

186. Shtraizent, N. *et al.* Autoproteolytic cleavage and activation of human acid ceramidase. *J. Biol. Chem.* **283,** 11253–9 (2008).

187. Pei, J. & Grishin, N. V. Peptidase family U34 belongs to the superfamily of N-terminal nucleophile hydrolases. *Protein Sci.* **12,** 1131–5 (2003).

188. Schulze, H., Schepers, U. & Sandhoff, K. Overexpression and mass spectrometry analysis of mature human acid ceramidase. *Biol. Chem.* **388,** 1333–43 (2007).

189. Liu, X. *et al.* Acid ceramidase upregulation in prostate cancer: role in tumor development and implications for therapy. *Expert Opin. Ther. Targets* **13,** 1449–58 (2009).

190. Elojeimy, S. *et al.* Role of acid ceramidase in resistance to FasL: therapeutic approaches based on acid ceramidase inhibitors and FasL gene therapy. *Mol. Ther.* **15,** 1259–63 (2007).

191. Musumarra, G., Barresi, V., Condorelli, D. F. & Scirè, S. A bioinformatic approach to the identification of candidate genes for the development of new cancer diagnostics. *Biol. Chem.* **384,** 321–7 (2003).

192. Strelow, A. *et al.* Overexpression of Acid Ceramidase Protects from Tumor Necrosis Factor-Induced Cell Death. *J. Exp. Med.* **192,** 601–612 (2000).

193. Mahdy, A. E. M. *et al.* Acid ceramidase upregulation in prostate cancer cells confers resistance to radiation: AC inhibition, a potential radiosensitizer. *Mol. Ther.* **17,** 430–8 (2009).

194. Eliyahu, E., Park, J.-H., Shtraizent, N., He, X. & Schuchman, E. H. Acid ceramidase is a novel factor required for early embryo survival. *FASEB J.* **21,** 1403–9 (2007).

195. Farber, S., Cohen, J. & Uzman, L. L. Lipogranulomatosis; a new lipo-glycoprotein storage disease. *J. Mt. Sinai Hosp. N. Y.* **24,** 816–37 (1957).

196. Park, J.-H. & Schuchman, E. H. Acid ceramidase and human disease. *Biochim. Biophys. Acta* **1758,** 2133–8 (2006).

197. Chavez, J. A., Holland, W. L., Bär, J., Sandhoff, K. & Summers, S. A. Acid ceramidase overexpression prevents the inhibitory effects of saturated fatty acids on insulin signaling. *J. Biol. Chem.* **280,** 20148–53 (2005).

198. Huang, Y. *et al.* Elevation of the level and activity of acid ceramidase in Alzheimer's disease brain. *Eur. J. Neurosci.* **20,** 3489–97 (2004).

199. Nilsson, Å. The presence of sphingomyelin- and ceramide-cleaving enzymes in the small intestinal tract. *Biochim. Biophys. Acta - Lipids Lipid Metab.* **176,** 339–347 (1969).

200. Okino, N. *et al.* Molecular cloning, sequencing, and expression of the gene encoding alkaline ceramidase from Pseudomonas aeruginosa. Cloning of a ceramidase homologue from Mycobacterium tuberculosis. *J. Biol. Chem.* **274,** 36616–22 (1999).

201. El Bawab, S. *et al.* Molecular cloning and characterization of a human mitochondrial ceramidase. *J. Biol. Chem.* **275,** 21508–13 (2000).

202. Canals, D., Perry, D. M., Jenkins, R. W. & Hannun, Y. A. Drug targeting of sphingolipid metabolism: sphingomyelinases and ceramidases. *Br. J. Pharmacol.* **163,** 694–712 (2011).

203. Galadari, S. *et al.* Identification of a novel amidase motif in neutral ceramidase. *Biochem. J.* **393,** 687–95 (2006).

204. Hwang, Y., Tani, M., Nakagawa, T., Okino, N. & Ito, M. Subcellular localization of human neutral ceramidase expressed in HEK293 cells. *Biochem. Biophys. Res. Commun.* **331,** 37–42 (2005).

205. Tani, M., Iida, H. & Ito, M. O-glycosylation of mucin-like domain retains the neutral ceramidase on the plasma membranes as a type II integral membrane protein. *J. Biol. Chem.* **278,** 10523–30 (2003).

206. Mitsutake, S. *et al.* Purification, characterization, molecular cloning, and subcellular distribution of neutral ceramidase of rat kidney. *J. Biol. Chem.* **276,** 26249–59 (2001).

207. Olsson, M., Duan, R.-D., Ohlsson, L. & Nilsson, A. Rat intestinal ceramidase: purification, properties, and physiological relevance. *Am. J. Physiol. Gastrointest. Liver Physiol.* **287,** G929–37 (2004).

208. Tani, M. *et al.* Molecular cloning of the full-length cDNA encoding mouse neutral ceramidase. A novel but highly conserved gene family of neutral/alkaline ceramidases. *J. Biol. Chem.* **275,** 11229–34 (2000).

209. Choi, M. S. *et al.* Neutral ceramidase gene: role in regulating ceramide-induced apoptosis. *Gene* **315,** 113–22 (2003).

210. Inoue, T. *et al.* Mechanistic insights into the hydrolysis and synthesis of ceramide by neutral ceramidase. *J. Biol. Chem.* **284,** 9566–77 (2009).

211. Kono, M. *et al.* Neutral ceramidase encoded by the Asah2 gene is essential for the intestinal degradation of sphingolipids. *J. Biol. Chem.* **281,** 7324–31 (2006).

212. Zhu, Q. *et al.* Chronic activation of neutral ceramidase protects beta-cells against cytokine-induced apoptosis. *Acta Pharmacol. Sin.* **29,** 593–9 (2008).

213. Snider, A. J. *et al.* Loss of neutral ceramidase increases inflammation in a mouse model of inflammatory bowel disease. *Prostaglandins Other Lipid Mediat.* **99,** 124–30 (2012).

214. Sun, W. *et al.* Upregulation of the human alkaline ceramidase 1 and acid ceramidase mediates calcium-induced differentiation of epidermal keratinocytes. *J. Invest. Dermatol.* **128,** 389–97 (2008).

215. Xu, R. *et al.* Golgi alkaline ceramidase regulates cell proliferation and survival by controlling levels of sphingosine and S1P. *FASEB J.* **20,** 1813–25 (2006).

216. Mao, C. *et al.* Cloning and characterization of a novel human alkaline ceramidase. A mammalian enzyme that hydrolyzes phytoceramide. *J. Biol. Chem.* **276,** 26577–88 (2001).

217. Pei, J., Millay, D. P., Olson, E. N. & Grishin, N. V. CREST--a large and diverse superfamily of putative transmembrane hydrolases. *Biol. Direct* **6,** 37 (2011).

218. Xu, R., Sun, W., Jin, J., Obeid, L. M. & Mao, C. Role of alkaline ceramidases in the generation of sphingosine and its phosphate in erythrocytes. *FASEB J.* **24,** 2507–15 (2010).

219. Hu, W. *et al.* Alkaline ceramidase 3 (ACER3) hydrolyzes unsaturated long-chain ceramides, and its down-regulation inhibits both cell proliferation and apoptosis. *J. Biol. Chem.* **285,** 7964–76 (2010).

220. Wertz, P. W. & Downing, D. T. Ceramidase activity in porcine epidermis. *FEBS Lett.* **268,** 110–2 (1990).

221. He, X. *et al.* A fluorescence-based high-performance liquid chromatographic assay to determine acid ceramidase activity. *Anal. Biochem.* **274,** 264–9 (1999).

222. Tani, M., Okino, N., Mitsutake, S. & Ito, M. Specific and sensitive assay for alkaline and neutral ceramidases involving C12-NBD-ceramide. *J. Biochem.* **125,** 746–9 (1999).

223. Nieuwenhuizen, W. F., van Leeuwen, S., Götz, F. & Egmond, M. R. Synthesis of a novel fluorescent ceramide analogue and its use in the characterization of recombinant ceramidase from Pseudomonas aeruginosa PA01. *Chem. Phys. Lipids* **114,** 181–91 (2002).

224. Bedia, C., Casas, J., Garcia, V., Levade, T. & Fabriàs, G. Synthesis of a novel ceramide analogue and its use in a high-throughput fluorogenic assay for ceramidases. *Chembiochem* **8,** 642–8 (2007).

225. Bedia, C., Camacho, L., Abad, J. L., Fabriàs, G. & Levade, T. A simple fluorogenic method for determination of acid ceramidase activity and diagnosis of Farber disease. *J. Lipid Res.* **51,** 3542–7 (2010).

226. Bhabak, K. P., Proksch, D., Redmer, S. & Arenz, C. Novel fluorescent ceramide derivatives for probing ceramidase substrate specificity. *Bioorg. Med. Chem.* **20,** 6154–6161 (2012).

227. Bhabak, K. P. *et al.* Development of a novel FRET probe for the real-time determination of ceramidase activity. *Chembiochem* **14,** 1049–52 (2013).

228. Camacho, L. *et al.* Acid ceramidase as a therapeutic target in metastatic prostate cancer. *J. Lipid Res.* **54,** 1207–20 (2013).

229. Endo, K., Akiyama, T., Kobayashi, S. & Okada, M. Degenerative spermatocyte, a novel gene encoding a transmembrane protein required for the initiation of meiosis in Drosophila spermatogenesis. *Mol. Gen. Genet.* **253,** 157–65 (1996).

230. Endo, K., Matsuda, Y. & Kobayashi, S. Mdes, a mouse homolog of the Drosophila degenerative spermatocyte gene is expressed during mouse spermatogenesis. *Dev. Growth Differ.* **39,** 399–403 (1997).

231. Cadena, D. L., Kurten, R. C. & Gill, G. N. The product of the MLD gene is a member of the membrane fatty acid desaturase family: overexpression of MLD inhibits EGF receptor biosynthesis. *Biochemistry* **36,** 6960–7 (1997).

232. Geeraert, L., Mannaerts, G. P. & van Veldhoven, P. P. Conversion of dihydroceramide into ceramide: involvement of a desaturase. *Biochem. J.* **327,** 125–32 (1997).

233. Michel, C. *et al.* Characterization of ceramide synthesis. A dihydroceramide desaturase introduces the 4,5-trans-double bond of sphingosine at the level of dihydroceramide. *J. Biol. Chem.* **272,** 22432–7 (1997).

234. Schulze, H., Michel, C. & van Echten-Deckert, G. Dihydroceramide desaturase. *Methods Enzymol.* **311,** 22–30 (2000).

235. Enomoto, A. *et al.* Dihydroceramide:sphinganine C-4-hydroxylation requires Des2 hydroxylase and the membrane form of cytochrome b5. *Biochem. J.* **397,** 289–95 (2006).

236. Fabrias, G. *et al.* Dihydroceramide desaturase and dihydrosphingolipids: debutant players in the sphingolipid arena. *Prog. Lipid Res.* **51,** 82–94 (2012).

237. Ternes, P., Franke, S., Zähringer, U., Sperling, P. & Heinz, E. Identification and characterization of a sphingolipid delta 4-desaturase family. *J. Biol. Chem.* **277,** 25512–8 (2002).

238. Shanklin, J. & Cahoon, E. B. DESATURATION AND RELATED MODIFICATIONS OF FATTY ACIDS1. *Annu. Rev. Plant Physiol. Plant Mol. Biol.* **49,** 611–641 (1998).

239. Mizutani, Y., Kihara, A. & Igarashi, Y. Identification of the human sphingolipid C4-hydroxylase, hDES2, and its up-regulation during keratinocyte differentiation. *FEBS Lett.* **563,** 93–7 (2004).

240. Beauchamp, E. *et al.* Myristic acid increases the activity of dihydroceramide Delta4-desaturase 1 through its N-terminal myristoylation. *Biochimie* **89,** 1553–61 (2007).

241. Omae, F. *et al.* DES2 protein is responsible for phytoceramide biosynthesis in the mouse small intestine. *Biochem. J.* **379,** 687–95 (2004).

242. Holland, W. L. *et al.* Inhibition of ceramide synthesis ameliorates glucocorticoid-, saturated-fat-, and obesity-induced insulin resistance. *Cell Metab.* **5,** 167–79 (2007).

243. Siddique, M. M. *et al.* Ablation of dihydroceramide desaturase 1, a therapeutic target for the treatment of metabolic diseases, simultaneously stimulates anabolic and catabolic signaling. *Mol. Cell. Biol.* **33,** 2353–69 (2013).

244. Shankar, S., Singh, G. & Srivastava, R. K. Chemoprevention by resveratrol: molecular mechanisms and therapeutic potential. *Front. Biosci.* **12,** 4839–54 (2007).

245. Idkowiak-Baldys, J. *et al.* Dihydroceramide desaturase activity is modulated by oxidative stress. *Biochem. J.* **427,** 265–74 (2010).

246. Rahmaniyan, M., Curley, R. W., Obeid, L. M., Hannun, Y. a & Kraveka, J. M. Identification of dihydroceramide desaturase as a direct in vitro target for fenretinide. *J. Biol. Chem.* **286,** 24754–64 (2011).

247. Triola, G., Fabriàs, G. & Llebaria, A. Synthesis of a Cyclopropene Analogue of Ceramide, a Potent Inhibitor of Dihydroceramide Desaturase. *Angew. Chemie* **113,** 2014–2016 (2001).

248. Triola, G., Fabriàs, G., Casas, J. & Llebaria, A. Synthesis of cyclopropene analogues of ceramide and their effect on dihydroceramide desaturase. *J. Org. Chem.* **68,** 9924–32 (2003).

249. Triola, G. *et al.* Specificity of the dihydroceramide desaturase inhibitor N-[(1R,2S)-2-hydroxy-1-hydroxymethyl-2-(2-tridecyl-1-cyclopropenyl)ethyl]octanamide (GT11) in primary cultured cerebellar neurons. *Mol. Pharmacol.* **66,** 1671–8 (2004).

250. Munoz-Olaya, J. M. *et al.* Synthesis and biological activity of a novel inhibitor of dihydroceramide desaturase. *ChemMedChem* **3,** 946–53 (2008).

251. Kohama, T. *et al.* Molecular Cloning and Functional Characterization of Murine Sphingosine Kinase. *J. Biol. Chem.* **273,** 23722–23728 (1998).

252. Liu, H. *et al.* Molecular cloning and functional characterization of a novel mammalian sphingosine kinase type 2 isoform. *J. Biol. Chem.* **275,** 19513–20 (2000).

253. Neubauer, H. a & Pitson, S. M. Roles, regulation and inhibitors of sphingosine kinase 2. *FEBS J.* (2013).

254. Wang, Z. *et al.* Molecular basis of sphingosine kinase 1 substrate recognition and catalysis. *Structure* **21,** 798–809 (2013).

255. Ren, S., Xin, C., Pfeilschifter, J. & Huwiler, A. A novel mode of action of the putative sphingosine kinase inhibitor 2-(p-hydroxyanilino)-4-(p-chlorophenyl) thiazole (SKI II): induction of lysosomal sphingosine kinase 1 degradation. *Cell. Physiol. Biochem.* **26,** 97–104 (2010).

256. Loveridge, C. *et al.* The sphingosine kinase 1 inhibitor 2-(p-hydroxyanilino)-4-(p-chlorophenyl)thiazole induces proteasomal degradation of sphingosine kinase 1 in mammalian cells. *J. Biol. Chem.* **285,** 38841–52 (2010).

257. Taha, T. A., Hannun, Y. A. & Obeid, L. M. Sphingosine kinase: biochemical and cellular regulation and role in disease. *J. Biochem. Mol. Biol.* **39,** 113–31 (2006).

258. Pitson, S. M. *et al.* Activation of sphingosine kinase 1 by ERK1/2-mediated phosphorylation. *EMBO J.* **22,** 5491–500 (2003).

259. Strub, G. M. *et al.* Sphingosine-1-phosphate produced by sphingosine kinase 2 in mitochondria interacts with prohibitin 2 to regulate complex IV assembly and respiration. *FASEB J.* **25,** 600–12 (2011).

260. Pitson, S. M. *et al.* Phosphorylation-dependent translocation of sphingosine kinase to the plasma membrane drives its oncogenic signalling. *J. Exp. Med.* **201,** 49–54 (2005).

261. Igarashi, N. *et al.* Sphingosine kinase 2 is a nuclear protein and inhibits DNA synthesis. *J. Biol. Chem.* **278,** 46832–9 (2003).

262. Chipuk, J. E. *et al.* Sphingolipid metabolism cooperates with BAK and BAX to promote the mitochondrial pathway of apoptosis. *Cell* **148,** 988–1000 (2012).

263. Olivera, A. *et al.* Sphingosine kinase expression increases intracellular sphingosine-1-phosphate and promotes cell growth and survival. *J. Cell Biol.* **147,** 545–58 (1999).

264. Marfe, G., Mirone, G., Shukla, A. & Di Stefano, C. Sphingosine Kinases Signalling in Carcinogenesis. *Mini Rev. Med. Chem.* (2015). at <http://www.ncbi.nlm.nih.gov/pubmed/25723458>

265. Shida, D., Takabe, K., Kapitonov, D., Milstien, S. & Spiegel, S. Targeting SphK1 as a new strategy against cancer. *Curr. Drug Targets* **9,** 662–73 (2008).

266. Watson, C. *et al.* High expression of sphingosine 1-phosphate receptors, S1P1 and S1P3, sphingosine kinase 1, and extracellular signal-regulated kinase-1/2 is associated with development of tamoxifen resistance in estrogen receptor-positive breast cancer patients. *Am. J. Pathol.* **177,** 2205–15 (2010).

267. Heffernan-Stroud, L. a & Obeid, L. M. *Sphingosine kinase 1 in cancer. Adv. Cancer Res.* **117,** 201–35 (Elsevier Inc., 2013).

268. Long, J. S. *et al.* Sphingosine kinase 1 induces tolerance to human epidermal growth factor receptor 2 and prevents formation of a migratory phenotype in response to sphingosine 1-phosphate in estrogen receptor-positive breast cancer cells. *Mol. Cell. Biol.* **30,** 3827–41 (2010).

269. Liu, H. *et al.* Sphingosine kinase type 2 is a putative BH3-only protein that induces apoptosis. *J. Biol. Chem.* **278,** 40330–6 (2003).

270. Hofmann, L. P., Ren, S., Schwalm, S., Pfeilschifter, J. & Huwiler, A. Sphingosine kinase 1 and 2 regulate the capacity of mesangial cells to resist apoptotic stimuli in an opposing manner. *Biol. Chem.* **389,** 1399–407 (2008).

271. Chumanevich, A. A. *et al.* Suppression of colitis-driven colon cancer in mice by a novel small molecule inhibitor of sphingosine kinase. *Carcinogenesis* **31,** 1787–93 (2010).

272. Gao, P. & Smith, C. D. Ablation of sphingosine kinase-2 inhibits tumor cell proliferation and migration. *Mol. Cancer Res.* **9,** 1509–19 (2011).

273. Weigert, A. *et al.* Sphingosine kinase 2 deficient tumor xenografts show impaired growth and fail to polarize macrophages towards an anti-inflammatory phenotype. *Int. J. Cancer* **125,** 2114–21 (2009).

274. Antoon, J. W., White, M. D., Driver, J. L., Burow, M. E. & Beckman, B. S. Sphingosine kinase isoforms as a therapeutic target in endocrine therapy resistant luminal and basal-A breast cancer. *Exp. Biol. Med. (Maywood).* **237,** 832–44 (2012).

275. Beljanski, V., Lewis, C. S. & Smith, C. D. Antitumor activity of sphingosine kinase 2 inhibitor ABC294640 and sorafenib in hepatocellular carcinoma xenografts. *Cancer Biol. Ther.* **11,** 524–34 (2011).

276. Snider, A. J., Orr Gandy, K. A. & Obeid, L. M. Sphingosine kinase: Role in regulation of bioactive sphingolipid mediators in inflammation. *Biochimie* **92,** 707–15 (2010).

277. Maines, L. W., Fitzpatrick, L. R., Green, C. L., Zhuang, Y. & Smith, C. D. Efficacy of a novel sphingosine kinase inhibitor in experimental Crohn's disease. *Inflammopharmacology* **18,** 73–85 (2010).

278. Fitzpatrick, L. R. *et al.* Attenuation of arthritis in rodents by a novel orally-available inhibitor of sphingosine kinase. *Inflammopharmacology* **19,** 75–87 (2011).

279. Mizugishi, K. *et al.* Essential role for sphingosine kinases in neural and vascular development. *Mol. Cell. Biol.* **25,** 11113–21 (2005).

280. Edsall, L. C., Van Brocklyn, J. R., Cuvillier, O., Kleuser, B. & Spiegel, S. N,N-Dimethylsphingosine is a potent competitive inhibitor of sphingosine kinase but not of protein kinase C: modulation of cellular levels of sphingosine 1-phosphate and ceramide. *Biochemistry* **37,** 12892–8 (1998).

281. Dickson, M. A. *et al.* A phase I clinical trial of safingol in combination with cisplatin in advanced solid tumors. *Clin. Cancer Res.* **17,** 2484–92 (2011).

282. Tonelli, F. *et al.* FTY720 and (S)-FTY720 vinylphosphonate inhibit sphingosine kinase 1 and promote its proteasomal degradation in human pulmonary artery smooth muscle, breast cancer and androgen-independent prostate cancer cells. *Cell. Signal.* **22,** 1536–42 (2010).

283. French, K. J. *et al.* Discovery and Evaluation of Inhibitors of Human Sphingosine Kinase Discovery and Evaluation of Inhibitors of Human Sphingosine Kinase 1. *Cancer Res.* **63,** 5962–5969 (2003).

284. Paugh, S. W. *et al.* A selective sphingosine kinase 1 inhibitor integrates multiple molecular therapeutic targets in human leukemia. *Blood* **112,** 1382–91 (2008).

285. Hengst, J. A. *et al.* Development of a sphingosine kinase 1 specific small-molecule inhibitor. *Bioorg. Med. Chem. Lett.* **20,** 7498–502 (2010).

286. Schnute, M. E. *et al.* Modulation of cellular S1P levels with a novel, potent and specific inhibitor of sphingosine kinase-1. *Biochem. J.* **444,** 79–88 (2012).

287. French, K. J. *et al.* Pharmacology and antitumor activity of ABC294640, a selective inhibitor of sphingosine kinase-2. *J. Pharmacol. Exp. Ther.* **333,** 129–39 (2010).

288. Hannich, J. T., Umebayashi, K. & Riezman, H. Distribution and functions of sterols and sphingolipids. *Cold Spring Harb. Perspect. Biol.* **3,** (2011).

289. Pruett, S. T. *et al.* Biodiversity of sphingoid bases ("sphingosines") and related amino alcohols. *J. Lipid Res.* **49,** 1621–39 (2008).

290. Bräse, S., Encinas, A., Keck, J. & Nising, C. F. Chemistry and biology of mycotoxins and related fungal metabolites. *Chem. Rev.* **109,** 3903–90 (2009).

291. Hanada, K. Serine palmitoyltransferase, a key enzyme of sphingolipid metabolism. *Biochim. Biophys. Acta - Mol. Cell Biol. Lipids* **1632,** 16–30 (2003).

292. Mandala, S. M., Thornton, R. A., Frommer, B. R., Dreikorn, S. & Kurtz, M. B. Viridiofungins, novel inhibitors of sphingolipid synthesis. *J. Antibiot. (Tokyo).* **50,** 339–43 (1997).

293. Fujita, T. *et al.* Fungal metabolites. Part 11. A potent immunosuppressive activity found in Isaria sinclairii metabolite. *J. Antibiot. (Tokyo).* **47,** 208–15 (1994).

294. Chiba, K. & Adachi, K. Discovery of fingolimod, the sphingosine 1-phosphate receptor modulator and its application for the therapy of multiple sclerosis. *Future Med. Chem.* **4,** 771–81 (2012).

295. Pyne, S., Bittman, R. & Pyne, N. J. Sphingosine kinase inhibitors and cancer: seeking the golden sword of Hercules. *Cancer Res.* **71,** 6576–82 (2011).

296. Bandhuvula, P., Tam, Y. Y., Oskouian, B. & Saba, J. D. The immune modulator FTY720 inhibits sphingosine-1-phosphate lyase activity. *J. Biol. Chem.* **280,** 33697–700 (2005).

297. Wascholowski, V., Giannis, A. & Pitsinos, E. N. Influence of the scyphostatin side chain on the mode of inhibition of neutral sphingomyelinase. *ChemMedChem* **1,** 718–21 (2006).

298. Tanaka, M., Nara, F., Suzuki-Konagai, K., Hosoya, T. & Ogita, T. Structural Elucidation of Scyphostatin, an Inhibitor of Membrane-Bound Neutral Sphingomyelinase. *J. Am. Chem. Soc.* **119,** 7871–7872 (1997).

299. Arenz, C. *et al.* Manumycin A and its analogues are irreversible inhibitors of neutral sphingomyelinase. *Chembiochem* **2,** 141–3 (2001).

300. Kuroda, I. *et al.* Pachastrissamine, a cytotoxic anhydrophytosphingosine from a marine sponge, Pachastrissa sp. *J. Nat. Prod.* **65,** 1505–6 (2002).

301. Ledroit, V., Debitus, C., Lavaud, C. & Massiot, G. Jaspines A and B: two new cytotoxic sphingosine derivatives from the marine sponge Jaspis sp. *Tetrahedron Lett.* **44,** 225–228 (2003).

302. Liu, J. *et al.* Stereoselective synthesis of jaspine B from D-xylose. *Carbohydr. Res.* **341,** 2653–7 (2006).

303. Kwon, Y. *et al.* Synthesis and biological evaluation of carbocyclic analogues of pachastrissamine. *Mar. Drugs* **13,** 824–37 (2015).

304. Jeon, H. *et al.* Syntheses of sulfur and selenium analogues of pachastrissamine via double displacements of cyclic sulfate. *Org. Biomol. Chem.* **9,** 7237–42 (2011).

305. Ballereau, S., Andrieu-Abadie, N., Saffon, N. & Génisson, Y. Synthesis and biological evaluation of aziridine-containing analogs of phytosphingosine. *Tetrahedron* **67,** 2570–2578 (2011).

306. Salma, Y. *et al.* Single- and double-chained truncated jaspine B analogues: asymmetric synthesis, biological evaluation and theoretical study of an unexpected 5-endo-dig process. *Tetrahedron* **67,** 4253–4262 (2011).

307. Salma, Y. *et al.* The natural marine anhydrophytosphingosine, Jaspine B, induces apoptosis in melanoma cells by interfering with ceramide metabolism. *Biochem. Pharmacol.* **78,** 477–85 (2009).

308. Rives, A., Ladeira, S., Levade, T., Andrieu-Abadie, N. & Génisson, Y. Synthesis of cytotoxic aza analogues of jaspine B. *J. Org. Chem.* **75,** 7920–3 (2010).

309. Yoo, H., Lee, Y. S., Lee, S., Kim, S. & Kim, T.-Y. Pachastrissamine from Pachastrissa sp. inhibits melanoma cell growth by dual inhibition of Cdk2 and ERK-mediated FOXO3 downregulation. *Phytother. Res.* **26,** 1927–33 (2012).

310. Canals, D. *et al.* Synthesis and biological properties of Pachastrissamine (jaspine B) and diastereoisomeric jaspines. *Bioorg. Med. Chem.* **17,** 235–41 (2009).

311. Yoshimitsu, Y. *et al.* Pachastrissamine (jaspine B) and its stereoisomers inhibit sphingosine kinases and atypical protein kinase C. *Bioorg. Med. Chem.* **19,** 5402–8 (2011).

312. Xu, J.-M. *et al.* Synthesis and preliminary biological evaluation of 1,2,3-triazole-Jaspine B hybrids as potential cytotoxic agents. *Eur. J. Med. Chem.* **80,** 593–604 (2014).

313. Kepp, O., Galluzzi, L., Lipinski, M., Yuan, J. & Kroemer, G. Cell death assays for drug discovery. *Nat. Rev. Drug Discov.* **10,** 221–37 (2011).

314. Nikoletopoulou, V., Markaki, M., Palikaras, K. & Tavernarakis, N. Crosstalk between apoptosis, necrosis and autophagy. *Biochim. Biophys. Acta* **1833,** 3448–59 (2013).

315. Elmore, S. Apoptosis: a review of programmed cell death. *Toxicol. Pathol.* **35,** 495–516 (2007).

316. Indran, I. R., Tufo, G., Pervaiz, S. & Brenner, C. Recent advances in apoptosis, mitochondria and drug resistance in cancer cells. *Biochim. Biophys. Acta* **1807,** 735–45 (2011).

317. Saraste, A. Morphologic and biochemical hallmarks of apoptosis. *Cardiovasc. Res.* **45,** 528–537 (2000).

318. Savill, J. & Fadok, V. Corpse clearance defines the meaning of cell death. *Nature* **407,** 784–8 (2000).

319. Galluzzi, L. *et al.* Molecular definitions of cell death subroutines: recommendations of the Nomenclature Committee on Cell Death 2012. *Cell Death Differ.* **19,** 107–20 (2012).

320. Tait, S. W. G., Ichim, G. & Green, D. R. Die another way--non-apoptotic mechanisms of cell death. *J. Cell Sci.* **127,** 2135–44 (2014).

321. Galluzzi, L., Blomgren, K. & Kroemer, G. Mitochondrial membrane permeabilization in neuronal injury. *Nat. Rev. Neurosci.* **10,** 481–94 (2009).

322. Bröker, L. E., Kruyt, F. A. E. & Giaccone, G. Cell death independent of caspases: a review. *Clin. Cancer Res.* **11,** 3155–62 (2005).

323. Edinger, A. L. & Thompson, C. B. Death by design: apoptosis, necrosis and autophagy. *Curr. Opin. Cell Biol.* **16,** 663–9 (2004).

324. Vanden Berghe, T., Linkermann, A., Jouan-Lanhouet, S., Walczak, H. & Vandenabeele, P. Regulated necrosis: the expanding network of non-apoptotic cell death pathways. *Nat. Rev. Mol. Cell Biol.* **15,** 135–47 (2014).

325. Yang, Z. & Klionsky, D. J. Eaten alive: a history of macroautophagy. *Nat. Cell Biol.* **12,** 814–22 (2010).

326. Galluzzi, L. *et al.* Autophagy in malignant transformation and cancer progression. *EMBO J.* (2015).

327. Gozuacik, D. & Kimchi, A. Autophagy as a cell death and tumor suppressor mechanism. *Oncogene* **23,** 2891–906 (2004).

328. Yang, Z. J., Chee, C. E., Huang, S. & Sinicrope, F. A. The role of autophagy in cancer: therapeutic implications. *Mol. Cancer Ther.* **10,** 1533–41 (2011).

329. Brech, A., Ahlquist, T., Lothe, R. A. & Stenmark, H. Autophagy in tumour suppression and promotion. *Mol. Oncol.* **3,** 366–75 (2009).

330. Cheong, H., Lu, C., Lindsten, T. & Thompson, C. B. Therapeutic targets in cancer cell metabolism and autophagy. *Nat. Biotechnol.* **30,** 671–8 (2012).

331. Janku, F., McConkey, D. J., Hong, D. S. & Kurzrock, R. Autophagy as a target for anticancer therapy. *Nat. Rev. Clin. Oncol.* **8,** 528–39 (2011).

332. Kroemer, G., Mariño, G. & Levine, B. Autophagy and the integrated stress response. *Mol. Cell* **40,** 280–93 (2010).

333. Kornienko, A., Mathieu, V., Rastogi, S. K., Lefranc, F. & Kiss, R. Therapeutic agents triggering nonapoptotic cancer cell death. *J. Med. Chem.* **56,** 4823–39 (2013).

334. Overmeyer, J. H., Kaul, A., Johnson, E. E. & Maltese, W. A. Active ras triggers death in glioblastoma cells through hyperstimulation of macropinocytosis. *Mol. Cancer Res.* **6,** 965–77 (2008).

335. Maltese, W. a & Overmeyer, J. H. Methuosis: Nonapoptotic Cell Death Associated with Vacuolization of Macropinosome and Endosome Compartments. *Am. J. Pathol.* **184,** 1–13 (2014).

336. Kerr, M. C. & Teasdale, R. D. Defining macropinocytosis. *Traffic* **10,** 364–71 (2009).

337. Bhanot, H., Young, A. M. & Overmeyer, J. H. Induction of Nonapoptotic Cell Death by Activated Ras Requires Inverse Regulation of Rac1 and Arf6. (2010).

338. Overmeyer, J. H., Young, A. M., Bhanot, H. & Maltese, W. A. A chalcone-related small molecule that induces methuosis, a novel form of non-apoptotic cell death, in glioblastoma cells. *Mol. Cancer* **10,** 69 (2011).

339. Overmeyer, J. H. & Maltese, W. A. Death pathways triggered by activated Ras in cancer cells. *Front. Biosci. Landmark Ed.* **16,** 1693–713 (2011).

340. Robinson, M. W., Overmeyer, J. H., Young, A. M., Erhardt, P. W. & Maltese, W. A. Synthesis and evaluation of indole-based chalcones as inducers of methuosis, a novel type of nonapoptotic cell death. *J. Med. Chem.* **55,** 1940–56 (2012).

341. Yu, H.-G. *et al.* Phosphoinositide 3-kinase/Akt pathway plays an important role in chemoresistance of gastric cancer cells against etoposide and doxorubicin induced cell death. *Int. J. Cancer* **122,** 433–43 (2008).

342. Harrer, H., Humpf, H. U. & Voss, K. A. In vivo formation of N-acyl-fumonisin B1. *Mycotoxin Res.* **31,** 33–40 (2015).

343. Garrido, M., Abad, J. L., Fabriàs, G., Casas, J. & Delgado, A. Azide-tagged sphingolipids: new tools for metabolic flux analysis. *Chembiochem* **16,** 641–50 (2015).

344. Lahiri, S. *et al.* Kinetic characterization of mammalian ceramide synthases: determination of K(m) values towards sphinganine. *FEBS Lett.* **581,** 5289–94 (2007).

345. Morissette, G., Moreau, E., C-Gaudreault, R. & Marceau, F. N-substituted 4-aminobenzamides (procainamide analogs): an assessment of multiple cellular effects concerning ion trapping. *Mol. Pharmacol.* **68,** 1576–89 (2005).

346. Collins, J. A., Schandl, C. A., Young, K. K., Vesely, J. & Willingham, M. C. Major DNA Fragmentation Is a Late Event in Apoptosis. *J. Histochem. Cytochem.* **45,** 923–934 (1997).

347. Delbridge, A. R. D., Valente, L. J. & Strasser, A. The role of the apoptotic machinery in tumor suppression. *Cold Spring Harb. Perspect. Biol.* **4,** (2012).

348. Li, J. *et al.* The AKT inhibitor AZD5363 is selectively active in PI3KCA mutant gastric cancer, and sensitizes a patient-derived gastric cancer xenograft model with PTEN loss to Taxotere. *J. Transl. Med.* **11,** 241 (2013).

349. Oki, E. *et al.* Akt phosphorylation associates with LOH of PTEN and leads to chemoresistance for gastric cancer. *Int. J. Cancer* **117,** 376–80 (2005).

350. Fulda, S. & Kögel, D. Cell death by autophagy: emerging molecular mechanisms and implications for cancer therapy. *Oncogene* (2015). doi:10.1038/onc.2014.458

351. Young, M. M., Kester, M. & Wang, H.-G. Sphingolipids: regulators of crosstalk between apoptosis and autophagy. *J. Lipid Res.* **54,** 5–19 (2013).

352. Bedia, C., Levade, T. & Codogno, P. Regulation of autophagy by sphingolipids. *Anticancer. Agents Med. Chem.* **11,** 844–53 (2011).

353. Wu, Y.-T. *et al.* Dual role of 3-methyladenine in modulation of autophagy via different temporal patterns of inhibition on class I and III phosphoinositide 3-kinase. *J. Biol. Chem.* **285,** 10850–61 (2010).

354. Bjørkøy, G. *et al.* Monitoring autophagic degradation of p62/SQSTM1. *Methods Enzymol.* **452,** 181–97 (2009).

355. Jung, C. H., Ro, S.-H., Cao, J., Otto, N. M. & Kim, D.-H. mTOR regulation of autophagy. *FEBS Lett.* **584,** 1287–95 (2010).

356. Tooze, S. A. & Yoshimori, T. The origin of the autophagosomal membrane. *Nat. Cell Biol.* **12,** 831–5 (2010).

357. Kar, R., Singha, P. K., Venkatachalam, M. a & Saikumar, P. A novel role for MAP1 LC3 in nonautophagic cytoplasmic vacuolation death of cancer cells. *Oncogene* **28,** 2556–68 (2009).

358. Wasik, a M. *et al.* WIN55,212-2 induces cytoplasmic vacuolation in apoptosis-resistant MCL cells. *Cell Death Dis.* **2,** e225 (2011).

359. Doherty, G. J. & McMahon, H. T. Mechanisms of endocytosis. *Annu. Rev. Biochem.* **78,** 857–902 (2009).

360. Clague, M. J., Urbé, S., Aniento, F. & Gruenberg, J. Vacuolar ATPase activity is required for endosomal carrier vesicle formation. *J. Biol. Chem.* **269,** 21–4 (1994).

361. Papini, E. *et al.* Bafilomycin A1 inhibits Helicobacter pylori-induced vacuolization of HeLa cells. *Mol. Microbiol.* **7,** 323–7 (1993).

362. Koivusalo, M. *et al.* Amiloride inhibits macropinocytosis by lowering submembranous pH and preventing Rac1 and Cdc42 signaling. *J. Cell Biol.* **188,** 547–63 (2010).

363. Commisso, C. *et al.* Macropinocytosis of protein is an amino acid supply route in Ras-transformed cells. *Nature* **497,** 633–7 (2013).

364. Yang, Z., Vadlamudi, R. K. & Kumar, R. Dynein light chain 1 phosphorylation controls macropinocytosis. *J. Biol. Chem.* **280,** 654–9 (2005).

365. Swanson, J. A. Shaping cups into phagosomes and macropinosomes. *Nat. Rev. Mol. Cell Biol.* **9,** 639–49 (2008).

366. Lim, J. P. & Gleeson, P. A. Macropinocytosis: an endocytic pathway for internalising large gulps. *Immunol. Cell Biol.* **89,** 836–43 (2011).

367. Chi, S. *et al.* Oncogenic Ras triggers cell suicide through the activation of a caspase-independent cell death program in human cancer cells. *Oncogene* **18,** 2281–90 (1999).

368. Grant, B. D. & Donaldson, J. G. Pathways and mechanisms of endocytic recycling. *Nat. Rev. Mol. Cell Biol.* **10,** 597–608 (2009).

369. Feliciano, W. D., Yoshida, S., Straight, S. W. & Swanson, J. A. Coordination of the Rab5 cycle on macropinosomes. *Traffic* **12,** 1911–22 (2011).

370. Minna, E. *et al.* miR-199a-3p displays tumor suppressor functions in papillary thyroid carcinoma. *Oncotarget* **5,** 2513–2528 (2014)

371. Kitambi, S. S. *et al.* Vulnerability of glioblastoma cells to catastrophic vacuolization and death induced by a small molecule. *Cell* **157,** 313–28 (2014).

372. Trabbic, C. J. *et al.* Differential Induction of Cytoplasmic Vacuolization and Methuosis by Novel 2-Indolyl-Substituted Pyridinylpropenones. *ACS Med. Chem. Lett.* **5,** 73–77 (2014).

373. Gilbertson, R. J. Driving glioblastoma to drink. *Cell* **157,** 289–90 (2014).

374. Gao, P., Peterson, Y. K., Smith, R. A. & Smith, C. D. Characterization of isoenzyme-selective inhibitors of human sphingosine kinases. *PLoS One* **7,** e44543 (2012).

375. Antoon, J. W., White, M. D., Burow, M. E. & Beckman, B. S. Dual inhibition of sphingosine kinase isoforms ablates TNF-induced drug resistance. *Oncol. Rep.* **27,** 1779–86 (2012).

376. French, K. J. *et al.* Antitumor activity of sphingosine kinase inhibitors. *J. Pharmacol. Exp. Ther.* **318,** 596–603 (2006).

377. Illuzzi, G. *et al.* Sphingosine kinase mediates resistance to the synthetic retinoid N-(4-hydroxyphenyl)retinamide in human ovarian cancer cells. *J. Biol. Chem.* **285,** 18594–602 (2010).

378. Tonelli, F. *et al.* The sphingosine kinase inhibitor 2-(p-hyroxyanilino)-4-(p-chlorophenyl)thiazole reduces androgen receptor expression via an oxidative stress-dependent mechanism. *Br. J. Pharmacol.* **168,** 1497–505 (2013).

379. Cingolani, F. *et al.* Inhibition of dihydroceramide desaturase activity by the sphingosine kinase inhibitor SKI II. *J. Lipid Res.* **55,** 1711–1720 (2014).

380. Çelik, H. & Koşar, M. Inhibitory effects of dietary flavonoids on purified hepatic NADH-cytochrome b5 reductase: Structure–activity relationships. *Chem. Biol. Interact.* **197,** 103–109 (2012).

381. Çelik, H., Koşar, M. & Arinç, E. In vitro effects of myricetin, morin, apigenin, (+)-taxifolin, (+)-catechin, (-)-epicatechin, naringenin and naringin on cytochrome b5 reduction by purified NADH-cytochrome b5 reductase. *Toxicology* **308,** 34–40 (2013).

382. Verma, S., Singh, A. & Mishra, A. Molecular construction of NADH-cytochrome b5 reductase inhibition by flavonoids and chemical basis of difference in inhibition potential: Molecular dynamics simulation study. *J. Appl. Pharm. Sci.* **02,** 33–39 (2012).

383. An, S., Zheng, Y. & Bleu, T. Sphingosine 1-Phosphate-induced Cell Proliferation, Survival, and Related Signaling Events Mediated by G Protein-coupled Receptors Edg3 and Edg5. *J. Biol. Chem.* **275,** 288–296 (2000).

384. Ricci, C. *et al.* In vitro anti-leukaemia activity of sphingosine kinase inhibitor. *Br. J. Haematol.* **144,** 350–7 (2009).

385. Kohno, M. *et al.* Intracellular role for sphingosine kinase 1 in intestinal adenoma cell proliferation. *Mol. Cell. Biol.* **26,** 7211–23 (2006).

386. Taha, T. A. *et al.* Loss of sphingosine kinase-1 activates the intrinsic pathway of programmed cell death: modulation of sphingolipid levels and the induction of apoptosis. *FASEB J.* **20,** 482–4 (2006).

387. Van Brocklyn, J. R. *et al.* Sphingosine kinase-1 expression correlates with poor survival of patients with glioblastoma multiforme: roles of sphingosine kinase isoforms in growth of glioblastoma cell lines. *J. Neuropathol. Exp. Neurol.* **64,** 695–705 (2005).

388. Zhang, H. *et al.* Inhibition of sphingosine kinase 1 suppresses proliferation of glioma cells under hypoxia by attenuating activity of extracellular signal-regulated kinase. *Cell Prolif.* **45,** 167–75 (2012).

389. Spassieva, S. D. *et al.* Cell density-dependent reduction of dihydroceramide desaturase activity in neuroblastoma cells. *J. Lipid Res.* **53,** 918–28 (2012).

390. Levade T, Sandhoff K, Schulze H, M. J. Acid ceramidase deficiency: Farber lipogranulomatosis. *InValleDet al Scriver's OMMBID (Online Metab. Mol. Bases Inherit. Dis. New York.* (2009).

391. Wu, B. X., Snook, C. F., Tani, M., Büllesbach, E. E. & Hannun, Y. A. Large-scale purification and characterization of recombinant Pseudomonas ceramidase: regulation by calcium. *J. Lipid Res.* **48,** 600–8 (2007).

392. Turk, B., Turk, V. & Turk, D. Structural and functional aspects of papain-like cysteine proteinases and their protein inhibitors. *Biol. Chem.* **378,** 141–50 (1997).

393. Otto, H.-H. & Schirmeister, T. Cysteine Proteases and Their Inhibitors. *Chem. Rev.* **97,** 133–172 (1997).

394. Proksch, D., Klein, J. J. & Arenz, C. Potent inhibition of Acid ceramidase by novel B-13 analogues. *J. Lipids* **2011,** 971618 (2011).

395. Schwarzmann, G., Arenz, C. & Sandhoff, K. Labeled chemical biology tools for investigating sphingolipid metabolism, trafficking and interaction with lipids and proteins. *Biochim. Biophys. Acta* **1841,** 1161–73 (2014).

396. Merrill, A. H. Sphingolipid and glycosphingolipid metabolic pathways in the era of sphingolipidomics. *Chem. Rev.* **111,** 6387–422 (2011).

397. Delgado, A., Casas, J., Llebaria, A., Abad, J. L. & Fabriás, G. Chemical tools to investigate sphingolipid metabolism and functions. *ChemMedChem* **2,** 580–606 (2007).

398. Delgado, A., Casas, J., Llebaria, A., Abad, J. L. & Fabrias, G. Inhibitors of sphingolipid metabolism enzymes. *Biochim. Biophys. Acta* **1758,** 1957–77 (2006).

399. Fazi, B. *et al.* Fenretinide induces autophagic cell death in caspase-defective breast cancer cells. *Autophagy* **4,** 435–41 (2008).

400. Li, J.-G. *et al.* Manumycin induces apoptosis in prostate cancer cells. *Onco. Targets. Ther.* **7,** 771–7 (2014).

401. Singha, P. K., Pandeswara, S., Venkatachalam, M. a & Saikumar, P. Manumycin A inhibits triple-negative breast cancer growth through LC3-mediated cytoplasmic vacuolation death. *Cell Death Dis.* **4,** e457 (2013).

402. Hurwitz, R., Ferlinz, K. & Sandhoff, K. The tricyclic antidepressant desipramine causes proteolytic degradation of lysosomal sphingomyelinase in human fibroblasts. *Biol. Chem. Hoppe. Seyler.* **375,** 447–450 (1994).

403. Elojeimy, S. *et al.* New insights on the use of desipramine as an inhibitor for acid ceramidase. *FEBS Lett.* **580,** 4751–6 (2006).

404. Filippova IYu, Lysogorskaya, E. N., Oksenoit, E. S., Rudenskaya, G. N. & Stepanov, V. M. L-Pyroglutamyl-L-phenylalanyl-L-leucine-p-nitroanilide--a chromogenic substrate for thiol proteinase assay. *Anal. Biochem.* **143,** 293–7 (1984).